Système de recommandation de patrons personnalisés de chemises pour hommes basé sur des mesures corporelles précises

Cheng Chi

CENTRALE LILLE

THESE

Présentée en vue

d'obtenir le grade de

DOCTEUR

En

Spécialité : Automatique, productique

Par

Cheng CHI

DOCTORAT délivré par CENTRALE LILLE

Titre de la thèse :

Personalized pattern recommendation system of men's shirts based on precise body measurement

Système de recommandation de patrons personnalisés de chemises pour hommes basé sur des mesures corporelles précises

Soutenue le 01/03/2022 devant le jury d'examen :

Président	**Xianyi ZENG, Professeur, ENSAIT**
Rapporteur	**Emilie DREAN, HDR, Université de Haute-Alsace (UHA)**
Rapporteur	**Katarzyna GRABOWSKA, Professeur, Lodz University of Technology**
Examinateur	**Antonella CURTEZA, Professeur, Gheorghe Asachi Technical University of Iaşi**
Co-encadrant	**Guillaume TARTARE, Docteur, ENSAIT**
Directeur de thèse	**Pascal BRUNIAUX, Professeur, ENSAIT**

Thèse préparée dans le Laboratoire **GEMTEX** – Laboratoire de Génie et Matériaux Textiles

École Doctorale : MADIS - Science Pour l'Ingénieur Lille Nord-de-France

centralelille

Acknowledgement

With the completion of my thesis, my Ph.D. study will soon come to an end. Despite many unexpected difficulties I have encountered, I still enjoy and gratefully this process. In the mid-stage of my Ph.D. that I was under tremendous pressure with the work stoppage caused by the Covid-19. I lost my way for a while. However, the help and encouragement from my supervisors and Ph.D. students helped me find the motivation to keep going again.

As my thesis draws to the end, I would like to take this opportunity to thank all those who have contributed in all kinds of ways and provided invaluable help in the preparation and completion of this research.

Firstly, I would like to thank my supervisor, Prof. Pascal Bruniaux of ENSAIT, for his constant encouragement, understanding and patience during my Ph.D. studies. Due to his constant care and patience, I was able to overcome all the difficulties with confidence.

I would also like to thank my Co-advisor Guillaume Tartare, Francois Dassonville from the GEMTEX laboratory, and the staff at ENSAIT for their guidance and enthusiastic help during my Ph.D. studies.

I would like to thank Professor Xianyi Zeng of ENSAIT in particular. He provided me with the opportunity to come to France for Ph.D. study and provided me with a constant stream of ideas and inspiration for my study. With Professor Zeng's guidance, my studies have been elevated. Professor Zeng is a generous and kind person. As a student, I have great admiration for such a senior academic. For all that you have done for me, Professor Zeng, I thank you heartily.

I would also like to thank my colleague, Dr. Hongshu Jin, a teacher at Wuhan Textile University, who sincerely provided me with valuable advice and guidance on human data collection in the pre-study stage.

I am very grateful to my friends, Kehui SONG, Chan HUI and Shengchang ZHANG, Ph.D. students in the GEMTEX laboratory, who provided me with a lot of valuable advice and technical help in the analysis of data and thesis writing. Without their help, my research process would not have been so smooth. In addition, I would like to thank my friends Kaichen WANG, Xin ZHAO, Chen CHEN, Hao SHEN, and Zhenglei HE, Ph.D. students in the GEMTEX laboratory, and Ph.D. student Zhujun WANG from Donghua University for their help and positive emotions during my study and life in France, so that difficulties have not defeated me during these past three years.

I would also like to thank Wuhan Textile University (China), the organization where I work, for offering me great support during my Ph.D. study, such as sufficient study time and subsistence allowance overseas.

My final thanks would go to my parents and my wonderful buddies for their love and support at every difficult moment. Without their utmost understanding and unfailing care, I would not have made any progress during my Ph.D. study overseas.

Finally, I would give my deepest apology to my wife. For various reasons, I have not been able to be with you and take care of you for the past three years, and this is my regret. Every day in the future, I hope to be by your side and love you with everything I have.

The completion of my thesis was the end of my PhD research. However, it is also a new starting point in my life. In the future, I will continue to pursue the career that I love.

CONTENTS

LIST OF FIGURES

LIST OF TABLES

GENERAL INTRODUCTION

With the rapid development of the economy, more and more consumers require the personalization of products. Apparel companies urgently need a new production model to respond to this requirement. Through this model, all activities in the complete product design and production process will focus more on the consumer's requirements. Mass customization is considered to be a successful model in the apparel industry. It requires apparel companies to produce customized garments quickly to suit different body shapes and individual requirements. Mass customization can satisfy the requirements of a specific population, provide adaptable products or services and realize the process of rapid customization at low cost. However, the complexity of consumer requirements has led to increased difficulty in garment design. For example, due to rising consumption levels and changes in people's diets, the body sizes of different consumer groups are becoming more and more different. This leads to the anthropometric data on which the ready-to-wear sizing system is based becoming outdated. Garments produced based on this system do not conform to current body sizes. More designers need to be employed for apparel companies, or the current design methods and processes need to be updated to solve this problem. However, employing more experienced designers would significantly increase costs. Therefore, changing the current design method and process is an effective way to solve the difficulties of modern apparel companies.

To match the design of products, environments, and systems to the target users, the target users' body characteristics must be considered first. Ergonomic research on anthropometry and human body shape analysis is essential for designing garment products. In the apparel industry, body shape is closely associated with garment manufacture and garment fit. The starting point for making comfortable garments is to understand and comprehensively characterize the differences in human body shape.

Currently, most body shape research is based on data obtained from 3D human models. 3D body scanning technology enhances traditional anthropometric body shape descriptions by extracting information on cross-sectional areas and segmental volumes. Most 3D human models used in the apparel industry are rigid geometric surface models in the standing position and do not consider factors such as skeletal structure, body composition (bone, fat and muscle) and body deformation associated with skin elasticity and body movements. If these factors are not integrated into 3D human models, the products produced on this basis may not be suitable for consumers. In addition, in a natural standing posture, it is difficult to obtain data on hidden areas (e.g., arm roots, groin, crotch) from a 3D scan. This also leads to the generated 3D body model not accurately reflecting the real human body shape. Therefore, it is important to propose a method for correcting 3D human models to solve the above problems.

In addition, garment pattern-making is a key part of satisfying the personalization of garments. However, whether through traditional manual garment pattern-making or computer-aided design (CAD) garment pattern-making software, pattern designers need to have a great wealth of professional knowledge and proficient skills to quickly make a better-fitting garment pattern. Meanwhile, these methods also have the following disadvantages: (1) the learning process is particularly long and difficult to promote, and the making process is time-consuming, limiting the improvement of production efficiency. Although the CAD garment pattern-making software can automatically grade, which improves production efficiency, it is only suitable for the overall grading of the standard dimension specifications. It cannot automatically adjust the changes of individual dimensions. Garments produced based on standard dimension specifications cannot satisfy the requirements of consumers for fit; (2) once the garment style changes, the structure drawing of the garment needs to be manually redrawn or adjusted, and inexperienced designers are unable to respond quickly to adjustments in garment patterns. Therefore, it is very useful for the garment industry to know how to develop garment products without experienced designers and pattern makers. This is

because the garment industry can reduce its reliance on designers and pattern makers. Virtual reality technology also plays an important role in modern mass garment customization. Due to the realistic 3D environment and real-time interaction supported by the technology, it has had a profound impact on the apparel manufacturing industry. It provides the basic technical conditions for the virtual design of new products and the associated manufacturing. In customized garment design, designers can use virtual reality technology to assess the fit of garment products.

In the current garment recommendation system, most garment CAD work focuses on the technical development of virtual garment assembly and its application to specific human body models. Few involve designer knowledge of the design area. It is well known that the garment designer plays a key role in the garment customization process. The knowledge obtained from the designer's experience should be utilized to develop virtual garment patterns. When a customer or young designer is unsure which garment is more suitable for a specific wearer in terms of garment style and body shape, the designer's knowledge can provide personalized recommendations based on the consumer's requirements. Therefore, personalized knowledge-based recommendations can provide more effective assistance to a wide range of consumers and young designers in choosing relevant customized garment products or design solutions with the knowledge of an experienced designer. For this reason, garment recommendation systems should be well developed to enable the formalization and development of designer knowledge for the rapid delivery of small quantities of customized garment design productions and solutions. Garment recommendation systems play an important role in e-shopping and CAD-based garment co-design.

In my PhD research, we propose an intelligent designer knowledge-based garment pattern recommendation system to design new personalized garment products. The designer's knowledge includes expert anthropometric knowledge and garment pattern-making knowledge. Firstly, by using experts' professional knowledge, we manually realize accurate human body data measurements as well as their interpretation and

classification, and extract more relevant human body features. In this approach, after a deep analysis, measured data irrelevant to human body shape have been excluded by designers. Furthermore, the relation between body shapes and previously identified body features have been modelled (Model I). Secondly, from this relational model, we label key positions on the corresponding 3D body model obtained from 3D body scanning and segment the whole 3D body model into semantically interpretable body parts. In this way, two databases have been created, enabling to identify features of all segmented body parts, whose combination corresponds to the whole body shape. Database I is composed of all body classification data (key body positions, segmented body parts, relevant body measures), manually measured by the involved designers. Database II includes all 3D body models for various body shapes, labelled and segmented according to the results of Database I. The adjusted 3D human body model contains important human semantic information on labelled key body position points and features on each body part. For a specific consumer, his/her personalized 3D body model can be obtained by taking a very few numbers of body measures on himself/herself, selecting the closest body parts from Database II, making an appropriate combination of the selected body parts, and adjusting parameters of all involved body parts (Model II). By using three-dimensional to two-dimensional (3D-to-2D) flattening technology, a 2D flatten graph of the 3D personalized basic pattern of the interpretable model is obtained and slightly adjusted to the form suitable for industrial production, i.e. PBP. And the PBP database (Database III) is built. In addition, to realize a fit-oriented personalized parametric pattern-making method, three models are required, including a basic pattern parametric model (Model III) (characterizing the relations between the basic pattern and its key influencing human dimensions (chest girth and back length)), a regression model (Model IV) which enables to infer from basic pattern to PBP for three body parts based on the one-to-one correspondence of key points between the PBPs and the basic patterns, and a personalized shirt pattern parametric model (Model V) (characterizing the structural relations between the

personalized shirt pattern (PBP*shirt*) and PBP).

The recommendation system also has an adjustment and feedback function. The recommended garment pattern and the relevant try-on for a specific body shape can be displayed virtually on the 3D platform. It can be adjusted if the user is not satisfied with the recommendation results. The design can be repeatedly evaluated and adjusted until the user is satisfied.

My PhD research aims to solve a series of key problems encountered in the parametric design of personalized garment patterns and provide several more effective and rational solutions for apparel companies. For that, it's necessary to summarize my PhD research, it consists of three main parts as follows.

1. Segment the body by anthropometric knowledge, and the segmented body parts are classified reasonably.

2. Combining manual, 3D, and body shape classification results to label and correct the scanned 3D human body model. Then, the corrected model is segmented, selected and combined to complete the parametric modelling of a personalized 3D human body that contains semantic information about the human body. The model can assist young designers to design 3D garments without enough knowledge.

3. Develop a fit-oriented personalized garment pattern parametric design process for users who do not have garment pattern-making knowledge.

The overall layout of this thesis is as follows.

Chapter 1: State of the Art and Basic Concepts

This chapter describes the current state of development of the various modules in the garment pattern recommendation system. This includes body data acquisition, body shape classification, 3D body modelling and garment pattern-making techniques, as well as concepts related to personalized garment design. In addition, we introduce the techniques used in various existing recommendation systems, especially for garment recommendations. Finally, the basic principles and overall scheme of a fit-oriented garment pattern recommendation system are given.

Chapter 2: Tools used in the Research

The relevant knowledge acquisition tools and computational tools used to realize the system are described. This includes the methods used for body data acquisition, the statistical methods used for body data analysis and modelling, and the various technical tools used for the 3D body modelling and parametric garment pattern design process.

Chapter 3: Human Upper Body Classification based on Manual Measurement Data

The segmented body parts shape classification method is described and a relationship model between feature measurements and body parts shape.

Chapter 4: 3D Human Upper Body Modelling

Firstly, the method of labelling human feature points and correcting the human body model is presented. Next, a parametric modelling method is described to obtain a personalized human body model for a specific user using the segmented corrected model.

Chapter 5: Parametric Garment Pattern-making

A parametric design process for fit-oriented personalized garment patterns is described and a method for evaluating garment fit. Finally, a personalized pattern recommendation system based on the above research is described.

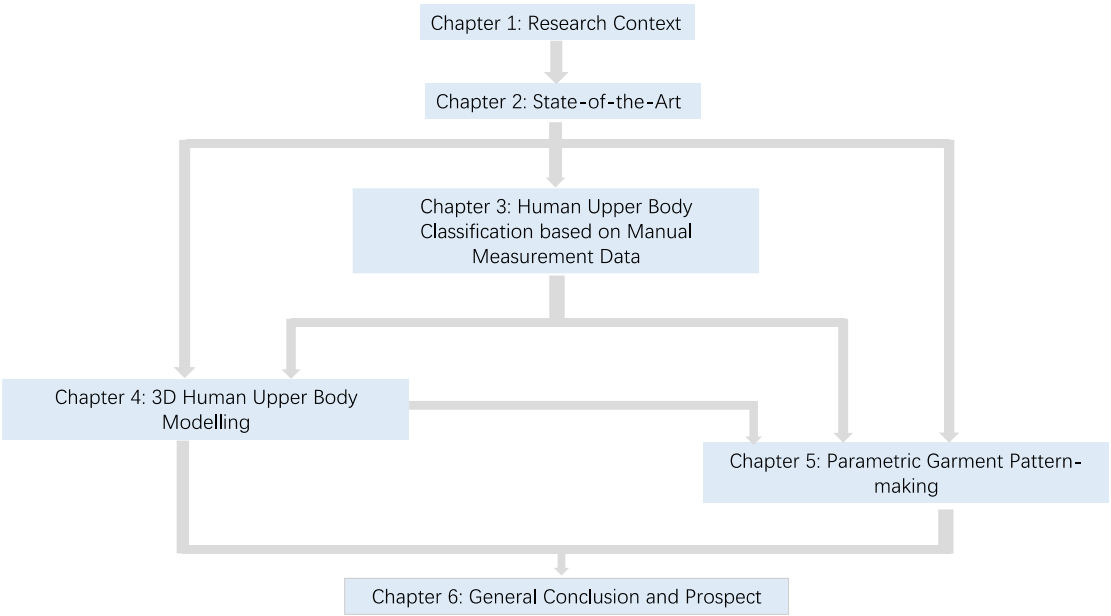

Figure 0-1: Organization of the chapters of this PhD Thesis.

CHAPTER 1: State of the Art and Basic Concepts

Introduction

This chapter reviews research work on the human body in the field of apparel, including anthropometric techniques, human body shape classification methods, 3D human body modelling, garment pattern-making techniques, and garment fitting. In addition, existing recommendation systems are analyzed, particularly for clothing. Based on the above concepts and techniques, the basic principles of a fit-oriented personalized garment pattern recommendation system is presented in this paper. The system integrates designers' pattern-making knowledge and anthropometric knowledge to adjust personalized garment patterns generated based on traditional pattern-making methods. Using this recommendation system, users can select the corresponding garment style and design the most suitable garment fit according to different individual requirements.

1.1 Research on human body shape

The human body is the center of clothing services. With the changing of lifestyles and demographics, new consumer requirements for clothing have arisen. Designers must satisfy the growing requirement for the fit of clothing. Moreover, the basis for creating comfortable clothing is understanding the specifics of the human body structure. Therefore, this has led to the research of the human body and its relationship with clothing. The uniqueness of the human body is that no two people are ever the same in terms of all measurable morphological features. Therefore, to create well-fitting clothes, comprehensive information about body measurements and shapes must first be provided. For this reason, it is essential to understand some basic concepts related to human morphology. Furthermore, the study of the human body is all based on

anthropometric measurements. Depending on the method of measurement, it can be divided into contact and non-contact measurements.

1.1.1 Morphological analysis of the human body

The model of the human being bears a specific scale. In the 1st century B.C., the Roman architect Marcus Vitruvius proposed a model called homo bene figuratus, 'the well-shaped man' [1]. The fifth-century Greek sculptor Polykleitos used the mathematical basis to segment the human body into seven equal parts [2], as in Figure 1-1. In the fifteenth century, Leonardo da Vinci refined Vitruviu's vague descriptions in his famous model of the 'Vitruvian Man', constructing a system of eight-head-heights [2], and it is used to this day, as shown in Figure 1-2. The proportions illustrated by Leonardo's model have been widely accepted as the 'golden proportion' [3]. However, in modern society, most people do not conform to this 'golden proportion', and no one is even absolutely symmetrical. Human imperfection and its limitations are a part of life and are acceptable.

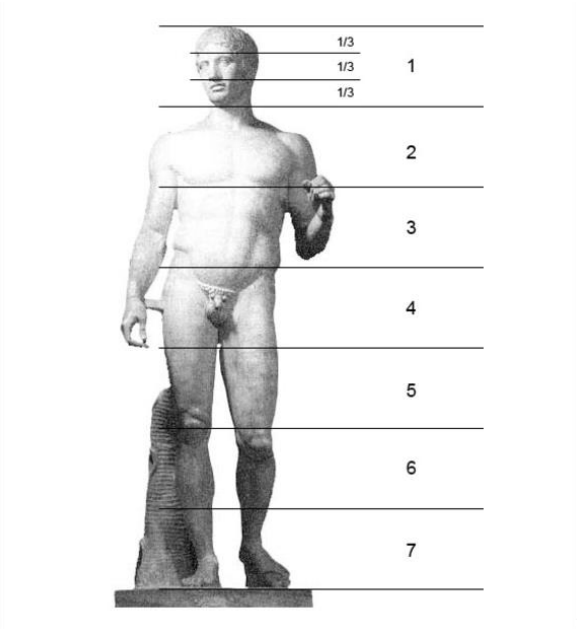

Figure 1-1: Seven-head body model.

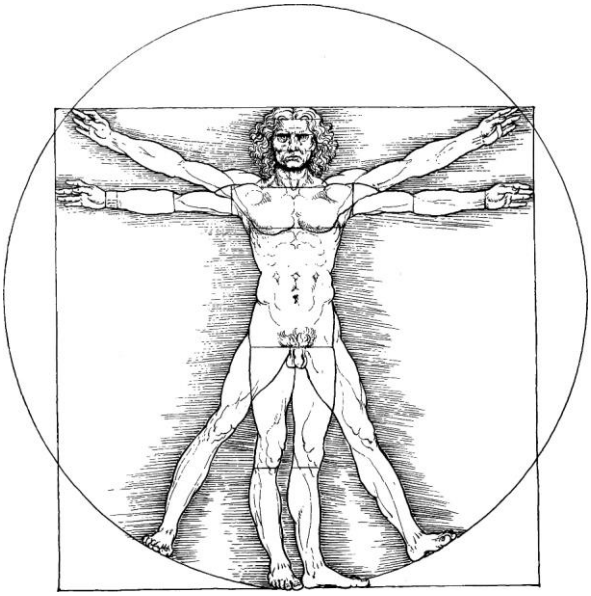

Figure 1-2: Vitruviu's man by Leonardo da Vinci

To quantify the knowledge about human measurements, anthropometry [4] was created. The aim of current anthropometric research is to explore and understand the real human body and its classification to satisfy the needs of the market today. Chaffin [5] proposes a most suitable definition of anthropometry. "Anthropometry is a science that deals with the measurement of size, weight, and proportions of the human body. It is empirical in nature and has developed quantitative methods to measure various physical dimensions". It is a knowledge dedicated to describing the quantification of the external geometry of the human body. As an application, the goal of anthropometry is to collect valuable information and make it usable for the designer's purposes. The garment industry is mainly concerned with anthropometric aspects of body dimensions and shapes [6, 7]. Body measurements are the basis of garment design [8]. For the purpose of this study, anthropometric data is also included to give better fit and comfort to the designed garments [9]. Therefore, accurate anthropometric procedure is necessary.

For the human body and its posture, it is not suitable to use physical terms such as up and down, front and back, etc. to represent body parts. In this situation, the definitions of anatomical terms for the position of the human body and the positional terms for the correct representation of body parts in garment styling are used. In this case, the ground

on which the body stands (the measuring surface) is defined as horizontal. The basic terms used in position are defined as follows (seen in Figure 1-3) [10]:

- Sagittal plane passes through the front and back of the body, dividing the body into left and right parts. If the two parts are equal in size, the plane is known as the Midsagittal plane. If the two parts are not equal, the plane is called the Parasagittal plane.
- Frontal plane parallels to the forehead, at right angles to the sagittal plane, dividing the body into anterior and posterior parts.
- Transverse planes, at right angles to the sagittal plane and parallel to the ground, divide the body into upper and lower parts.

The intersection of the above planes makes it possible to define three reference anatomical axes perpendicular to the reference plane.

- Longitudinal axis, perpendicular to the transverse plane.
- Anteroposterior axis, perpendicular to the frontal plane.
- Mediolateral axis, perpendicular to the sagittal plane.

The planes describe the static position of the body, while the axes determine rotation and define the movement.

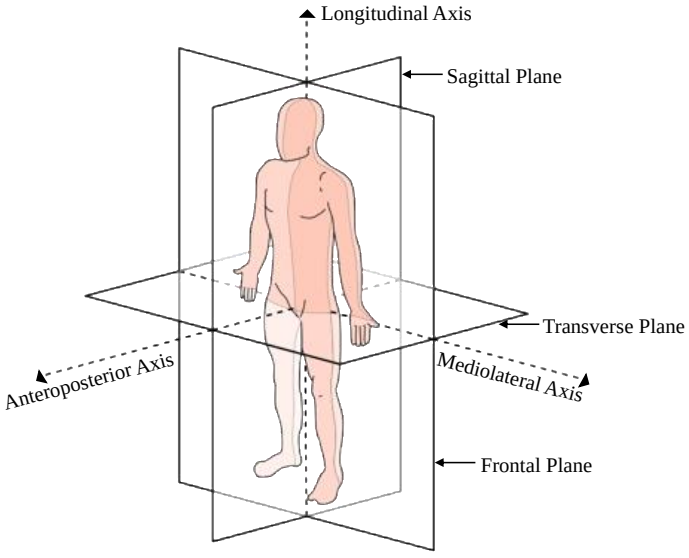

Figure 1-3: Body reference planes and axes.

Due to the softness of the body surface and the fact that the human body is non-stationary, it is very difficult to exclude errors during the measurement process completely. Therefore, to obtain the correct measurement values, the next step requires the correct labelling of the measuring points and the measuring baselines on the body before the measurement is taken. The specific body landmarks are defined by uniform standards (e.g., ISO-7250, ISO-8559, JIS L0111-1983). A comprehensive summary of male anthropometric points based on Japanese anthropometric standards [11] was presented by the Japanese Bunka Fashion College[12], as shown in Figure 1-4. Table 1-1 presents the definitions of the necessary measurement points for making garments, which can be taken on the skin.

The anthropometric data to be incorporated into the anthropometric database must be accurate and interpretable. It is also necessary for create well-fitting garments. Therefore, all steps in the development of anthropometrics need to minimize errors from the beginning.

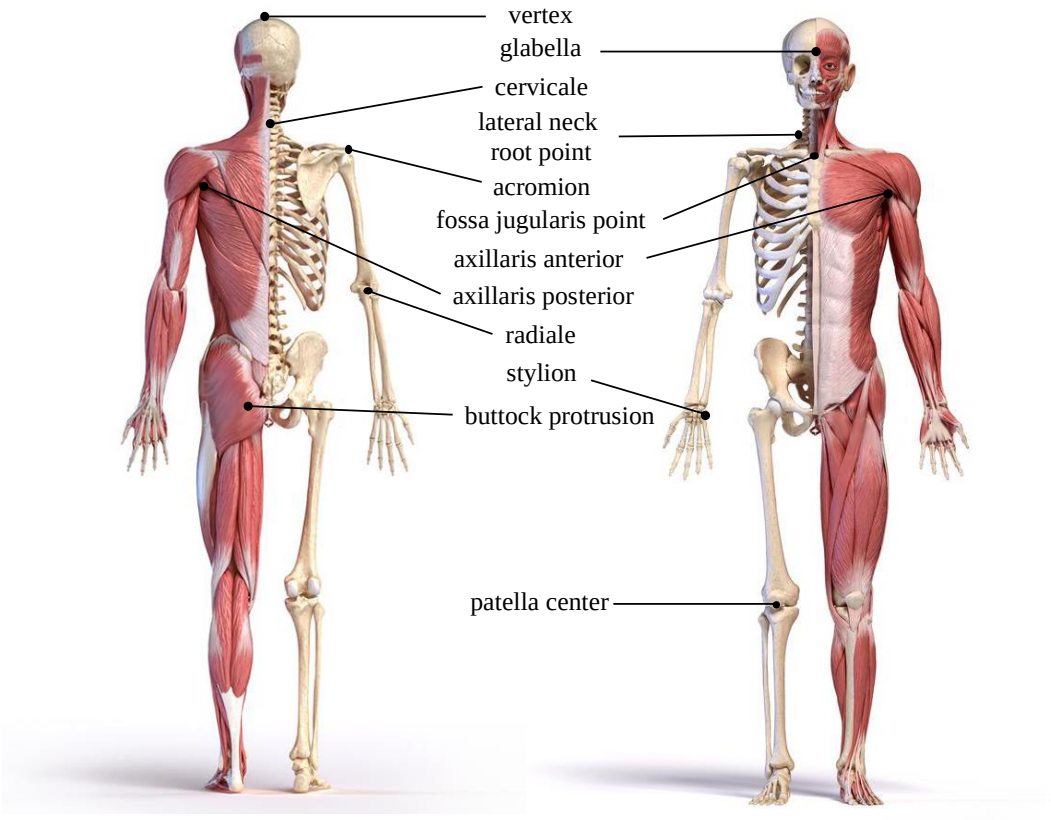

Figure 1-4: Anthropometric points for garment making on the human body.

Table 1-1: Definition of anthropometric points for garment making.

NO.	Body Measurement Point	Definition
1	Vertex	The highest point in the sagittal plane directly above the head.
2	Glabella	The most prominent point on the median sagittal plane between the root of the nose and the eyebrows, when viewed from the side.
3	Cervical	The point of the tip of the seventh cervical spine.
4	Lateral neck root point	At the lateral cervical triangle, the intersection of the anterior border of the trapezius muscle and the curve connecting the cervical fossa to the cervical point on the lateral part of the neck.
5	Acromion	The most lateral point of the outer edge of the scapula, usually equal to the shoulder height.
6	Fossa jugularis point	The intersection of the line connecting the superior border of the right and left lateral clavicular terminal with the median sagittal plane.
7	Axillary anterior	The point superior to the anterior axillary fissure.
8	Axillary posterior	The point at the upper end of the posterior axillary fissure.
9	Radiale	The most superior point of the upper border of the radius.
10	Stylion	The most inferior point of the stemmed prominence of the radius.
11	Buttock protrusion	The most prominent point at the posterior of the hip.
12	Patella center	Mid-point of the line joining the superior and inferior edges of the patella.

1.1.2 Anthropometric measuring methods

Anthropometry makes it possible to digitize the human body features. Only through anthropometry can specific data on the relevant parts of the human body so that there is a reliable reference for the dimensions of the relevant parts in the garment pattern design, thus ensuring the fit, comfort, and beauty of the garment. In general, anthropometry refers to the measurement of the external conditions of the human body. It can be divided into static and dynamic measurements [13]. Static measurement studies the static body shape, vertical and horizontal dimensions of the human body. Dynamic measurement studies human movement, changes in muscle and skin stretch, joint movement, and direction of movement. In particular, static anthropometry is the technique most closely related to garment pattern-making and most widely used [14]. With the development of science and technology, anthropometric techniques and methods have also changed. Its development has gone through three stages. From the traditional Martin measurements (obtaining the length and girth of the body), moving gradually to two-dimensional photogrammetry of the human silhouette, to the three-dimensional measurements of the human body shape now in use [15]. The characteristics of the acquired measurements are different depending on the tools used in the measurement process. The most commonly used measurement in anthropometry is one-dimensional data, such as height and chest girth. A capture of morphology can

be achieved by two or three-dimensional measurement methods. The following is a discussion of the different measurement methods and the application of the results [16].

1.1.2.1 One-dimensional measurement method

From the end of the 19th century, anthropologists used tape and calipers to measure the human body. Until now, designers still use this method to measure the human body. These methods are time-consuming, require manual recording of results, and are highly dependent on people. Martin measurement is a method proposed by anthropologist Rudolph Martin in his textbook 'Lehrbuch der Anthropologie' published in 1928, which has been widely used globally. The measurement items include height (vertical projection length), left and right width (horizontal projection length), front and back thickness (horizontal projection length), angle, perimeter (real horizontal length), and real length [16]. The main instruments used in one-dimensional anthropometry are described as follow (Figure 1-5) [6]:

- anthropometer (Figure 1-5.a)
- large sliding calipers (Figure 1-5.b)
- small sliding calipers (Figure 1-5.c)
- spreading calipers (Figure 1-5.d)
- measure tape (Figure 1-5.e)

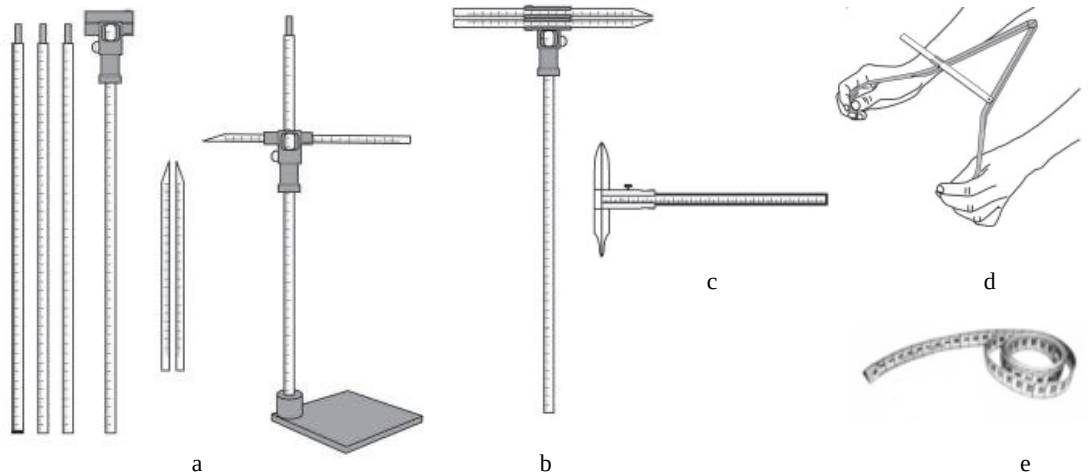

Figure 1-5: Martin measurement instruments.

1.1.2.2 Two-dimensional measurement method

In order to obtain the human body image related to design and the necessary information related to the garment pattern theory, it is also necessary to obtain the human body surface angle and cross-section morphology from the two-dimensional human body contour, except to obtain the one-dimensional length data directly from the human body. Two-dimensional measurement methods include contact measurement and non-contact measurement. The contact measurement includes taking the body surface angle directly from the human body with the angle measuring instrument and obtaining the vertical or horizontal cross-section shape with the profiler and other equipment. By overlaying these cross-sections, three-dimensional data information can be obtained. Noncontact measurement includes photogrammetry etc., which quantifies the position of each part by projection length and angle [16], as shown in Figure 1-6.

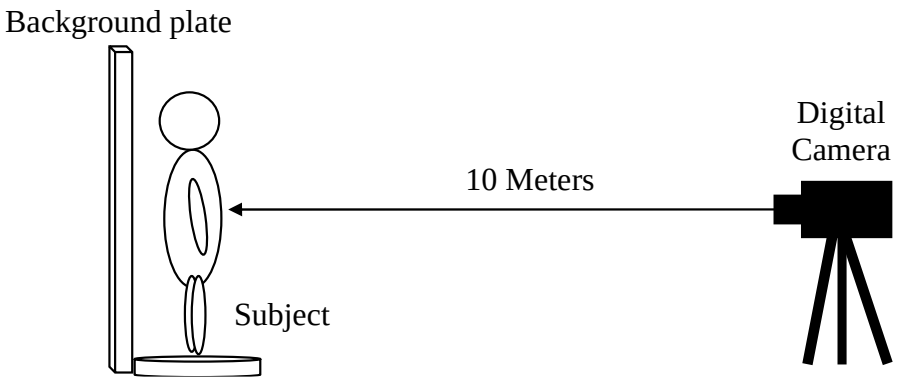

Figure 1-6: 2D Photogrammetry instruments.

Photogrammetry is a non-contact measurement method that uses optical technology to take digital photographs of the human body under test, and indirect measurements are made based on the photographs. The method is fast and inexpensive to measure but does not directly obtain three-dimensional information about the human body. Manual measurements and statistical analysis need be used to support this approach [17]. The main body shape data obtained by photogrammetry, including length, thickness, width, angle, and other data, can estimate the contour shape of the front and side of the body shape, providing valuable references for the design of human body model, body shape

classification, clothing size modification and clothing structure design [18]. Lin Yueh-Ling et al. proposed a systematic approach to automatically find human contour feature points from frontal and side images of the human body. The chain-code based algorithm automatically extracts 55 feature points and 26 body dimensions [19]. Meunier et al. used two cameras to simultaneously take images of the front and side of the human body and build mathematical model calculations and found no significant difference from the manual measurement data [20]. Patrick et al. proposed a method of measuring human dimensions through two-dimensional pictures of the human body. The results of variance analysis were compared with those of the manual measurements, and it was concluded that there was no significant difference between the two [21]. Marianne et al. performed human-size measurements on five athletes using a manual measurement method and a 2-dimensional non-contact photographic method, and then calculated human-size based on the Yeadon model approach and found that the mean standard deviation of the absolute accuracy of the two methods was 2. 1% and 2. 87% [22]. Herianto et al. based on the need for more efficient and convenient body size collection for clothing e-commerce. It is proposed to obtain dimensions from camera pictures, where manual and photogrammetric methods are compared and statistically analyzed, resulting in high accuracy and reliability [23].

1.1.2.3 Three-dimensional measurement method

Three-dimensional anthropometry appeared in the mid-1980s. It is to measure the dimension of each part of the human body model and the body shape of the human body and then to study the human body's morphological characteristics and technical methods. It is used in human database construction, clothing customization, ergonomics, medicine, and museum display [24, 25]. Technical methods include contact measurement, such as the gypsum wrapping method. As well as non-contact measurement methods, such as mole fringe or laser. At present, this method has leaped forward in development. Using this method and computer, we can get the two-

dimensional unfolded drawing of the human body surface from the 3D data of the human body and generate a 2D garment pattern [16].

(1) Contact measurement method

General contact methods are the three-dimensional cutting method and the gypsum-wrapping method. The three-dimensional cutting method is to set the straight and horizontal yarns on the cloth to the horizontal and vertical (X, Y) lines on the flat unfolding diagram, and wrap the human body in a pillar shape with the cloth, with the gaps closed off as a way to make the cloth fit the body and obtain the human form. The gypsum wrapping method is a method of acquiring the human form with a gypsum-applied band, which is effective for acquiring the body in a stationary state and for acquiring the human form in a motor state.

The gypsum model can be used as a resource for observing the body part shape of the human body. Especially the arm root and the groin, which are impossible to observe from the human body itself or a 3D human body model but can be well observed through the gypsum model, which is one of its significant advantages. For example, through the gypsum model, we can find the difference in the shape of arm root of different body types. You can also obtain the body surface flatten graph. The flatten graph can be used as a basis for the design of paper patterns, or it can be used to understand the relationship between the 3D human body model and the 2D flatten graph [12].

(2) Non-contact measurement method

Compared with the contact method, the noncontact method has the advantages of high automation, short time, and high accuracy [26]. Noncontact measurement methods can be divided into two categories, active and passive, depending on the measurement method.

The active method transforms the image into point cloud and then measures the point cloud data by the algorithm. The active method includes the grid method, scanning method, etc.

The grid method includes the Moire method, the layered method, and the phase method, as shown in Figure 1-7. Moire Fringes scanning technology is less accurate than laser scanning, but the acquisition speed is faster than laser, so the data is collected relatively stable. Moreover, the camera captures not only geometric information about the human body but also texture information. But the amount of computation would be enormous to get the full data on the human body surface [27]. Layered method uses a white light source to project a sine curve on the surface of the object. TC2 American textile and garment technology center uses the white light stratified section method to obtain three-dimensional human body data [26]. Phase method is a phase measurement technique based on an optical interferometer, which uses general white light illumination to project the grating onto the human body surface. The phase measurement of the grating image is projected onto the human body surface to obtain the three-dimensional dimensions of the human body, and the three-dimensional coordinates of any point on the body image. Through human-computer interaction, online and offline measurements can be easily made, and the need for single-agent and rapid measurements in the field can be met [28].

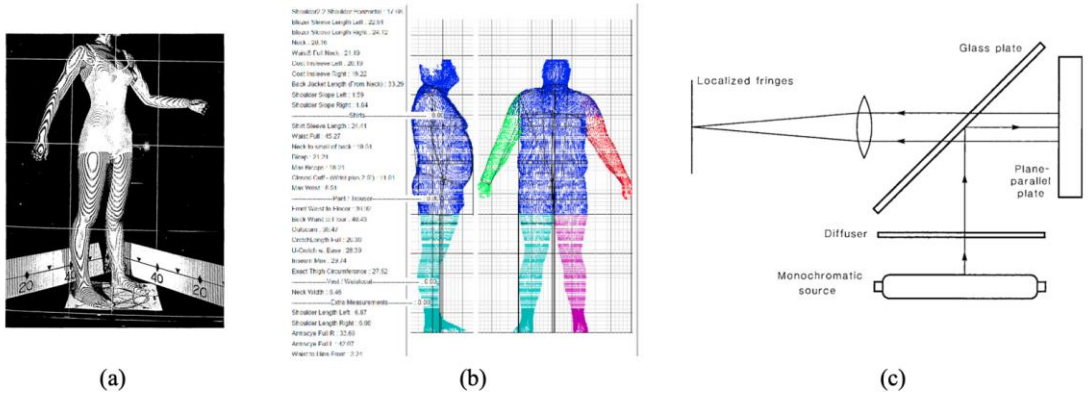

Figure 1-7: Grid methods: (a) Moire method [27]; (b) Layered method [28]; (c) Phase method [29].

Since the 1980s, the rapid development of three-dimensional body scanning technology in the modern clothing industry has been widely used. They can capture information about the human surface without touching the body, using optical technology combined with a 3D scanner, which can produce many measurements on the body in just a few

seconds. The scanner software system combines two-dimensional models of different scanning units to form a smooth and complete three-dimensional human body model. Based on this three-dimensional model, it is possible to describe the three-dimensional characteristics of the human body and build the corresponding digital model. Digital mannequins can be automatically integrated into commercial apparel CAD systems, such as Lectra in France and Gerber in the US. Among the many possible applications for 3D body scanning, the most important is the use of point cloud data to generate virtual or physical garment models and the use of key signage and anthropometric data to guide the design and sizing of garments.

Laser scanning uses multiple laser rangefinders to receive the reflected light of the laser on the human body surface in different directions, based on the position of the light, time interval, the angle of the optical axis to calculate a number of coordinate values of the same height of the human body, so as to obtain all the data of the human surface. Cyberware in the UK is the one that uses laser scanning 3D measurement technology to obtain 3D images, as shown in Figure 1-8(a). The entire scanning and movement process is controlled through the software of the workstation. It takes only a few seconds to complete a single scan. Users can view the results of the scans using the image tools on the workstation and combine multiple scans to form a complete model. Laser scanning systems are relatively expensive, and lasers are harmful to the human eye and must be scanned with closed eyes, with the advantage of high accuracy [30].

The infrared scanning method avoids the fear of laser, directly obtains the net body size, and eliminates the dress's influence. CCD camera first takes the human body's physical characteristics and human dress profile, as shown in Figure 1-8(b). The control module arm automatically moves intermittently from top to bottom, and the sensing head moves back and forth on the cross arm to scan the whole body. The computer first processes the contour size of the CCD to obtain the dimensional frame model, then processes the thermal image data from the sensor head to correct the human body data frame model to complete the anthropometry [31].

In recent years, with the advent of the Kinect sensor device (seen in Figure 1-8(c), the method of obtaining real-world depth images in millimeters by optical triangulation to complete 3D reconstruction and then measure them has become mainstream [32], as shown in Figure 1-8(c). Jun-Ming Lu et al. divided the 3D images into 2D contours and analyzed them, using minimal dimensional detection, grayscale detection, and human contour lines to obtain marker points and marker lines to measure the human body but the measurement sample range was small [33]. Jing Tong et al. used three Kinect devices, two to scan the upper and lower parts of the human body and one to capture the middle torso part of the human body from the relative direction and then splice the alignment. However, unsuccessful alignment occurs due to the poor quality of the depth data [34]. Yi Chen et al. used two Kinect devices to obtain point cloud images from the front and front posterior of the subjects, respectively. After measurement, the time required for measurement was short, avoiding the error caused by subject movement. However, the data accuracy was low [35]. Alexander Weiss et al. implemented a home-based 3D human reconstruction system based on a single Kinect [36].

(a) (b) (c)

Figure 1-8: Scanning method instruments: (a) laser scanning [37]; (b) infrared scanning [38]; (c) Kinect sensor [39].

The passive methods refer to photographic imaging to take direct images of the human body for measurement. The main methods are monocular, binocular, multiocular, etc [40]. The monocular vision method uses a single camera that treats the subject for body image acquisition. Its simple construction makes it easy to calibrate the camera. The method includes both the focus method and the out-of-focus method [41].

The binocular vision method (seen in Figure 1-9(a)), also commonly referred to as

stereoscopic photogrammetry, acquires frontal and lateral images of the human body by simultaneous image acquisition with two cameras with orthogonal lines of sight. Then a series of image processing methods are used to analyze the correspondence of the same feature point in two images. However, the measurement accuracy is not high, and matching the front and side image feature points is always a technical difficulty. The better-known 3D camera method results from research at the University of Loughborough in the UK [42].

The multi-vision method (seen in Figure 1-9(b)) reduces the difficulty of matching between images by increasing the shooting equipment. For example, Gu et al. constructed a double-sided positive hexagonal shooting environment using 12 cameras to simultaneously capture 12 upper and lower body images at different angles [43]. However, due to its large number of construction equipment, complex structure, strict equipment angle placement, and other problems, resulting in large measurement errors, but it also reduces the efficiency of human measurement.

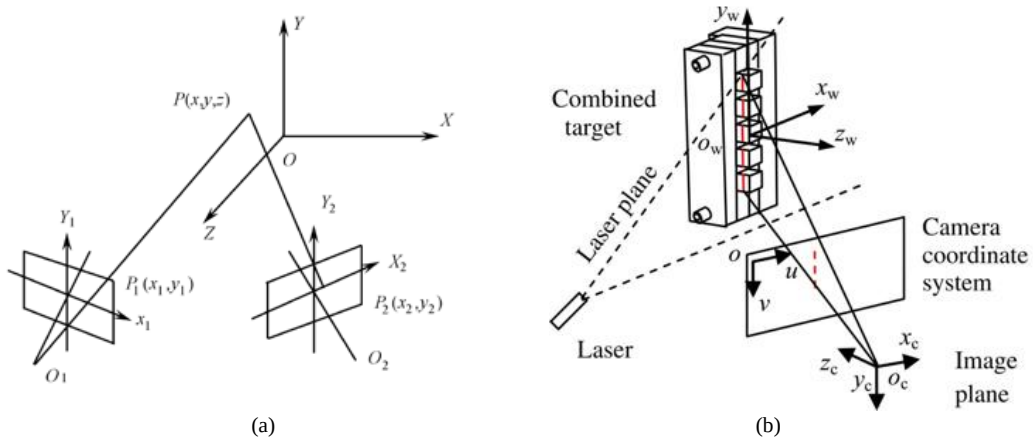

Figure 1-9: Photographic method: (a) binocular vision principle [31]; (b) multi-vision principle [44].

In anthropometry, the required amount of data on the human body is obtained through automated measurement techniques. Human characteristics are analyzed using statistical or data mining methods [43, 45]. In the garment industry, companies use automated measurement technology to obtain user dimension data to customize garments [46–48]. However, the automated measurement technology is not yet perfect.

For example, it is impossible to obtain accurate dimension data on the user's hidden areas (due to self-occlusion) in their natural standing position. In order to obtain complete and accurate data, manual measurements must be combined to use. How to perfectly combine manual measurement and automatic measurement, and map the manual measurement data based on skeletal features and designer's knowledge onto the 3D rigid human body model so that the 3D human body models applied to the apparel industry can be more interpreted and more accurately reflect real human characteristics is what needs to be focused on in the future.

1.1.3 Human body shape classification

Body shape refers to the physical features and types of the human body. In a multicultural society, body shape can change dramatically depending on their cultural and ethnic background. Researches have shown that body shape is related to geography, age, marital status, nutritional status, etc. Traditional methods of classifying the human body shapes are mainly based on the visual effect of the overall or partial contours of the body, with no clear boundaries between different body shapes. The classification of the human body shape varies from country to country. They give their national criteria based on the physical characteristics of their people. The U.S. ASTM standard uses age, weight, height, and chest girth as a single independent indicator to classify a woman's body shape, rather than girth differences such as chest waist and chest hip differences, reflecting changes in body shape [49, 50]. Both Japanese and German standards classify body type according to height and then classify the isometric lines on both sides according to the standard hip girth. The difference is that the standards for height classification are different [51]. The Chinese standard classifies the human body shape into four types: Y, A, B, and C, according to the difference between the human chest and waist girth. While these classifications intuitively reflect the body shape, they do not accurately define it. Therefore, the above standards do not fully address the need for clothing design conformity.

In garment design and mass customization, body shape analysis is particularly important to meet the individual needs of the target population. The refinement of the body shape classification has helped to improve the coverage and applicability of products. Lenda Jo Connell et al. have studied the human body using shape analysis theory. They argue that people wearing the same size clothing may have different body shapes. Moreover, people of different body shapes wearing the same clothes may reflect different dressing effects [52]. Therefore, accurate body shape analysis is an important basis for meeting consumer demand for apparel conformation. Elizabeth Newcomb et al. studied the body shape and physical characteristics of young Mexican American women aged 18 to 25 years for apparel sales fitness research [53]. Marklin et al. conducted body measurements on U.S. power workers. The results informed the design of power workers' apparel, tools, vehicles, etc., reducing the risk of worker injury and optimizing product performance [54]. The study of body shape can guide the production and sale of clothing, building a bridge between the producer and the consumer, with standards to be followed in both the production process as a producer and the purchase process as an end consumer. However, many garment companies only produce less than five body types [54]. This does not meet the needs of the average consumer for clothing fit and variety.

In practice, different bodies have different morphological characteristics. Existing classification criteria tend to be rather coarse and do not fit well with real requirements. Researchers have studied the human body shape classification from different angles and at different levels. The human body shape classification results are often not the same due to the different parameters selected for body type characteristics. Therefore, most of the research on the selection of human body type classification aims to find the optimal parameters that can characterize human body shape characteristics [55]. These optimal parameters are called critical dimensions. In 1941, O'Brien and Shelton first proposed an anthropometric study of clothing design using critical dimensions [56]. Existing human body shape classifications are mainly implemented using classical

statistical methods such as factor analysis, principal component analysis, and regression analysis [52–56], and classical data mining techniques such as neural networks [57, 58]. This paper categorizes the body shape classification method into two main categories: overall and partial contours.

1.1.3.1 Overall human body shape classification

There have been many researches classify the human body as a whole through different body indicators, such as circumference, angle, section, etc.

(1) Circumference

Karla Simmons et al. classify body shape into nine types based on body girth (bust, waist, hip, upper and abdominal girth) dimensions, including hourglass, oval, triangle, inverted triangle, rectangle, diamond, spoon, positive hourglass, and inverted hourglass. A comparative analysis gives the characteristics of each body shape and assigns a numerical range to each body shape [64]. Meng-Jung Chung et al. used two-order clustering analysis to classify primary and secondary school students aged 6-18 years into nine levels based on age, gender, and clothing size [65]. Adriana Petrova et al. studied 24 participants aged 35-55 years. They classified the study subjects into three body shapes, namely lean body, average body, and obese body, based on their waist-hip difference and the waist-hip ratio [66]. Deepti Gupta divided human body shape into five body types by body shape statistical analysis tools, including obese, moderately obese, mildly obese, normal, and strong [67]. Vuruskan A et al. used subjective visual analysis to achieve body type classification and used basic human body dimensions such as the chest, waist, and hip circumference as assessment parameters to classify human body shape into five types: hourglass, inverted hourglass, scoop, triangle, and oval [68]. Renata Hrženjak et al. used factor analysis and clustering analysis to classify the body types of Croatian girls between 13 and 20 years old according to their height, chest, waist, and hip girth to obtain three body shapes [69].

(2) Angle

Woo Kyung Lee et al. extracted basic feature points by defining and measuring representative body size and proposed a body shape classification method based on angular features [70]. Yong Lim Choi et al. grouped the lateral body shape of the human body into four levels based on the lateral body angle of the human surface, improving the accuracy of body shape classification [61]. Sun Jie used the US TC2 3D anthropometric system to measure the dimensions of young women and used K-mean clustering analysis to classify women's body shapes into four levels based on the body surface angles that characterize body shape (shoulder angle, thoracic angle, hip angle, and lateral angle) [71].

(3) Profile/Section

Ni et al. extracted longitudinal contour curves, including sagittal and coronal contour curves, established a classifying method for the body shape of young women by the radius of curvature of the contour curve feature points [72]. Wang et al. believe that it is inaccurate to distinguish body shape by the cross-sectional sagittal ratio. Therefore, the girth and area of the horizontal cross-section of the human body were obtained by self-programming. The cross-sectional area of the chest, waist, and hip girth to the square of the circumference was selected for clustering analysis. The body type was subdivided into three levels: flat, intermediate, and round [73]. Yao et al. established a method based on the longitudinal cross-sectional curve morphological index to subdivide the torso body shape of young women to describe the differences in body shape characteristics of various body shapes in the anterior and posterior center lines, back, chest, hips, shoulders and side slits; finally, they constructed four types of body shape corresponding to the prototype paper samples and analyzed the relationship between the paper samples and human body shape, which can provide a reference for the design of conformation of the prototype paper samples of young women [74].

1.1.3.2 Human body part shape classification

Besides classified the human body as an overall, some scholars have also classified the

body part shape according to its features. The shoulders, neck, chest, and hip have been the focus of research.

(1) Chest/Breast

Lee Hyun Young et al. used reverse engineering software to study the morphology of the mammary floor contour lines of the female breast, performed morphological analysis, and extracted the curvature of the mammary floor contour line feature points for classification [75]. Chang Lixia et al. subdivided breast morphology into nine categories by extracting characteristic indicators that affect the breasts of young women [76].

(2) Hip

Through principal component analysis, Song et al. selected waist contour, hip contour, hip convexity, and abdominal convexity as feature indicators and classified the waist and hip morphology of 18 to 35-year-old women in the Size USA series into three levels: curves, slashes, and straight lines. The automatic customization of trouser samples and the method of conformity determination were further investigated [77, 78]. Alexander et al. studied the effect of hip morphology and dimension changes on clothing sales in obese women in the U.S. national size line [79]. Wang Jun studied the waist-hip body features and categories of specific populations to analyze the factors influencing the structural design confirmation of pants. The waist and buttocks of young women in the Northeast region are divided into three levels: the first type is straight, flat buttocks, short and thin; the second type is convex buttocks, round body; and the third type is the curved, high and flat body [80].

(3) Torso

Chin-Man Chen et al. quantified the upper body features of female college students by using angular measurements of body surface angles at the positions of shoulder obliquity, thoracic convexity, dorsal curvature, and shoulder peak using a 3D scanner and two software systems [25]. Peng Li uses discrete cosine transform (DCT) to analyze

the female torso morphology obtained from 3D scan data, compresses the dense 3D point cloud surface into small format vector data to preserve the shape, and then uses principal component analysis to decompose the shape changes into component morphological components, which can provide a basis for the description and classification of 3D torso morphology [81]. Mi Kyung Yoon proposes a method for defining and classifying the lateral body shape of the upper body based on the directional angle of the three-dimensional space vector. This method of three-dimensional analysis improves the accuracy of body type classification compared to existing two-dimensional analysis methods [82].

(4) Neck

Shanshan Wang extracted the relevant data of the human neck through three-dimensional anthropometry and analyzed the cross-sectional shape of the neck, neck circumference shape, neck height shape, neck curvature shape, and three-dimensional shape of the neck, respectively, to provide a theoretical reference for the design of male clothing collar [83].

(5) Shoulder

Zhang Jinhua et al. subdivided the shoulder morphology of young women using three-dimensional measurements [84]. Jin Juanfeng established a method to subdivide the shoulder body shape based on the feature point radius of curvature to sagittal diameter ratio and further characterized the curve variation characteristics of four types of shoulder cross-sections by comparing the curve morphology the shoulder point cross-section [85].

The scholars mentioned above have studied human body shape classification from the body part shape, body surface angle, body surface contour information, frontal and lateral contour information, age stage, and other aspects, which has some significance. For the apparel industry, through the corresponding methods to use the human body data and use this as a criterion to classify, we can not only understand the human body shape, understand the average value and data distribution state of human body data used

in pattern design, and obtain different types of paper pattern design data, but also can apply the classification results to the construction of 3D human body parametric model for clothing so that the apparel industry to information and intelligent direction forward. However, the existing whole classification method lacks the response to the body part features of the human body. In contrast, the body part classification method only considers the feature of one body part. It does not consider the impact of other body parts on the body shape. In addition, less research has been done on the hidden parts of the person, such as the shape of the arm root. Moreover, the shape of the cuffs (corresponding to arm root shape) is closely related to the structural design of the garment, which to some extent affects the fit and comfort of the garment. It is not to be ignored and is worth researching.

1.2 Research on 3D human body modelling

Personalized 3D modelling is being used in depth and widely in the apparel industry. 3D models of the human body come in various manifestations, such as surface models, solid models, and physical models, each with its advantages and disadvantages. The human body surface is complex. A suitable method should be chosen to obtain a three-dimensional human body model according to different needs.

The human body modeling method focuses on how to construct realistic virtual human body models in a computer [86]. Initially, modeling with simplified lines could only be done for models with relatively simple geometry. The full development of 3D modeling techniques has also made possible the inclusion of object-oriented models such as skeletons, skin and joints, and faces [87]. At present, in terms of acquiring 3D human models, 3D human modelling mainly consists of the scanning model method, the creation model method, and the reconstruction model method [88]. Each of these methods has its advantages and disadvantages, and how to quickly and accurately obtain mannequins in different shapes remains the focus of many scholars' research.

1.2.1 Scanned model method

Human models obtained using scanners can accurately reflect the surface features of the human body. As a result, more and more researchers are using scanners to scan different groups of people to obtain dimensional information about different shapes of the human body [89]. The use of body scanners to obtain 3D human body models has high accuracy, but it also has obvious disadvantages. Firstly, full-body scanners are expensive and take up much space, so only larger research institutions or clothing shops will introduce these 3D scanners. Secondly, using the scanner to obtain a body model requires the user to travel to a specific location for scanning, which is not widely available to most people who need to create their own personalized 3D body model. Even when conditions allow, scanning the user is very complex. The user has to wear a specific straitjacket to ensure that the scanned model is as accurate as possible to the human body shape. At the same time, the user must remain in a static position during the scan. Otherwise, the model may show double shadows, noise, etc. The human model obtained with a 3D scanner is usually a static 3D image that designers cannot edit (seen in Figure 1-10), so its application is limited. Therefore, the method of acquiring 3D human models with the help of 3D scanning equipment is not suitable for a large number of general users in the Internet environment [35, 90, 91].

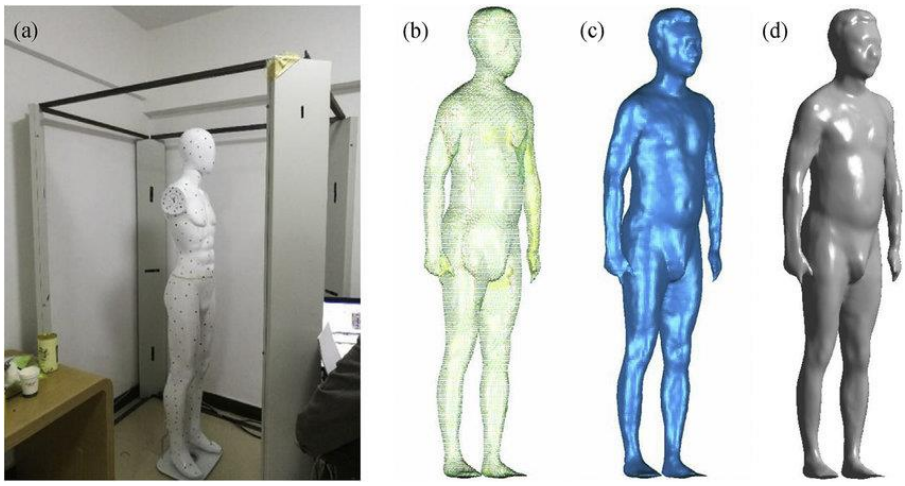

Figure 1-10: (a) 3D body scanning system and 3D body model of (b) point cloud, (c) triangulated irregular network mesh, (d) curved surface [92].

1.2.1 Model creation method

Creating human models includes wireframe modelling, solid modelling, surface modelling and physical modelling methods.

(1) Wireframe modelling

This modeling is a very early method used to represent the human body and was first applied in CAD/CAM in computer graphics [93]. Its advantages are low data volume and simple definition, so editing and modifying operations are fast and suitable for traditional proofing. The disadvantage of wireframe modeling is that there is little data to accurately characterize the human body, leading to ambiguity and ambiguity. It does not accurately display the non-duality characteristics of the three-dimensional human body. To compensate for the shortcomings of wireframe modeling. A new combination of line segments, circles, arcs, text, and B-spline is designed as a conceptual element. It is no longer a pointless graphic element to represent a three-dimensional human body model, such as intermittent dots, lines, and surfaces. The designer can accurately display the three-dimensional human body, which contains many body elements and sections. However, the interaction between the elements and the cross-section is large and prone to singularity, and the accuracy of the equipment can also lead to measurement errors. The complex relationship between the elements is prone to disturbance. So this method cannot be widely applied in practice [94].

(2) Solid modeling

Compared to wireframe modeling, this modeling proposed in the early 1960s can express more complete information, and the resulting mannequins will not be dichotomous [95]. Solid modeling enables local control of the mannequin with a better sense of reality and automatic fading of the human body. However, solid modeling is slow, inefficient, and time-consuming because it constructs all the external and internal

data to the human body, which is huge. The entity modeling approach is classified and elaborated in detail by Yong Li et al. [96]. At present, the main representations of the human entity modeling system include somatotropic decomposition, tectonic entity geometry, boundary representation, and polyhedral modeling.

(3) Surface modeling

This modeling is one of the most widely used methods of 3D human body modeling [97, 98]. Surface modeling is better than wireframe modeling in describing the geometric topological relationships of the human body. Because curve modeling has 3D information, it can realistically display realistic 3D effects and automatic fading, and its realism is better expressed. However, surface modeling lacks representation of human entities, so this method cannot be profiled. Modeling methods include triangular surface slice approximation and parameterized surface modeling.

(4) Physical modelling

The physical modelling method not only models the surface of the human body but also introduces the physical properties of the body itself and the external environment to which it is subjected. With more information being introduced, the physical modelling method can achieve more realistic modelling results. It can effectively characterize the human dynamic features. Researchers often use the numerical solution of a system of differential equations to calculate dynamic systems and express the human body's dynamic motion. Therefore, the physical modelling method is much more complex in terms of computation. However, the method can compensate for the lack of traditional human modelling methods and has been developed rapidly since it was proposed [99, 100].

1.2.2 Model reconstruction method

To minimize costs and environmental impacts, an increasing number of scholars are preferring to use the reconstruction model over creating the 3D human body models that match individual human body features. Various methods for reconstructing human

models are based on the open literature: image-based model reconstruction, template model-based scaling, and anthropometry-based model reconstruction [101, 102].

(1) Image-based human modelling

Image-based human modelling is a reconstruction method [103–105], which uses digital devices by taking 2D images of the front, back, and side of the human body to reconstruct 3D models. They extract shape information, such as body contours or anthropometric data, which can be used as a basis for their reconstruction work. It is convenient to obtain human model data using this method. However, the photographing environment should be strictly controlled, and the quality of photographs and image pre-processing are required. Moreover, the personalized information of the user may be leaked while uploading images.

(2) Template model-based scaling

Template model-based scaling is another reconstruction method [106–109], which enables to generate human models by transforming an individual template model. However, the results are less realistic and cannot accurately reflect the surface features of the human body. In these models, correlations between body parts are not considered, resulting in a significant loss of human body features.

(3) Anthropometry-based human modelling

The anthropometry-based model reconstruction method has higher accuracy and is time efficient than the above-mentioned methods. Seo et al. [110, 111] proposed a personalized human modelling method based on anthropometric parameters. Multiple human skin surface models obtained from a 3D scanner were interpolated based on the input values of eight anthropometric parameters to generate personalized human skin surface models. To further improve the realistic model, Koo et al. [112] used a manually labelled human model to measure its 13 anthropometric dimensions and personalized the human model by establishing a mapping between these dimensions and the human body shape. Based on the anthropometric definition, Zhang et al. [113] extracted 30 human dimensions from the example model, obtained statistical relationships between

the human dimensions, implemented the recovery of all 30 human dimensions from multiple input human dimensions, and obtained a radial basis function (RBF) model for the mapping between dimensions and human surface vertices, thus recovering human surface data from dimensional data. Zeng et al. [114] designed a 3D human body re-modelling system. They proposed a novel feature selection-based local mapping technique to achieve automatic anthropometric parametric modelling of all human body surfaces. The proposed method could take a limited number of anthropometric parameters (i.e. 3-5 measurements) as input, avoiding complex measurements, and thus allowing for a better user experience in real-world scenarios.

Although the above researches achieved impressive results in static scenes, they only targeted objects that contained only rigid body changes. However, the three-dimensional modeling of the human body is different from the modeling of static objects. As the existing models are rigid, they cannot consider factors such as skeletal structure, body composition (bone, fat, and muscle), and body deformation associated with skin elasticity and movement [115–117]. For example, the most serious problem in 3D anthropometry is the lack of landmarks. Many landmarks on the bones, which are usually manually identified by designers, cannot be accurately determined from the 3D human model surface shape. Although 3D anthropometry yields quick results, the results obtained are inaccurate and uninterpretable because they cannot correctly identify body features [118, 119]. The results are even worse when non-standard body shapes (e.g., hunchbacks and pot bellies) are measured [120]. Additionally, most designers are currently unable to measure the human body accurately. They cannot respond quickly and effectively when using 3D human body models that lack human body information as a reference for measurements or design. Therefore, it is reasonable to propose an efficient and time-saving human body model that contains semantic information (e.g., key position labelling and optimized body parts segmentation) to help designers efficiently and accurately design new garment products.

1.3 Research on garment pattern generation

Garment fit is one of the key elements of garment quality and customer satisfaction, which determines whether the produced garments can be chosen by more people [78]. Due to the increase of consumption levels and changes in the diet of people, the body dimensions of different consumer groups are becoming more and more different, which has led to the fact that the anthropometric data on which ready-to-wear sizing system has been based is obsolete. The garments produced based on this system do not fit current body dimensions [121]. Personalized customization is considered to be an effective way of improving the fit of garments [122–124]. However, with the popularity of personalized customization, garment pattern-making as a key factor to improve the efficiency of garment production [125, 126] needs to become faster and better.

1.3.1 Pattern generation based on traditional pattern-making methods

Traditional manual garment pattern-making methods, even with computer-aided design (CAD) garment pattern-making software help, the pattern designers need to have a great wealth of professional knowledge and proficient skills to make a better-fit garment pattern [127] quickly. Meanwhile, these methods also have the following disadvantages [128, 129]: (1) the learning process is particularly long and difficult to promote, and the making process is time-consuming, limiting the improvement of production efficiency. Although the CAD garment pattern-making software can automatically grade, which improves production efficiency, it is only suitable for the overall grading of the standard dimension specifications. It cannot automatically adjust the changes of individual dimensions. Garments produced based on standard dimension specifications cannot satisfy the requirements of consumers for fit; (2) once the garment style changes, the structure drawing of the garment needs to be manually redrawn or adjusted, which cannot automatically and quickly respond to the adjustment of the garment pattern.

1.3.2 Pattern generation based on artificial neural networks

To solve the above problems, researchers have developed some new techniques for generating garment patterns. The garment pattern generation technique based on an artificial neural network (ANN) simulates the designer's pattern-making process, defining the anthropometric dimensions as the input data of this model and the X, Y coordinates of the garment pattern as the output data of this model [130]. Chan et al. proposed an ANN model to predict the pattern parameters of men's shirts [131]. Liu et al. developed a backpropagation artificial neural network (BP-ANN) model to predict the lower body dimensions used for pants pattern design [132]. Wang et al. proposed a radial basis function artificial neural networks (RBF-ANN) predictive model to improve the prediction accuracy of body dimensions used for garment pattern-making [133]. The key technique of these methods is to establish the relationship between the human body data and the garment pattern. However, the garment pattern is a combination of curves and straight lines, which is difficult to describe using specific data, resulting in unreasonable output garment patterns. Therefore, it is limited to simple garment patterns and is not widely used.

1.3.3 Pattern flattening based on 3D human or garment models

There are also many researchers who are exploring the method of creating garment patterns directly from 3D human body models, i.e., 3D-to-2D flattening technology [125, 126, 134]. With this 3D-to-2D flattening technology, customized garment patterns can be obtained directly without measuring the human body [135, 136] However, the most serious problem in 3D garment design and anthropometry is the lack of feature point labels. Many labels on the bones, which are usually manually identified by designers, cannot be accurately determined from the 3D human model surface shape. Lacking accurate labelling of body feature points makes it impossible for most

designers who lack the knowledge of anthropometry to respond quickly and effectively when using such 3D human body models to design. In addition, this method does not accurately determine the ease allowance between the body and the garment. Therefore, it is only suitable for designing simple and tight-fitting garments.

1.3.4 Pattern generation based on parametric

Compared with the methods mentioned above, the parametric garment pattern-making technology can better satisfy the requirements of the apparel industry [137]. Parametric garment pattern-making technology uses the dimensions of the human body feature parts related to the garment structure as constraint values (i.e., parameters, such as chest girth, back length, etc.). By defining the geometric and dimensional relationships between the various geometric objects in a garment pattern, a garment pattern can be quickly adjusted by dimension-driven to generate the new garment pattern [138, 139]. In garment pattern-making, both body shape and dimension are significant for garment fit [140]. However, current parametric garment pattern-making technology only considers the differences between dimensions [78, 121]. For this reason, the made garment patterns tend to ignore the individual shape differences, such as the convex chest, hunched back, and slipped shoulders, which reduces the custom garment fit [141]. Although researchers have proposed some methods of garment pattern adjustment to eliminate body part unfit, such as shoulder unfit, there is no systematic adjustment method to improve the overall garment fit [57, 142]. Therefore, it is significant to propose a personalized parametric garment pattern-making method oriented to fit that considers both human body dimension differences and each body part shape differences to help consumers, especially those not in the standard body shape and dimension, achieve the rapid generation of personalized garment patterns.

1.4 Research on garment fitting

The definition of fit varies in the apparel field, depending on fashion culture, industry

norms, and individual perceptions of fit [143–145]. The reasonableness and authenticity of the garment fitting results are directly related to the realization of the style of the garment and the effect of the making process. Therefore, it is particularly important to use appropriate evaluation methods to obtain reasonably effective evaluation results. The evaluation of garment fit provides a reference for consumers to make decisions about shopping. The current research methods for evaluating garment fit can be divided into two categories: objective evaluation methods and subjective evaluation methods, which are summarized below.

1.4.1 Garment fitting subjective evaluation

The subjective evaluation method evaluates whether a person looks and feels fit for himself or others after putting on the clothes. Researchers and practitioners in the apparel industry are faced with a new challenge: how to get Kansei information about what customers are wearing, such as needs, preferences, evaluations, etc. Kansei engineering [146], born in Japan, provides a powerful research tool for exploring and analyzing such issues. Its founder, Mitsuo Nagamachi, defines Kansei engineering as a customer-oriented new product development technique that aims to translate the feelings or imagery consumers have about a product into translation into design elements. Since the 1980s, Kansei engineering has been widely used in the Japanese industry, especially in the automotive, home appliance, and textile industries. In recent years, it has expanded into the Kansei design, Kansei evaluation, and even cross-cultural Kansei research [147, 148]. At the same time, it attracts scholars from different countries and fields, and scholars in the field of textile and apparel have also carried out relevant research.

Na Youngjoo explores the relationship between styling elements such as women's collars, sleeves, skirt silhouettes, and color and the customer's perceptions using the Kansei engineering method [149]. Bensaid S et al. conducted a 15-dimensional tactile analysis of nine different organizational structures of machine fabrics using semantic

analysis. The results showed that the fabric organization parameters have a significant effect on customer tactility [150]. Wang Ying et al. of Suzhou University have concretized each sensual need from three aspects: comfort, safety, and aesthetics, and transformed them into relevant elements of detailed clothing design [151].

1.4.2 Garment fitting objective evaluation

Since garment fit depends on various factors, such as physical comfort, psychological comfort, and appearance, understanding garment fit from the consumer's perspective is very complex. Objective evaluation methods use objective methods such as image processing and mathematical modelling to evaluate garment form through quantitative analysis. Currently, the development of CAD systems has allowed for 3D virtual try-on simulations of garments, as shown in Figure 1-11. In the case of virtual try-on, human body models are obtained by 3D scanning. These human body models represent specific dimensions or shapes of the target group or individual customers. The significance of this technology is to reduce the production of real garment patterns. Moreover, to be more efficient and effective in the product development and quality control process. However, the wearer cannot feel whether a garment fits his form correctly as a real try-on [152]. Different solutions have been proposed to evaluate the fit of garments for virtual try-on to solve this problem.

Figure 1-11: Virtual try-on of garments [153].

For example, garment fit has been evaluated based on the experience and knowledge

of the designer, using measurements such as ease allowance between the 3D garment and the 3 D human body [154, 155], or based on pressure, stress, and fit maps generated by virtual try-on software [134, 156]. However, the evaluation quality can be criticized as it depends heavily on the mathematical model [157]. Liu et al. proposed a Naive Bayes-based model to evaluate the fit of garments [140]. Digital garment pressures acquired at different measurement points are the input to the model, and the output is a prediction of the garment fit (fit or unfit). The learning model uses real garment fit data and digital garment pressures. After the learning process, their model can quickly and automatically predict the fit of garments without the need for any real try-on, as shown in Figure 1-12.

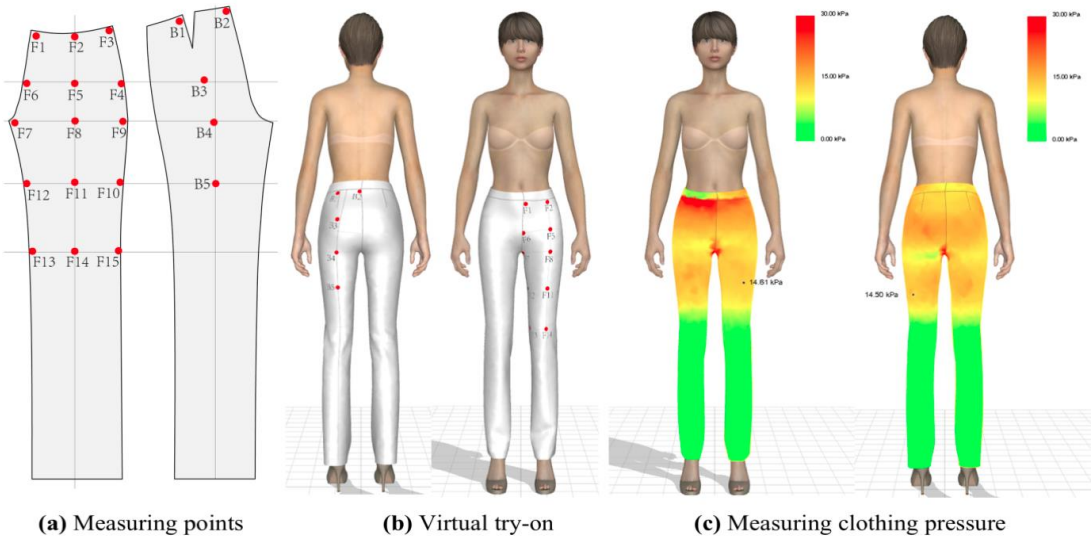

Figure 1-12: Digital clothing pressure measurement by virtual try-on [140].

1.5 General Notions of recommendation system

With the increasing amount of information on the Internet, users cannot get the part of the information that is useful to them. The efficiency of information utilization decreases in the face of the massive amount of information [158]. How to make good use of this information has become a concern for researchers and enterprises. A recommendation system is a decision support system based on massive data (information) mining [159]. By studying user interests and preferences and

personalized computing, the system discovers the user's interests. It thus guides the user to his or her information needs [160]. Currently, recommendation systems have been widely used in books, videos, e-commerce, and finance. This section will analyze existing recommendation systems and their applications in the apparel industry.

1.5.1 Existing recommendation systems

Efficient and accurate recommendation techniques are very important for a system that will provide excellent and valuable recommendations to users. Current recommendation systems generally consist of three important modules: the user modelling module, the recommendation object module, and the recommendation algorithm module (see Figure 1-13). Typical recommendation algorithms include content-based filtering, collaborative filtering, utility-based recommendation, association rule-based recommendation, knowledge-based recommendation, hybrid filtering, etc. [161, 162].

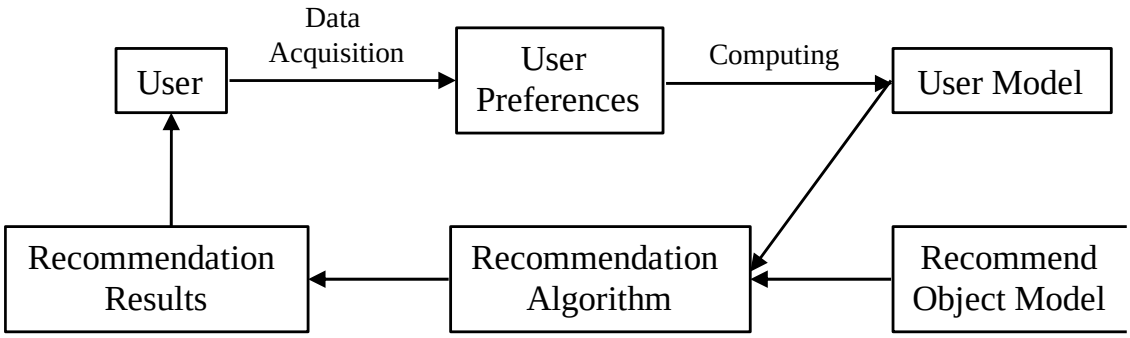

Figure 1-13: A general recommendation system structure.

1.5.2 Existing recommendation systems in apparel industry

In the apparel industry, there is also much focus on the research and development of recommendation systems. Current researches include color, garment pattern, fabric, and style[163]. The Fitme.com website, developed in Silicon Valley, connects Size Genie to clothing sellers through a relational network. When consumers log in to the shopping website to purchase clothes, they can choose different styles and brands according to

their preferences [164]. The Right Size is a recommendation system that focuses on clothing size recommendations, and it also recommends styles to consumers. The system captures consumers' preferences for clothing size, brand, and style, which is used as a reference to recommend the best choice to customers. Consumers are required to answer some questions about their personal preferences when registering. The system will collect these answers and use them as selection parameters to determine consumers' preferences [165]. However, a traditional garment design process is mainly dependent on the experience and knowledge of the designer. As a result, the design process cannot be based on consumer preferences totally. Intelligent garment recommendation systems are based on rules extracted from the expert (designer) knowledge and experience and use computer intelligence methods to recommend suitable garments to specific groups of people. Yang presented a case study of an online clothing recommendation system based on decision tree mining rules and empirical clothing knowledge [166]. P.Y and Mok proposed an interactive genetic algorithm (IGA)-based fashion design system for lay users (general customers) to create their favorite fashion designs in a user-friendly manner. The system effectively generates fashion design sketches that reflect user preferences [167].

Conclusion

There has been much research on the content and methods of garment recommendations by apparel industry practitioners. However, in the practical garment design process, many young designers do not necessarily know what products are suitable for the target consumers. High-level designers have accumulated a wealth of experience and knowledge in different areas of the apparel industry, particularly in personalized garment design. This experience and knowledge should not be lost but should be integrated and applied in future virtual garment design. Moreover, to provide advice to young designers through an adapted model or system. Personalized recommendations based on multiple experts' (designer) knowledge will enhance the consumer's

experience of the garment customization process.

Therefore, the purpose of this study is to propose a recommendation system for personalized patterns for users by using a parametric garment pattern-making hybrid model integrating the designer's pattern-making knowledge and anthropometric knowledge and 3D-to-2D flattening technology. The experience and knowledge of the designer will be formalized and digitized and saved in databases to improve the quality and efficiency of the garment pattern-making. The recommendation system can be used even the user does not have knowledge of garment pattern-making. Personalized garment pattern-making solutions based on specific measurements and preferences will be delivered quickly. Suppose the user is not satisfied with the results. In this case, feedback can be provided to adjust the garment pattern until it fits the body perfectly.

CHAPTER 2: Tools used in the Research

Introduction

This chapter will first present the concept of knowledge-base. Then, the methods for acquiring human body measurements data, both from manual measurements based on expert knowledge and 3D human data from 3D scanners are described. With this aim, we design some experiments. Thirdly, we present various virtual reality-based CAD software for fashion knowledge visualization and product design. Finally, we also present the different theories used in the analysis of human body data in order to set up models in the following chapters.

This chapter answers the complex question of recommending a personalized garment pattern oriented to fit, without any contact, for customers who do not have any expertise in garment-related knowledge, and virtual try-on on the Internet.

The first contribution in this area has been to establish a body shape identification process for new customers (Figure 2-1). For this purpose, by using experts' professional knowledge, we manually realize accurate human body data measurements as well as their interpretation and classification, and extract more relevant human body features. In this approach, after a deep analysis, measured data irrelevant to human body shape have been excluded by designers. And Database I is composed of all body classification data (key body positions, segmented body parts, relevant body measures), manually measured by the involved designers. Furthermore, the relation between body shapes and previously identified body features have been modelled (Model I).

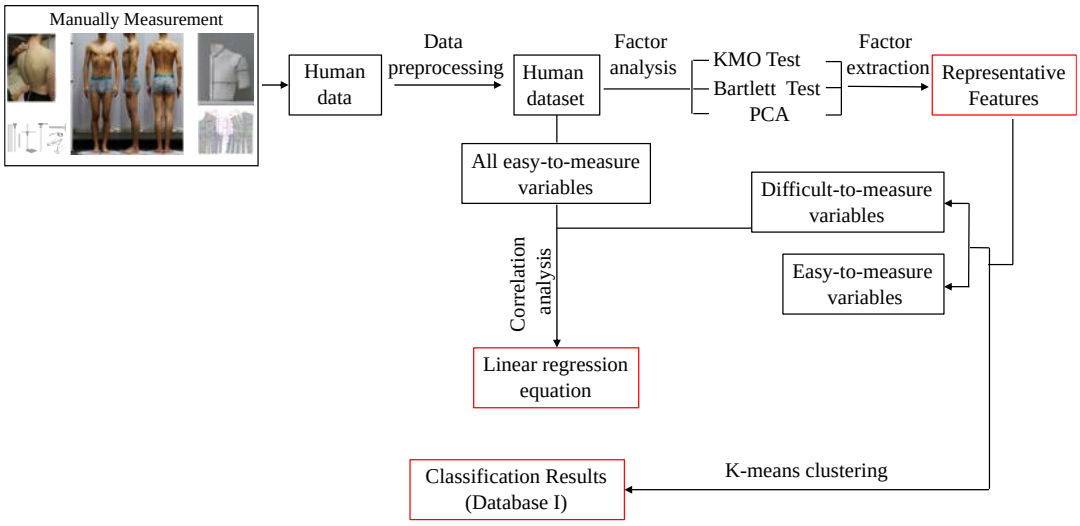

Figure 2-1: Body part shape identification process (Model I).

The second contribution is modelling a new parametric 3D human body for new customers by using key position labelling and body parts segmentation (Figure 2-2). From the above relational model, key positions are labeled on the corresponding 3D body model obtained from 3D body scanning and segment the whole 3D body model into semantically interpretable body parts. In this way, Database II has been created, enabling to identify features of all segmented body parts, whose combination corresponds to the whole upper body shape. Database II includes all 3D body models for various body shapes, labelled and segmented according to the results of Database I. The adjusted 3D human body model contains important human semantic information on labelled key body position points and features on each body part. For a specific consumer, his/her personalized 3D body model can be obtained by taking a very few numbers of body measures on himself/herself, selecting the closest body parts from Database II, making an appropriate combination of the selected body parts, and adjusting parameters of all involved body parts.

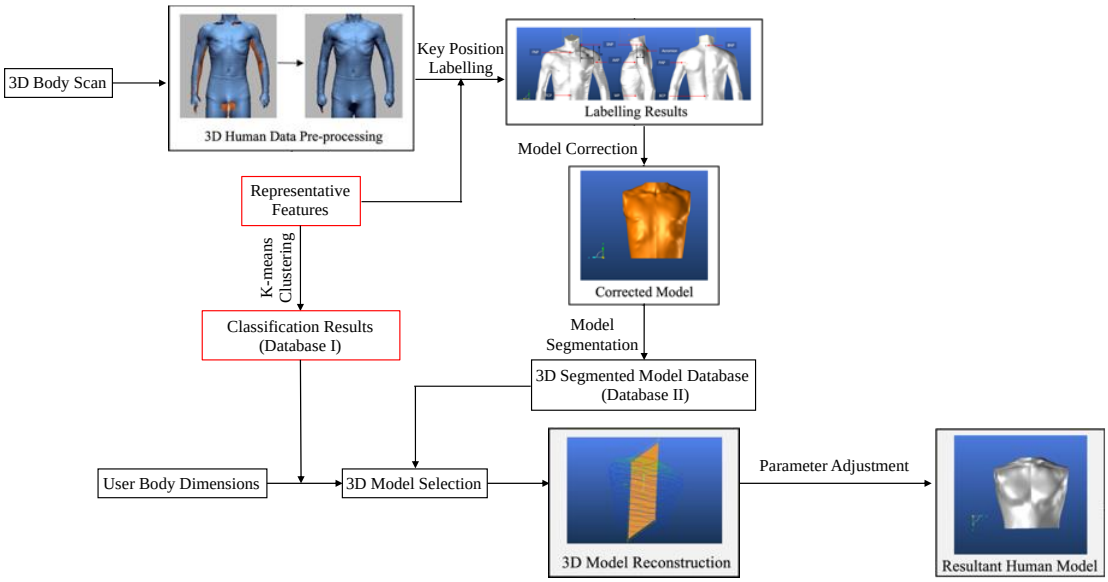

Figure 2-2: Parametric 3D human body modelling process (Model II).

The third contribution is modelling a personalized parametric garment pattern model oriented to fit by integrating designer's knowledge and the above parametric 3D human body model (Figure 2-3). The 3D personalized basic pattern is drawn on the corrected model based on the above key feature points. By using three-dimensional to two-dimensional (3D-to-2D) flattening technology, a 2D flatten graph of the 3D personalized basic pattern of the interpretable parametric model is obtained and slightly adjusted to the form suitable for industrial production, i.e., PBP (Personalized Basic Pattern), and the PBP database (Database III) is built. In addition, the three models include a basic pattern parametric model (Model III) (characterizing the relations between the basic pattern and its key influencing human dimensions (chest girth and back length)), a regression model (Model IV) which enables to infer from basic pattern to PBP for three body parts based on the one-to-one correspondence of key points between the PBPs and the basic patterns, and a personalized shirt pattern parametric model (Model V) (characterizing the structural relations between the personalized shirt pattern (PBP_{shirt}) and PBP).

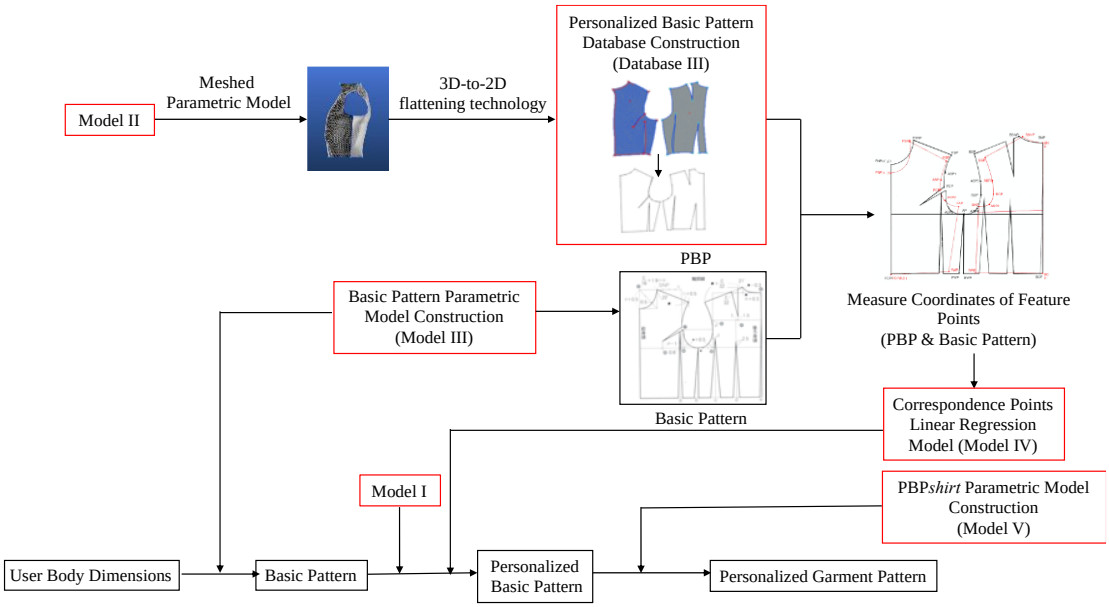

Figure 2-3: Personalized parametric garment pattern modelling process.

Finally, an intelligent recommendation system for personalized parametric garment patterns by integrating the above contributions (Figure 2-4). The initial input items of the recommendation system are the body dimension constraint parameters, including chest girth, back length, and the body feature dimensions used to determine each body part shape as well as three shirt style constraint parameters (slim, regular, and loose). By using Model III, the corresponding basic pattern can be generated through the user's chest girth and back length. Body feature dimensions determine the three body parts shapes. Then, Model IV is used to generate the PBP for the corresponding body parts shape. Based on the shirt style chosen by the user, Model V is used to generate the PBP$_{shirt}$ from the PBP. By using virtual try-on technology, the garment pattern is assembled onto the corrected 3D human body model. Finally, the user evaluates the virtual garment. The garment is produced if the result is satisfactory; otherwise, the pattern is adjusted by using adjustable parameters until it satisfies the requirements.

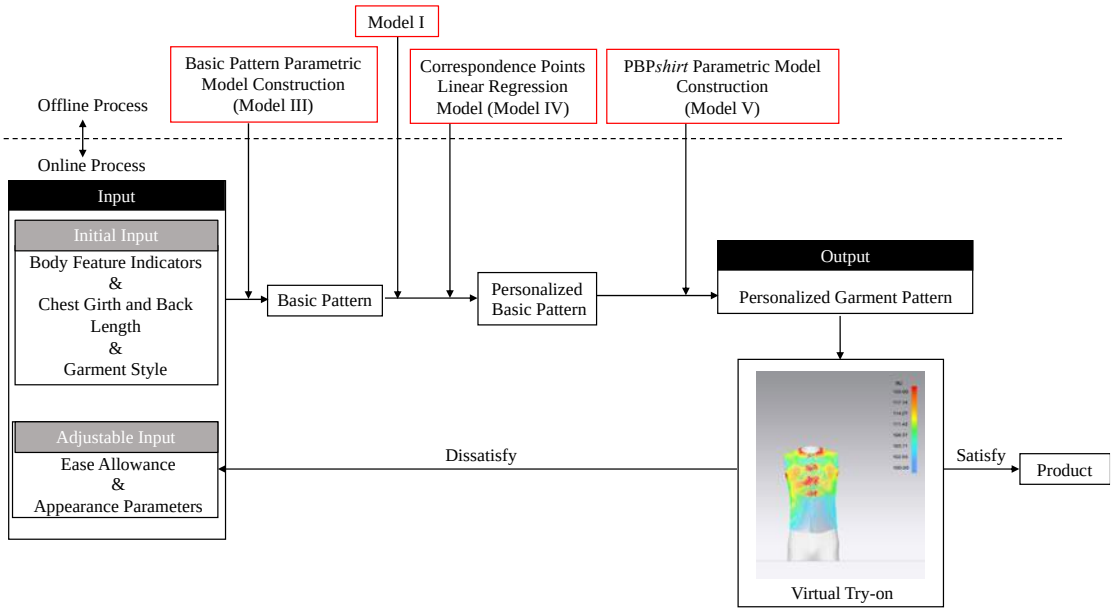

Figure 2-4: An overview of Personalized parametric garment pattern recommendation system.

2.1 Knowledge-based anthropometric and garment pattern-making

In this thesis, the designer's knowledge is the basis for all research work. It includes knowledge of anthropometry and knowledge of garment pattern-making. To analyze the designer's knowledge, this section will introduce the general concept of knowledge.

2.1.1 Classification of Knowledge

Knowledge can be divided into explicit and tacit knowledge according to how it is acquired [168]. Explicit knowledge can be explicitly expressed and obtained from verbal instructions, textbooks, references, software, and databases and is easy to learn [169]. Tacit knowledge is practical skills or expertise and refers to knowledge that people acquire in terms of skills and understanding, including informal, hard-to-express skills and experiences and insights, intuition, inspiration, etc. Tacit knowledge resides in the brains of experts, and it dominates a variety of human applications [170].

Tacit knowledge has a significant influence on anthropometry and garment pattern-making. Without the involvement of a designer with extensive professional experience, the accuracy of anthropometric measurements and the fit of garments would be

significantly reduced. However, it can take many years to train a designer to become a professional designer. This situation limits the development of fashion houses. All apparel companies would like to be able to extract and formally use the wealth of knowledge that professional designers have and use it freely to ensure the sustainable development of their garment products. At the same time, the extracted knowledge can be used by amateurs who do not have knowledge of fashion design. This can help apparel companies to break away from their dependence on specific designers and make the process of developing garment products more efficient, systematic, and adapted to the individual needs in the context of mass customization.

2.1.2 Knowledge Acquisition

Knowledge can be acquired from three sources [171].

(1) Indirect knowledge: experts provide their empirical and unstructured knowledge related to past experiences by answering well-organized questionnaires in many real-life scenarios.

(2) Direct knowledge: experts (dress designers and pattern designers) express their structured and formal knowledge directly in the form of generalized rules and relationships.

(3) Knowledge from data: knowledge can be learned automatically and progressively from data.

In this research, a knowledge-based recommendation system for garment patterns has been proposed. There are three parts where the designer's knowledge needs to be used. The first part is the anthropometric database. Modelling based on anthropometric knowledge to establish the relationship between anthropometric items and body shape. A more accurate and rational classification of the body shape is achieved. The second part is parametric pattern making. During the human-computer interaction process, the computer translates the entire pattern-making work into a number of executable codes. This solves the time-consuming and difficult adjustment problems of the traditional 2D

pattern-making process. The third part uses some intelligent algorithms to construct suitable regression models by learning from experimental data. The proposed model can predict the personalized base fit of a garment by obtaining the base pattern. By integrating the three previous technical modules, a feasible solution for the personalization of garment patterns has been provided.

2.2 Tools for human body data acquisition

As this work focuses on young men's shirt pattern-making, it only needs the measurements related to men's upper body positions. The general principle can be easily adapted to other body positions and other garment types.

2.2.1 Anthropometric subject selection

The dataset used for this study was based on measurements of 33 young men ages 18–25 years. The impacts of race, socioeconomic status, and lifestyle were considered to some extent. The 33 participants were students (first-year university students to postgraduate students) and are representative of the general population of young men. The cumulative data acquisition time for each sample was approximately four hours.

2.2.2 Human upper body segmentation

As shown in Figure 2-5, to ensure the accuracy and interpretability of the body classification results, the upper body of the subjects was segmented into three parts (the arm root, shoulder, and torso [below the shoulder]) according to the structural characteristics of young male upper bodies and corresponding garment patterns [88].

The shoulder shape refers to the shape between the shoulder line, the cross-section where the neck baseline is located, and the cross-section in which the curve of shoulder width is located.

The arm root shape is determined by the arm root line, which is a round curve through the acromion point, shoulder point, axillary anterior point, and axillary posterior point.

The shape of this round curve corresponds to the arm root shape.

The torso (below the shoulder) shape refers to the shape between the cross-section where the horizontal line of waist circumference is located, and the cross-section where the shoulder width curve is located.

To achieve the final classification result that includes both global and body part features of the human body, this study proposes to assemble the final classification results of each part to obtain a complete body shape that contains sufficient human features. The detailed process is described in Section 4.2.

Shoulder part | Arm root part | Torso (below the shoulder) part

Figure 2-5: Upper body segmentation manually realized by designers.

2.2.3 Manual measurement of human body data acquisition (Experiment 1)

Anthropometric measurements are carried out indoors at a temperature of 22 to 25 °C and a humidity of 40% to 60% to ensure that the subject feels comfortable and breathes naturally. The subjects are uniformly dressed in close-fitting underwear, and the surveyors have professional anthropometric knowledge and skills. For each subject, three kind of manual measurements are used (body surface measurements (Martin's ruler and tape measurements), two-dimensional photogrammetry, and gypsum paper film flattened graph measurements). The measurement items include length, width, height, perimeter, and angle data [16]. Due to the soft and non-static body surface, it is difficult to eliminate errors during the manual measurement. We use the human skeletal structure as the basis for manual measurements, combined with the designer's anthropometric knowledge, to make manual measurements more accurate and

interpretable. We label key feature points manually on the real human body, such as shoulder points, front neck points, etc. Finally, 41 manual measurements have been measured. Each measurement has to be repeated to minimize errors.

2.2.3.1 Experiment equipment and method

(1) Martin Measurement

The anthropometric measurements have been taken using a tape and Martin's ruler, and 14 relevant measurements have been taken, including height, width, girth, and length, according to the required measurements, as shown in Figure 2-6. The surveyors are experienced enough to use the measuring instruments and carry out the measurements professionally. A uniform standard of measurement was used to keep within the permissible limits of error.

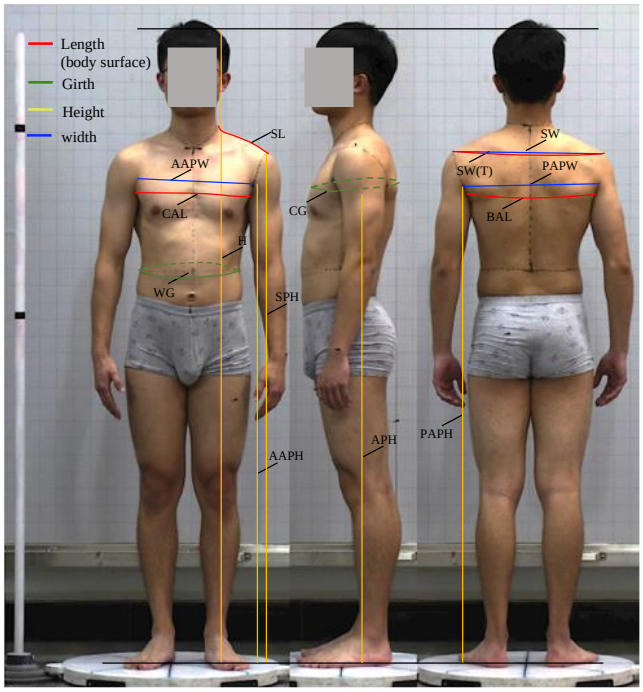

Figure 2-6: Anthropometric items measured by Martin Measurement.

(2) 2D Photogrammetry Measurement

In this study, photographs were taken with a Canon® EOS5D Mark II DSLR camera at a distance of 10 metres, a lens height of approximately 1 metre, and at three angles: front, side, and back. The participant was kept in a natural standing position with their

feet together, their arms naturally down, and their eyes forward. A 50 cm marker was placed on the side of the body as a reference for scale. Body shape data obtained by photogrammetry include height, thickness, depth, and angle. As shown in Figure 2-7, there are 8 2D photo measurement items included in this method.

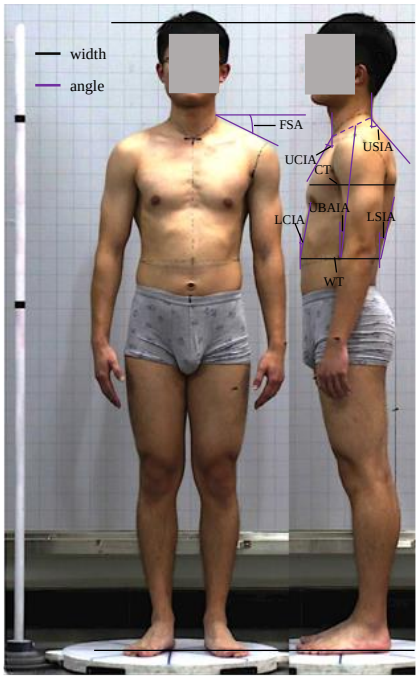

Figure 2-7: Anthropometric items measured by photogrammetry.

(3) Gypsum Paper Film Flattened Graph Measurement

3D gypsum models and 2D flattened graphs are useful modalities for body shape observations and measurements. The plaster model can be used as a resource for observing the morphology of the human body, especially the morphology of locations such as the arm root and the groin; these sites are impossible to observe on the human body itself or on a 3D human model but can be accurately observed through plaster models. This is one of the strengths and advantages of this methodology. For example, using plaster model, we can determine differences in the shape of the arm root for different body shapes. A body surface flattened graph can also be obtained. The flattened graph can be used as a basis for the design of paper patterns and to understand association between the 3D form of the human body and the flattened graph. To collect the complete form and morphological parameters of the male upper body for each participant, we carried out a gypsum membrane experiment along with 2D flattening.

As shown in Table 2-2, there are 19 flattened graph measurement items evaluated in this method. The processing of flattened graph is as follows:

(a) Draw the reference line or reference point on the body surface including chest line, waist line, shoulder line, arm root line etc.;

(b) Paste a cast of more than three layers of plaster on the skin, and removed from the body surface when it solidifies, shown as fig 2-8(a);

(c) Making flatten graphs of gypsum inner wall, shown as fig 2-8(b);

(d) Cutting flatten graphs to flatten graph of body surface, shown as fig 2-8(c).

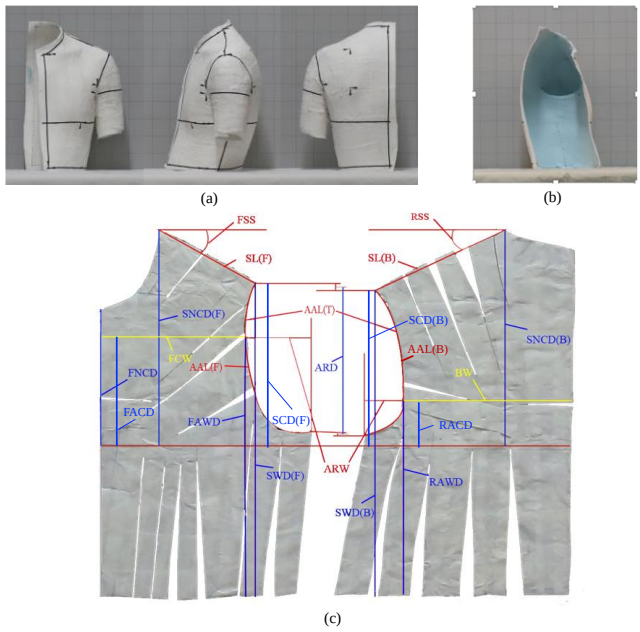

Figure 2-8: Gypsum Paper Film Flattened Graph making process and measurement items.

2.2.3.2 Manual measurement items

The manual measurements carried out in this research are all based on human skeletal features and anthropometric definitions, as detailed in Table 2-1. The statistical values of anthropometric parameters for the subjects used in this study are presented in Table 2-2.

Table 2-1: The upper body measurements and anthropometric definitions of young men used in this study.

No.	Body Measurment	Definition
1	Height	The vertical distance from the top point of the head to the ground with the subject's heels together.
2	Axillary point height	The vertical height from the ground to the axillary point.
3	Anterior axillary point height	The vertical height from the ground to the anterior axillary point.
4	Posterior axillary point height	The vertical height from the ground to the posterior axillary point.
5	Shoulder point height	The vertical height from the ground to the shoulder point.
6	Chest girth	The horizontal girth through the left and right axillary points.
7	Chest arc length	Body surface solid length from right anterior axillary point to left anterior axillary point
8	Waist girth	The horizontal girth of the thinnest part of the waist between the lower edge of the rib cage and the upper edge of the iliac crest.
9	Anterior axillary point width	The horizontal distance between the anterior points of the left and right axillae.
10	Posterior axillary point to waistline	The horizontal distance between the posterior points of the right and left axillae.
11	Back arc length	Body surface solid length from right posterior axillary point to left posterior axillary point.
12	Shoulder width	The straight line distance between the left and right shoulder peak points.
13	Total shoulder width	Body surface solid length between the left and right shoulder peak points.
14	Shoulder length	Body surface length from the lateral point of the cervical root to the point of the shoulder peak.
15	Upper chest tilt angle	Taking the chest bump point as its apex, the angle between the line connecting the chest bump and the anterior neck point and the horizontal line.
16	Lower chest tilt angle	Taking the chest bump point as the apex, the angle between the line connecting the chest bump and the projection on the waistline section where it is located and the vertical line.
17	Tilt angle of upper body axis	Connecting the midpoint of the line connecting the anterior and posterior most prominent parts of the waist and the midpoint of the line connecting the anterior and posterior neck points, the angle between this line and the horizontal line.
18	Upper angle of scapula	It is the angle between the line joining the most convex point of the scapula and the point of the seventh cervical vertebra and the vertical line.
19	Angle of inclination of lower scapula	The angle between the line passing through the most convex point of the scapula and the point of its projection on the waistline section and the vertical line.
20	Chest thickness	Over the nipple point, the horizontal straight line distance between the most prominent part of the front and back of the chest in the sagittal plane.
21	Waist thickness	The horizontal linear distance in the sagittal plane between the anterior and posterior most prominent parts of the waist at the minimum waist circumference.
22	Front shoulder angle	The lateral neck point is taken as the vertex of the angle, and the angle between this vertex and the shoulder peak point and the horizontal line.
23	Distance from shoulder point to waistline (front)	The vertical distance from the shoulder point to the horizontal waistline on the front piece of the flattened graph.
24	Distance from shoulder point to waistline (back)	The vertical distance from the shoulder point to the horizontal waistline on the back piece of the flattened graph.
25	Distance between the concave part of rare armhole arc and waistline	The vertical distance between the most concave part of the armhole arc and the horizontal waistline of the back piece of the flattened graph.
26	Distance between the concave part of front armhole arc and waistline	The vertical distance between the most concave part of the armhole arc and the horizontal waistline of the front piece of the flattened graph.
27	Distance from side neck point to chest line (front)	The vertical distance from the point of the lateral neck to the horizontal chest line on the front piece of the flattened graph.
28	Distance from side neck point to chest line (back)	The vertical distance from the point of the lateral neck to the horizontal chest line on the back piece of the flattened graph.
29	Front shoulder length	The straight line distance from the point of the lateral neck to the point of the shoulder peak on the front piece of the flattened graph.
30	Back shoulder length	The straight line distance from the point of the lateral neck to the point of the shoulder peak on the back piece of the flattened graph.
31	Back shoulder angle (°)	The angle between the lateral point of the neck as the apex of the angle and the shoulder peak and the horizontal line on the back piece of the flattened graph.
32	Front shoulder angle (°)	The angle between the lateral point of the neck as the apex of the angle and the shoulder peak and the horizontal line on the front piece of the flattened graph.
33	Armhole arc length (back)	The length from the shoulder peak point, through the anterior axillary point to the axillary point on the back piece of the flattened graph.
34	Armhole arc length (front)	The length from the shoulder peak point, through the anterior axillary point to the axillary point on the front piece of the flattened graph.
35	Armhole arc length (total)	The girth starting at the point of the shoulder peak and passing through the anterior point of the axilla and the posterior point of the axilla to the starting point.
36	Arm root depth	The vertical distance from the midpoint of the vertical distance between the axillary points of the front and back pieces to the midpoint of the vertical distance between the shoulder peak points of the front and back pieces on the flattened graph.
37	Arm root width	The horizontal distance between the most concave point in the front armhole arc and the most concave point in the back armhole arc on the flattened graph.
38	Distance between the back-shoulder point to the chest line	The vertical distance from the shoulder point to the horizontal chest line on the back piece of the flattened graph.
39	Distance between the front-shoulder point to the chest line	The vertical distance from the shoulder point to the horizontal chest line on the front piece of the flattened graph.
40	Distance between the most concave part of the rear-armhole arc to the chest line	The vertical distance from the most concave point of the armhole arc to the horizontal chest line on the back piece of the flattened graph.
41	Distance between the most concave part of the front-armhole arc to the chest line	The vertical distance from the most concave point of the armhole arc to the horizontal chest line on the front piece of the flattened graph.

Table 2-2: Upper body measurement items for young males and anthropometric statistics used in this study.

No.	Measurment Method	Body Measurment	Body parts	Abbreviation	Mean	SD	Min	Max
1	Body Surface	Height	Torso (below the shoulder)	H	172,75	4,98	165,00	187,00
2		Axillary point height		APH	127,46	5,20	119,30	142,60
3		Anterior axillary point height		AAPH	130,76	5,02	122,30	146,20
4		Posterior axillary point to waistline		PAPH	129,27	4,85	122,10	144,80
5		Shoulder point height		SPH	140,02	5,00	132,50	156,10
6		Chest girth		CG	87,09	6,02	75,00	104,00
7		Chest arc length		CAL	34,88	3,13	29,40	40,50
8		Waist girth		WG	72,65	5,46	62,00	83,50
9		Anterior axillary point width		AAPW	32,56	1,66	28,70	35,80
10		Posterior axillary point to waistline		PAPW	33,45	2,16	29,20	38,00
11		Back arc length		BAL	38,05	4,46	32,00	58,00
12		Shoulder width	Shoulder	SW	37,98	2,25	33,70	43,90
13		Total shoulder width		SW(T)	42,57	4,04	37,00	56,00
14		Shoulder length		SL	14,34	2,30	10,00	23,50
15	2D Photogrammetry	Upper chest tilt angle	Torso (below the shoulder)	UCIA	28,07	4,92	20,00	37,50
16		Lower chest tilt angle		LCIA	3,12	6,10	-12,00	16,00
17		Tilt angle of upper body axis		UBAIA	5,87	2,34	1,00	10,00
18		Upper angle of scapula		USIA	27,23	6,81	12,00	40,00
19		Angle of inclination of lower scapula		LSIA	10,81	6,33	-18,00	20,00
20		Chest thickness		CT	21,72	1,66	18,50	24,70
21		Waist thickness		WT	19,53	1,83	16,00	24,30
22		Front shoulder angle	Shoulder	FSA	24,64	3,39	18,00	30,00
23	Gypsum paper film flatten graph	Distance from shoulder point to waistline (front)	Torso (below the shoulder)	SWD(F)	36,75	2,54	29,60	42,00
24		Distance from shoulder point to waistline (back)		SWD(B)	35,99	2,48	30,40	40,40
25		Distance between the concave part of rare armhole arc and waistline		RAWD	24,05	2,41	19,00	28,40
26		Distance between the concave part of front armhole arc and waistline		FAWD	27,61	3,47	18,60	34,00
27		Distance from side neck point to chest line (front)	Shoulder	SNCD(F)	22,01	2,56	14,70	25,90
28		Distance from side neck point to chest line (back)		SNCD(B)	25,02	2,45	20,60	31,00
29		Front shoulder length		SL(F)	13,34	1,57	9,50	16,00
30		Back shoulder length		SL(B)	16,36	2,17	12,20	22,90
31		Back shoulder angle (°)		RSS	24,42	5,06	12,00	32,50
32		Front shoulder angle (°)		FSS	22,45	5,17	11,00	32,00
33		Armhole arc length (back)	Arm root	AAL(B)	19,31	4,59	1,30	30,40
34		Armhole arc length (front)		AAL(F)	19,92	1,95	15,50	23,60
35		Armhole arc length (total)		AAL(T)	39,24	5,56	18,40	50,00
36		Arm root depth		ARD	15,90	1,48	12,40	18,90
37		Arm root width		ARW	10,26	1,61	6,60	12,90
38		Distance between the back-shoulder point to the chest line		SCD(B)	17,78	3,29	13,30	26,20
39		Distance between the front-shoulder point to the chest line		SCD(F)	18,53	2,35	11,90	23,10
40		Distance between the most concave part of the rear-armhole arc to the chest line		RACD	5,84	3,00	1,00	12,50
41		Distance between the most concave part of the front-armhole arc to the chest line		FACD	9,40	3,40	3,60	17,60

Note: Mean stands for average; SD stands for standarddeviation; Min stands for minimum; Max stands for maximum; Red font unit: ∘; Black font unit: cm.

2.2.4 3D human body data acquisition (Experiment 2)

2.2.4.1 Experiment equipment

The 3D scanning instrument used in this study was the OKIO-Body Scan 3D body scanning system (Beijing TEN YOUN 3D Technology CO. LTD, Beijing, China). The 3D model obtained from the scan is a surface model defined by a network of curves extracted from a scanned human body.

2.2.4.2 Measurement conditions and requirements

In order to obtain a 3D model of the subjects, 3D scans have been taken of the same

subjects who have previously been measured manually, in a laboratory with an ambient temperature of 27°C ± 3°C and a humidity of 60% ± 10%, which satisfies the environmental criteria for anthropometric measurements. The subjects are naked, wearing a tight white underwear with a tight-fitting headgear to avoid folds of clothing and hairstyles that could cause measurement errors. No watches, necklaces, rings, or other jewellery should be worn to prevent interference with the measurement. During the scan, the subject should be fully relaxed and stand still at the designated footprint mark. Both eyes look straight ahead, shoulders in a natural position, breathing evenly, and arms spread out about 30 degrees. The standing position is shown in Figure 2-6. Multiple scans are taken and the best scan is chosen based on quality of the imaging results.

2.3 CAD tools for 3D human body modelling and garment pattern-making

In this study, several computer-aided design (CAD) software are applied to construct a virtual design platform for the proposed design method, permitting 3D scanning, 3D human body modeling, 3D garment construction, 2D pattern design and 3D virtual try-on (see Figure 2-9).

(1) Human Solution ScanWorX

To obtain a 3D human body model of the subject, Human Solution's 3D SCAN Tecmath was used. During the scanning process, the data are exported to ScanWorX [172], [173]. ScanWorX is a software that imports data from the scanner and digitizes it. The scanned data is then purified and smoothed in pre-processing.

(2) Geomagic Design X

Geomagic Design X [174], [175] can transform 3D scan data into high-quality feature-based CAD models. The software combines automatic, guided solid model extraction uniquely while being extremely accurate. In addition, it offers numerous features for fitting accurate surfaces to organic 3D scans, surface sheet editing, and point cloud

processing. In this study, the Geomagic Design X software is used to analyze further and pre-process the point cloud data exported from the scanner to obtain a smooth object surface. In addition, Geomagic Design X ensures that the 3D shapes are re-trigonometrically profiled, and holes due to scanning are filled. The most difficult areas to recover are the armholes and crotch areas. They were carefully processed by using software tools for cleaning, boundary creation, and hole filling. On this basis, a unique surface shaped by several small faces has been obtained.

(3) DesignConcept

DesignConcept [135], [176] by Lectra is a "2D and 3D" software solution for 3D design based on TOPSOLID, a software package from another French company, MISSLER. DesignConcept can create points, lines, curves, and surfaces in a 3D environment, thus allowing the transformation of 3D garment prototypes into 2D flattening graphics to be worked on and reconstruction of 3D human body models. In this research, combining DesignConcept 2D with DesignConcept 3D offers unique flexibility for designing and optimizing garment patterns and 3D human body modelling.

(4) Alpha Myu

Alpha Myu [177] is a 2D garment CAD system developed by Yuka & Alpha Co., Ltd. that has attracted the attention of the garment industry due to its ease of use. Users can automatically record and perform routine tasks that are repeated in pattern-making, effectively increasing productivity.

(5) CLO 3D

CLO 3D [178, 179] software developed by CLO Virtual Fashion Inc. It can be used to create and edit 2D garment patterns and perform a virtual try-on process. 2D and 3D are simulated in parallel, so users can immediately see the effect of modifications such as panels, colors, textures, and details. The ability to check the shape and fit of the garment in real-time during development and modify the design on the fly.

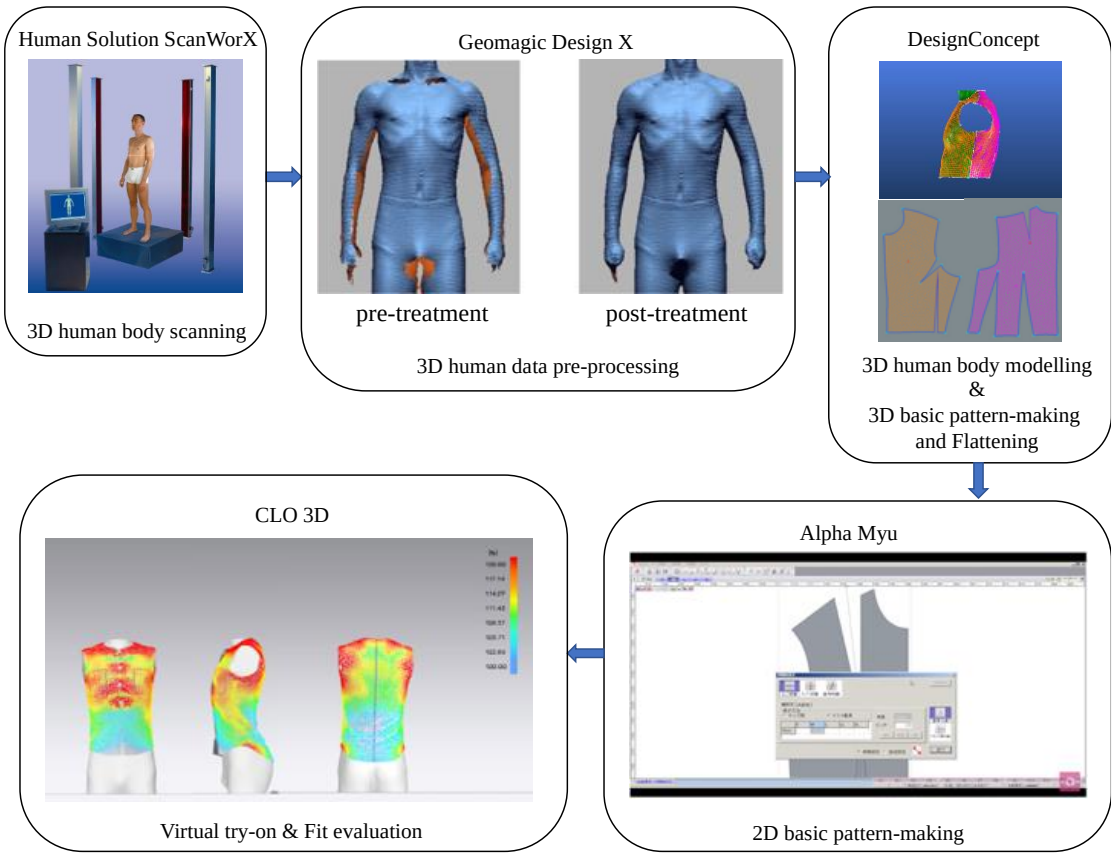

Figure 2-9: Different fashion CAD software used in this research, their functions and relations.

2.4 Mathematic modeling tools for human body analysis and parametric garment pattern-making

2.4.1 Factor analysis

The factor analysis method reflects most of the information of the original indicator variables with a relatively small number of common factor variables and reduces the difficulty of analyzing the problem by determining the weights through the contribution of each indicator [180], the equation of factor analysis is:

$$X_1 = a_{11}F_1 + a_{12}F_2 + a_{13}F_3 + \cdots + a_{1m}F_m + \varepsilon_1$$
$$X_2 = a_{21}F_1 + a_{22}F_2 + a_{23}F_3 + \cdots + a_{2m}F_m + \varepsilon_2$$
$$X_3 = a_{31}F_1 + a_{32}F_2 + a_{33}F_3 + \cdots + a_{3m}F_m + \varepsilon_3$$
$$\vdots$$
$$X_p = a_{p1}F_1 + a_{p2}F_2 + a_{p3}F_3 + \cdots + a_{pm}F_m + \varepsilon_p$$

where X = (X_1, X_2, ... X_p) is the observable random raw variable, F = (F_1, F_2, ... F_m) is the common factor; a_{pm} is the loading of the P_{th} variable on the m_{th} factor, indicating the dependence and relative importance of the P_{th} variable X_P on the m_{th} factor F_m, and ε_p is the error term. The general steps of the analytical factor analysis are:

1) confirm the suitability of the data variables to be analyzed for factor analysis

2) conduct a preliminary factor analysis and select the factor variables

3) Factor rotation and interpretation of the factor variables.

4) Calculation of factor scores and composite scores for further analysis.

The purposes of the factor analysis in this research are: reducing the number of anthropometric items and detecting structure in the relationships among anthropometric items.

2.4.2 Kaiser-Meyer-Olkin test and Bartlett's test

In this study, the Kaiser-Meyer-Olkin (KMO) test and Bartlett's test of sphericity were used to test whether factor analysis is relevant for data processing using SPSS software (SPSS, Inc., Chicago, IL, US) [181]. KMO values were > 0.5, indicating that factor analysis is worthwhile. The Sig. value is 0, indicating that the hypothesis of a null association was rejected and providing evidence that factor analysis may be suitable for this data.

In this study, the Kaiser-Meyer-Olkin test and Bartlett's test have been used to test the suitability of anthropometric data for principal component analysis.

The parameter equations of the KMO test (1) and the Bartlett test (2) are as follows:

$$KMO = \frac{\sum\sum_{i\neq j} r_{ij}^2}{\sum\sum_{i\neq j} r_{ij}^2 + \sum\sum_{i\neq j} r_{ij\cdot 1,2\cdots k}^2} \quad (1)$$

$$X^2 = \frac{(N-k)\ln(S_p^2) - (\sum_{i=1}^{k}(n_i-1)\ln(S_i^2))}{1+\frac{1}{3(k-1)}(\sum_{i=1}^{k}\left(\frac{1}{n_i-1}\right) - \frac{1}{N-k})} \quad (2)$$

2.4.3 Principle component analysis

PCA is generally used to characterize human-related designs and has been shown to be effective in addressing issues of human identification, anthropometric analysis, and ergonomic design. In current study, the purpose of PCA was to reduce the dimensionality of the anthropometric measurement items dataset while retaining the items in the dataset that contributed most to variance. Therefore, in this study, principal component factor analysis was applied to the experimental samples using SPSS software to explore the main factors influencing the body shape characteristics of each body part separately [182]–[184].

The principle is that PCA performs a linear transformation of the input variable vectors to represent all the original data in a low-dimensional space with minimal information loss. The q observations in the original n-dimensional space, corresponding to the n input variables, form a data distribution characterized by eigenvectors and eigenvalues that can be easily computed from the variance-covariance matrix. PCA aims to find the smallest subspace in the n-dimensional space that maintains the shape of this distribution. The first component of the transformed variable vector represents the original variable vector in the direction of the largest eigenvector of the variance-covariance matrix, the second component of the transformed variable vector in the second-largest direction, and so on. The general steps of the principal component analysis are [185]:

(1) Column or row vector of size N^2 represents the set of M images (B_1, B_2, B_3…B_M) with size N*N.

(2) The training set image average (μ) is described as:

$$\mu = \frac{1}{m}\sum_{i=1}^{M} B_i$$

(3) The average image by vector (W) is different for each trainee image.

$$\Phi_i = B_i - \mu \ (i = 1,2, \dots m)$$

(4) Total Scatter Matrix or Covariance Matrix is calculated from Φ as shown below

$$C = \frac{1}{m}\sum_{n=1}^{M} \Phi_i \Phi_i^T = AxA^T$$

where $\Phi = [\Phi_1, \Phi_2, \dots \Phi_M]$

(5) Measure the eigenvectors U_i and eigenvalues λ_i of the covariance matrix C.

$$Cv_i = \lambda_i v_i$$

(6) For image classification, this feature space can be utilized. Measure the vectors Ω^T of weights.

$$\Omega^T = [W_1, W_2, \dots, W_{M'}]$$

whereby,

$$W_k = U_K^T(B_i - \mu)(1 \leq K \leq M')$$

2.4.4 Correlation analysis

In statistics, correlation means measuring the distance of two variables relative to their independence from each other. The most familiar measure of the correlation between two quantities is the Pearson's Product Moment Correlation Coefficient (PPMCC or PCC, often denoted by r or Pearson's r in articles.) The PCC is used to measure the degree of correlation (linear correlation) between two variables, X and Y, and has a value between -1 and 1. In the natural sciences, this coefficient is widely used to measure the linear correlation between two variables. Karl Pearson evolved it from a similar but slightly different idea proposed by Francis Galton in the 1880s [186], [187]. The rule of thumb in terms of correlation is that r > 0.5 means that the correlation is strong. A strong correlation means that a change in an easily measured item will lead to a correct prediction of a hard-to-measure item. Although correlation cannot be interpreted as causality, the test can test whether two variables fluctuate together.

When applied to populations, PCC is also referred to as the population correlation coefficient and is represented by the Greek letter ρ. For two random variables X and Y, the formula for ρ is given as:

$$\rho_{X,Y} = \frac{Cov(X,Y)}{\sigma_X \sigma_Y} = \frac{E(X - \mu_X)(X - \mu_Y)}{\sigma_X \sigma_Y}$$

The covariance and the standard deviations can be estimated with a limited number of samples. Therefore, the corresponding estimation for PCC, also known as the sample correlation coefficient, commonly used English lowercase letter r:

$$r = \frac{\sum_{i=1}^{n}(X_i - \bar{X})(Y_i - \bar{Y})}{\sqrt{\sum_{i=1}^{n}(X_i - \bar{X})^2}\sqrt{\sum_{i=1}^{n}(Y_i - \bar{Y})^2}} = \frac{1}{n-1}\sum_{i=1}^{n}\left(\frac{X_i - \bar{X}}{s_X}\right)\left(\frac{Y_i - \bar{Y}}{s_Y}\right)$$

where, $\bar{X} = \frac{1}{n}\sum_{i=1}^{n} X_i$, and $s_X = \sqrt{\frac{1}{n-1}\sum_{i=1}^{n}(X_i - \bar{X})^2}$

When the law of large numbers can be applied, the sample correlation coefficient is a consistent estimate of the population correlation coefficient as long as the sample means, variances, and covariance are consistent.

In this research, among representative measurement items used for clustering, some measurement items and methods have particularly stringent requirements for the professionalism of the surveyors and the quality of the measuring instruments and measuring environment. Although these measurement items can better express body shape characteristics, this methodology increases the difficulty of data acquisition and is inconvenient for daily measurement. The purpose of correlation analysis is to identify the measurement items that are highly correlated with these items and are convenient for daily manual measurements, such as chest circumference and height. The corresponding linear regression equation was established based on the results of the correlation analysis.

2.4.5 K-means clustering

The basic principle of the K-means clustering [77], [188] algorithm is to divide n points (an observation or an instance of the sample) into k (random) clusters so that each point belongs to the cluster corresponding to the nearest mean (i.e., the cluster center), and then iterate until the iterations converge. Assume that the original set of samples is (X_1, X_2, ..., X_n) and X_n is a D-dimensional vector. Given the number of classifications K,

the samples are divided into K classes. The same group of classifications has the maximum similarity. Even if the value of $\operatorname{argmin}\sum_{i=1}^{k}\sum_{x\in S_i}\| x - \mu_i \|^2$ is the smallest, where $S = \{S_1, S_2, \cdots, S_i\}$ and μ_i is the mean of class S_i. The process is as follows.

(1) Select K elements randomly from the total experimental samples (D) and use them as the initial clustering centers for K classes.

(2) The distances of the remaining elements to the K cluster centers are then calculated. The elements are assigned to the class with the smallest distance.

(3) Calculate the clustering centers of the new K classes according to the results obtained in (2). This is calculated as the arithmetic mean of all the elements in each class in each dimension.

(4) Re-cluster all the elements in the D according to the new clustering centers calculated in (3) until the clustering results do not change. In this paper, the K-means clustering algorithm will cluster each body part of the segmented human upper body.

2.4.6 Linear regression

In statistics, linear regression [189], [190] is a type of regression analysis that models the relationship between one or more independent and dependent variables using the least squares function known as a linear regression equation. Such a function is a linear combination of one or more model parameters called regression coefficients. Only one independent variable is called simple linear regression, and more than one independent variable is called multivariable linear regression. Linear regression is the first type of regression analysis that has been rigorously studied and is widely used in practice. This is because models that are linearly dependent on their unknown parameters are easier to fit and the statistical properties of the resulting estimates are easier to determine than models that are non-linearly dependent on their unknown parameters.

The relationship between a variable Y depending on p variables $x_1, \cdots, x_p$ in the following way [191]:

$$Y = \beta_0 + \beta_1 x_1 + \cdots + \beta_p x_p + \varepsilon$$

Where:

- Y: response variable (also dependent variable, output, endogeneous variable, explained variable, ...)
- $x_1, \cdots, x_p$: regressors (also predictors, independent variables, exogeneous variables, explanatory variables, covariables, input, ...)
- ε is a noise (measurement error)

Since ε is a noise, it satisfies $\mathbb{E}(\varepsilon) = 0$ and then:

$$\mu(x_1, \cdots, x_p) = \mathbb{E}(Y | x_1, \cdots, x_p) = \beta_0 + \beta_0 x_1 + \cdots + \beta_p x_p$$

Using vectorial notation $\underline{x} = (1, x_1, \cdots, x_p)$ and $\underline{\beta} = (\beta_0, \beta_1, \cdots, \beta_p)^t$, model can be written:

$$Y = \underline{x}^t \underline{\beta} + \varepsilon$$

We are given n observations

$$(x_{i1}, \cdots, x_{ip}, y_i) \quad i = 1, \cdots, n$$

from which we intend to carry out statistical inference.

By least square method we get an estimate for the regression model, that is $\widehat{\beta_0}$, ..., $\widehat{\beta_p}$ and estimates for their precisions. This enables us to deal with the relevant statistical issues.

Therefore, in this study, a relational model between the corresponding representative body index and body shape for each body part is built based on the results of the body shape classification. With this model, the user can predict their body part shape by entering specified anthropometric items. In addition，according to the position of the coordinate points, a linear regression model of the key points on the PBP and the corresponding key points on the basic model are developed.

Conclusion

In this chapter, various anthropometric methods, scientific and technical tools are presented, and useful theories are used in this research. The large number of tools used

in the study shows how extensive and complex a field personalized parametric garment pattern-making is.

Based on the analysis of these tools' advantages and disadvantages. In Chapter 3, the relationship between human feature dimensions and body part shape is modelled using factor analysis, K-means clustering and linear regression, etc. (Model I). In Chapter 4, various CAD tools are used to reconstruct a 3D personalized parametric human body model (Model II) in combination with Model I. In Chapter 5, linear regression is adopted to construct parametric garment pattern-making models, include Model III (characterizing the relations between the basic pattern and its key influencing human dimensions (chest girth and back length)), Model IV (infer from basic pattern to PBP for three body parts based on the one-to-one correspondence of key points between the PBPs and the basic patterns), and Model V (characterizing the structural relations between the personalized shirt pattern (PBP_{shirt}) and PBP).

CHAPTER 3: Human Upper Body Classification based on Manual Measurement Data

Introduction

This chapter focuses on the mathematical models related to the classification of male upper body shapes. First, we screened all body measurements according to the designer's knowledge. This ensures that measurements that are not relevant to the corresponding body part have been excluded before the body measurements being dimensionality reduction processed. Then, factor analysis was applied to the screened measurements using the statistical software SPSS. Several feature measurements with a high principal component contribution in each of the three body parts were extracted, i.e., the feature measurements that significantly impacted the three body parts. Based on these feature measurements, the three body parts were classified separately using a K-means clustering algorithm. In order to facilitate user operation, correlation analysis was used to establish a linear relationship between human body items which are easy to measure and those which are difficult to measure. Finally, MATLAB software was used to build a body shape classification model, which easily measurable anthropometric items as input and the shape of body parts as output.

3.1 Manual measurement data analysis

To reduce the number of anthropometric items and elucidate the complex relationships between anthropometric items, we used factor analysis (which is widely applied for data reduction and structure detection) to process the data. The final factor extraction results were used for body shape classification.

3.1.1 Human data effectiveness testing

As shown in Table 3-1, all KMO values were > 0.5, indicating that factor analysis is worthwhile. The Sig. value is 0, indicating that the hypothesis of a null association was rejected and providing evidence that factor analysis may be suitable for this data.

Table 3-1: Kaiser-Meyer-Olkin (KMO) and Bartlett test results.

KMO and Bartlett's Test			
Arm root	Kaiser-Meyer-Olkin Measure of Sampling Adequacy.		0,617
	Bartlett's Test of Sphericity	Approx. Chi-Square	214,752
		df	36
		Sig.	0,000
Shoulder	Kaiser-Meyer-Olkin Measure of Sampling Adequacy.		0,723
	Bartlett's Test of Sphericity	Approx. Chi-Square	115,67
		df	28
		Sig.	0,000
Torso (Below the shoulder)	Kaiser-Meyer-Olkin Measure of Sampling Adequacy.		0,568
	Bartlett's Test of Sphericity	Approx. Chi-Square	742,90
		df	231
		Sig.	0,000

Note: df stands for degrees of freedom; Sig. stands for minimum significance.

3.1.2 Principle factor extraction and explanation

3.1.2.1 Shoulder

About the shoulder, Figure 3-1 shows that the curve decreases rapidly at the beginning but becomes slower after the third factor. Table 3-2 shows that the cumulative contribution of the first third factors is 87.3%. In our study, if the cumulative contribution rate threshold is 85%, we need to select the first third components. Therefore, we consider that all datasets can be represented by these third factors.

The maximum variance method is used to implement an orthogonal rotation of the factor loading matrix to clarify the meaning of the factors. The rotated factor loading matrix is shown in Table 3-2. The first principal factor has larger loadings on SW, SL, SW(T), and RSS, which is a composite reflection of the width of the shoulder; the

second principal factor has larger loadings on SL(F), SL(B), and FSS, which is a composite reflection of the length of the shoulder; the third principal factor has larger loadings on FSA, which is a composite reflection of the angle of the shoulder. According to the meanings of the factors, factors 1, 2, and 3 are named width, length, and angle factors, respectively.

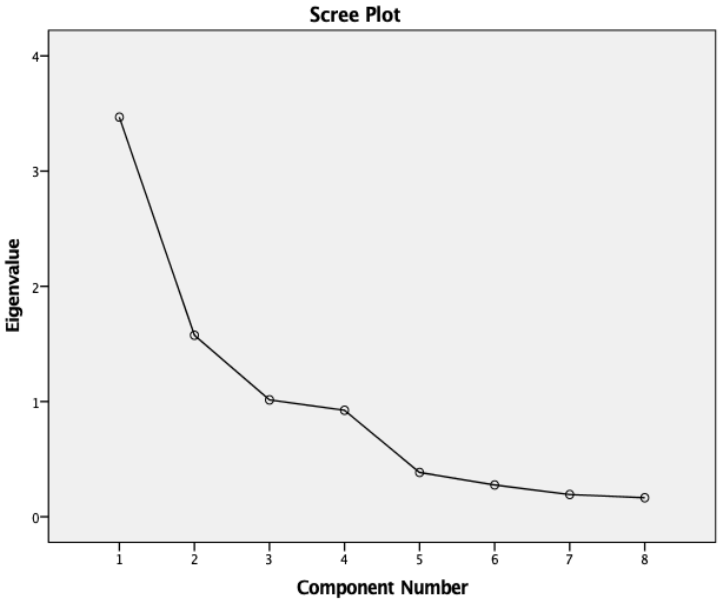

Figure 3-1: Scree plot (shoulder)

Table 3-2: Rotated component matrix of shoulder anthropometric measurement.

Rotated Component Matrix[a]

Body Part	No.	Items	Component		
			1	2	3
Shoulder	1	SW	0,898	0,157	0,031
	2	SL	0,857	0,037	0,168
	3	SW(T)	0,831	0,357	-0,035
	4	RSS	0,412	0,022	-0,050
	5	SL(F)	0,299	0,866	-0,005
	6	SL(B)	0,548	0,747	-0,091
	7	FSS	-0,378	0,723	0,388
	8	FSA	0,079	0,056	0,970
		% of Variance	43,354	25,741	18,183
		Cumulative %	43,354	69,095	87,278

Extraction Method: Principal Component Analysis. Rotation Method: Varimax with Kaiser Normalization.

3.1.2.2 Arm root

About the arm root, Figure 3-2 shows that the curve decreases rapidly at the beginning but becomes slower after the fourth factor. Table 3-3 shows that the cumulative contribution of the first four factors is 89.2%. In our study, if the cumulative contribution rate threshold is 85%, we need to select the first four components. Therefore, we consider that all datasets can be represented by these four factors.

The maximum variance method was used to implement an orthogonal rotation of the factor loading matrix to clarify the meaning of the factors. The rotated factor loading matrix is shown in Table 3-3. The first principal factor had larger loadings on SCD(B), RACD, FACD, and SCD(F), which is a composite reflection of the longitudinal height of the arm root; the second principal factor had larger loadings on AAL(F), ARD, and AAL(T), which is a composite reflection of the arm root circumference; the third principal factor had larger loadings on AAL(B), and the fourth principal factor had larger loadings on ARW. According to the meanings of the factors, factors 1, 2, 3, and 4 were named height, girth, AAL (B), and ARW factors, respectively.

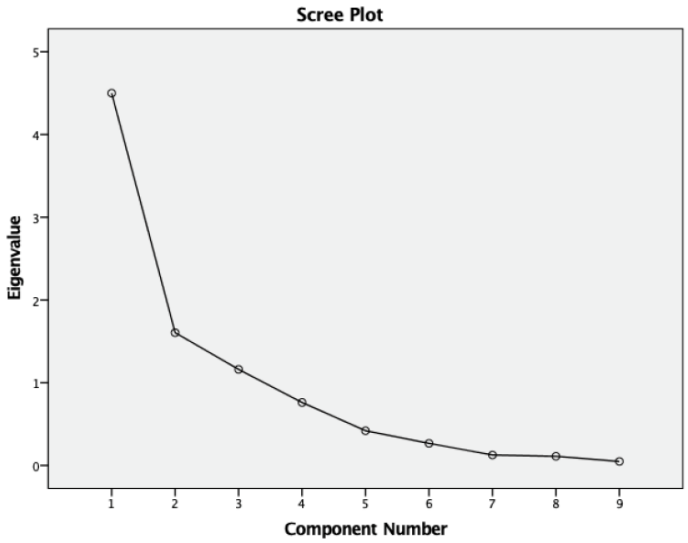

Figure 3-2: Scree plot (arm root).

Table 3-3: Rotated component matrix of arm root anthropometric measurement.

Rotated Component Matrix[a]

Body Part	No.	Items	Component			
			1	2	3	4
Arm Root	1	SCD(B)	0,885	0,087	0,345	0,093
	2	RACD	0,850	-0,068	0,385	0,082
	3	FACD	0,758	0,279	-0,242	0,261
	4	SCD(F)	0,748	0,552	-0,008	0,031
	5	AAL(F)	0,038	0,881	0,070	0,363
	6	ARD	0,245	0,876	0,261	0,018
	7	AAL(T)	0,132	0,657	0,632	0,150
	8	AAL(B)	0,172	0,200	0,914	0,074
	9	ARW	0,199	0,222	0,118	0,941
	% of Variance		50,000	17,832	12,903	8,459
	Cumulative %		50,000	67,832	80,735	89,194

Extraction Method: Principal Component Analysis. Rotation Method: Varimax with Kaiser

3.1.2.3 Torso (below the shoulder)

About the torso (below the shoulder), Figure 3-3 shows that the curve decreases rapidly at the beginning but becomes slower after the seventh factor. Table 3-4 shows that the cumulative contribution of the first seven factors is 86.7%. In our study, if the cumulative contribution rate threshold is 85%, we need to select the first seven components. Therefore, we consider that all datasets can be represented by these seven factors.

The maximum variance method was used to implement an orthogonal rotation of the factor loading matrix to clarify the meaning of the factors. The rotated factor loading matrix is shown in Table 3-4. The first principal factor had larger loadings on PAPH, AAPH, APH, SPH, H, which is a composite reflection of the longitudinal height of the human body; the second principal factor had larger loadings on WG, WT, CT, and CG, which is a composite reflection of the torso girth; the third principal factor had larger loadings on SWD(B), RAWD, SWD (F), and FAWD, which is a composite reflection the longitudinal length of the torso; the fourth principal factor had larger loadings on CAL and AAPW, which is a composite reflection the transverse length of the front chest;

the fifth principal factor had larger loadings on UBAIA, LSIA, UCIA and USIA, which is a composite reflection the angle of the torso; the sixth principal factor had larger loadings on BAL and PAPW, which is a composite reflection the transverse length of the back; the sixth principal factor had larger loadings on LCIA. According to the meanings of the factors, factors 1, 2, 3, 4, 5, 6 and 7 were named height, girth, longitudinal torso, front chest, angle, back and LCIA factors, respectively.

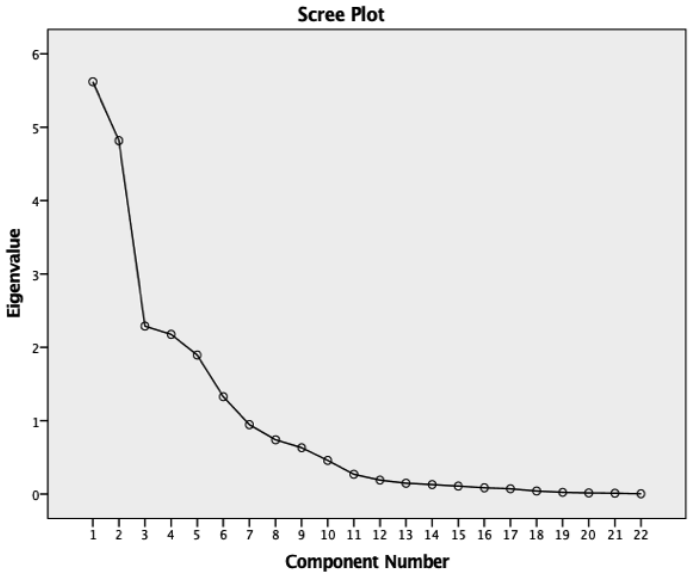

Figure 3-3: Scree plot (torso (below the shoulder)).

Table 3-4: The results of torso principal components analysis.

Rotated Component Matrix[a]								
Body Part	No.	Items	Component					
			1	2	3	4	5	6	7
Torso (below the shoulder)	1	PAPH	0,979	0,002	0,121	0,039	-0,035	0,001	-0,042
	2	AAPH	0,974	0,009	0,123	0,115	0,000	0,016	-0,041
	3	APH	0,964	-0,103	0,110	0,019	-0,099	-0,007	-0,047
	4	SPH	0,957	0,086	0,124	0,091	-0,055	-0,045	-0,094
	5	H	0,938	0,000	0,115	0,047	0,046	0,166	0,005
	6	WG	0,071	0,910	-0,035	0,226	0,011	0,102	0,138
	7	WT	-0,202	0,874	0,018	0,105	-0,003	0,151	0,203
	8	CT	0,092	0,853	-0,097	-0,067	0,058	0,164	-0,362
	9	CG	-0,039	0,740	-0,124	0,352	0,032	0,392	0,028
	10	SWD(B)	0,219	0,017	0,859	-0,307	-0,070	-0,098	0,141
	11	RAWD	0,118	-0,067	0,808	-0,348	-0,005	0,024	-0,019
	12	SWD(F)	0,210	-0,126	0,791	0,344	-0,073	0,079	-0,076
	13	FAWD	0,103	-0,041	0,730	0,294	0,101	-0,239	-0,363
	14	CAL	0,222	0,206	-0,112	0,806	0,042	-0,025	-0,136
	15	AAPW	0,120	0,379	-0,007	0,731	-0,144	0,278	-0,055
	16	UBAIA	-0,121	-0,146	0,004	0,145	0,921	-0,015	0,191
	17	LSIA	0,168	0,186	-0,078	-0,459	0,690	0,120	0,103
	18	UCIA	-0,096	0,443	-0,066	-0,029	0,660	-0,059	-0,470
	19	USIA	0,186	0,404	-0,068	0,086	-0,465	-0,403	0,321
	20	BAL	0,014	0,245	-0,033	0,193	0,098	0,801	0,108
	21	PAPW	0,185	0,448	-0,117	-0,086	-0,063	0,758	0,111
	22	LCIA	-0,225	0,134	-0,147	-0,231	0,158	0,183	0,831
		% of Variance	25,547	21,897	10,406	9,895	8,611	6,032	4,299
		Cumulative %	25,547	47,444	57,849	67,744	76,355	82,388	86,686

Extraction Method: Principal Component Analysis. Rotation Method: Varimax with Kaiser Normalization.

3.1.3 Feature measurements selection

To make the user's measurement easy, a feature measurement from each principal factor is found. Then these items are used for body classification. The selection is based on a high correlation with the corresponding principal factor and relative ease of measurement. Accordingly, feature measurements for the shoulder include SW, SL(F), and FSA. Feature measurements for the arm root include SCD(B), AAL(F), AAL(B), and ARW. Feature measurements for the torso (below the shoulder) include PAPH, WG, SWD(B), CAL, UBAIA, BAL and LCIA.

3.2 Classification model for segmented upper body shapes (Model I)

Based on the feature measurements obtained previously, we use the K-means method for body part shape clustering. It has been widely used in various applications. The K-means algorithm requires that the number of classes or categories be determined before running. Feature measurements and classification results for the three body parts will be used to manually label and correct the scanned 3D human body models. The details are described in Chapter 4.

3.2.1 Shoulder classification

Three variables were selected from the principal component analysis, including SW, SL(F), and FSA. Table 3-5(a) shows the ANOVA results when the four feature shoulder items are clustered into three, four, and five classes. When the experimental samples are divided into four and five classes, the probability of the F test is <0.05, showing that clustering into three and five classes is reasonable. From convenience for industrial production, we decide to divide the shoulder shapes into three classes. According to the final clustering centre shown in Table 3-5(b), the intermediates of different shoulder shapes are found.

Table 3-5(a): Analysis of variance in typical indices

ANOVA								
Parts	NO.	Items	Cluster		Error		F	Sig.
			Mean Square	df	Mean Square	df		
Shoulder	3	SW	34,389	2	3,259	30	10,551	0,000
		SL(F)	9,100	2	2,120	30	4,293	0,023
		FSA	139,108	2	3,336	30	41,699	0,000
	4	SW	32,530	3	2,378	29	13,679	0,000
		SL(F)	4,346	3	2,371	29	1,833	0,163
		FSA	94,132	3	3,307	29	28,466	0,000
	5	SW	29,926	4	1,673	28	17,885	0,000
		SL(F)	9,670	4	1,540	28	6,280	0,001
		FSA	64,728	4	4,264	28	15,181	0,000

Note: df stands for degree of freedom; F stands for F-statistics; Sig. stands for minimum signigicance.

Table 3-5(b): Final cluster centers and capacity of shoulder shape

Final Cluster Centers			
Items	Cluster		
	1	2	3
SW	40,5	36,9	37,4
SL(F)	14,6	12,6	13,2
FSA	25,0	20,8	27,5
Sample capacity	8	11	14

3.2.2 Arm root classification

Four variables were selected from the principal component analysis, including AAL(F), AAL(B), SCD(B), and ARW. Table 3-6(a) shows the ANOVA results when the four feature arm root items are clustered into three, four, and five classes. When the

experimental samples are divided into four and five classes, the probability of the F test is <0.05, showing that clustering into four and five classes is reasonable. From convenience for industrial production, we decide to divide the arm root shapes into four classes. According to the final clustering centre shown in Table 3-6(b), the intermediates of different arm root shapes are found.

Table 3-6(a): Analysis of variance in feature measurements

ANOVA								
Parts	NO.	Items	Cluster		Error		F	Sig.
			Mean Square	df	Mean Square	df		
Arm root	3	AAL(F)	6,797	2	3,722	30	1,826	0,178
		AAL（B）	118,445	2	4,178	30	28,350	0,000
		SCD(B)	106,625	2	4,819	30	22,125	0,000
		ARW	12,458	2	2,013	30	6,189	0,006
	4	AAL(F)	22,529	3	1,988	29	11,332	0,000
		AAL（B）	92,941	3	2,876	29	32,314	0,000
		SCD(B)	55,704	3	6,576	29	8,470	0,000
		ARW	13,051	3	1,591	29	8,201	0,000
	5	AAL(F)	20,066	4	1,606	28	12,492	0,000
		AAL（B）	69,050	4	3,073	28	22,473	0,000
		SCD(B)	54,119	4	5,048	28	10,720	0,000
		ARW	9,409	4	1,702	28	5,527	0,002

Note: df stands for degree of freedom; F stands for F-statistics; Sig. stands for minimum signigicance.

Table 3-6(b): Final cluster centers and capacity of arm root shape

Final Cluster Centers				
Items	Cluster			
	1	2	3	4
AAL(F)	21,3	18,2	19,5	19,3
AAL（B）	20,3	18,2	26,7	9,7
SCD(B)	17,5	16,2	23,9	22,5
ARW	11,0	8,9	11,1	12,5
Sample capacity	17	12	3	1

3.2.3 Torso (below the shoulder) classification

Seven variables were selected from the principal component analysis, including PAPH, WG, SWD(B), CAL, UBAIA, BAL and LCIA. Table 3-7(a) shows the ANOVA results when the seven features torso (below the shoulder) items are clustered into six, seven, and eight classes. When the experimental samples are divided into eight classes, the probability of the F test is <0.05, showing that clustering into eight classes is reasonable. According to the final clustering center shown in table 3-7(b), the intermediates of different torso (below the shoulder) shapes are found.

Table 3-7(a): Analysis of variance in typical indices

	NO.	Items	ANOVA					
			Cluster		Error		F	Sig.
			Mean Square	df	Mean Square	df		
Torso (below the shoulder)	6	PAPH	89,625	5	12,193	27	7,351	0,000
		WG	52,278	5	26,798	27	1,951	0,119
		SWD(B)	5,286	5	6,520	27	0,811	0,552
		CAL	25,922	5	7,178	27	3,612	0,012
		UBAIA	7,372	5	5,322	27	1,385	0,261
		LCIA	189,154	5	10,502	27	18,012	0,000
		BAL	91,263	5	7,374	27	12,377	0,000
	7	PAPH	80,986	6	11,208	26	7,226	0,000
		WG	68,126	6	22,160	26	3,074	0,021
		SWD(B)	10,971	6	5,256	26	2,087	0,089
		CAL	14,960	6	8,986	26	1,665	0,170
		UBAIA	11,689	6	4,247	26	2,752	0,033
		LCIA	136,910	6	15,687	26	8,728	0,000
		BAL	74,965	6	7,908	26	9,480	0,000
	8	PAPH	67,405	7	12,220	25	5,516	0,001
		WG	81,867	7	16,474	25	4,969	0,001
		SWD(B)	12,860	7	4,498	25	2,859	0,025
		CAL	23,086	7	6,472	25	3,567	0,009
		UBAIA	12,985	7	3,586	25	3,621	0,008
		LCIA	125,704	7	13,976	25	8,994	0,000
		BAL	65,497	7	7,877	25	8,315	0,000

Table 3-7(b): Final cluster centers and capacity of torso (below the shoulder) shape

Final Cluster Centers								
Items	Cluster							
	1	2	3	4	5	6	7	8
PAPH	122,7	128,6	125,7	125,4	144,8	128,0	129,3	133,5
WG	82,0	67,8	69,4	65,8	71,0	76,2	76,1	75,5
SWD(B)	34,1	36,8	36,0	37,0	40,0	33,5	37,9	36,7
CAL	40,0	33,5	31,9	35,5	37,0	36,6	31,6	36,8
UBAIA	10,0	4,7	9,0	3,5	7,0	4,9	4,9	6,8
BAL	58,0	36,7	35,3	37,5	37,0	38,7	39,3	37,4
LCIA	13,0	2,5	8,1	-12,0	2,0	2,7	12,5	-2,4
Sample capacity	1	9	4	1	1	8	3	6

3.3 The correlation analysis between the easy-to-measure items and difficult-to-measure items

Among feature measurements used for clustering, some measurement items and methods have particularly stringent requirements for the professionalism of the surveyors and the quality of the measuring instruments and measuring environment,

such as gypsum paper film flattened graph measurement items. Although these measurement items can better express body shape characteristics, this methodology increases the difficulty of data acquisition and is inconvenient for daily measurement. The purpose of correlation analysis is to identify the measurement items that are highly correlated with these items and are convenient for daily measurements, such as chest girth and height. The corresponding linear regression equation was established based on the results of the correlation analysis. According to experts' measurement experience, SL(F), AAL(F), AAL(B), SCD(B), ARW, and SWD(B) (which are not convenient for daily measurement) were selected from the feature measurements. From the correlation analysis shown in Table 3-8, it can be seen that the correlations between each feature measurement and other measurements which are convenient for daily measurement. Therefore, a linear regression equation can be used to express this relationship. Table 3-9 presents the resulting linear regression equations.

Table 3-8: The correlation between principal factors and variables.

Correlations						
	Shoulder		Arm root			Torso
Items	SL(F)	AAL(F)	AAL(B)	SCD(B)	ARW	SWD(B)
AAPW	0,037	.617**	0,010	-0,161	0,272	-0,167
PAPW	0,128	.432*	.371*	-0,004	0,305	-0,100
SW	.358*	0,162	-0,030	-0,214	-0,136	-0,259
SW(T)	.517**	0,155	-0,066	-0,212	-0,108	-0,206
CG	0,012	.636**	0,208	0,004	.489**	-0,252
CAL	-0,112	.420*	-0,121	-.454**	-0,114	-0,298
CBL	-0,145	-0,031	0,154	-0,136	-0,114	.383*
WG	-0,190	.705**	.439*	0,277	.497**	-0,050
BAL	0,030	0,194	0,087	-0,330	0,096	-0,169
CFL	0,183	-0,001	-0,090	-0,310	-0,013	.426*
ARG	-0,137	.519**	0,281	0,268	.427*	-0,034
SL(F)	1	-0,210	-0,098	-0,146	-0,017	-0,157
AAL(F)	-0,210	1	0,240	0,193	.546**	0,105
AAL(B)	-0,098	0,240	1	.445**	0,247	0,274
SCD(B)	-0,146	0,193	.445**	1	0,335	.553**
ARW	-0,017	.546**	0,247	0,335	1	0,237
SWD(B)	-0,157	0,105	0,274	.553**	0,237	1

*. Correlation is significant at the 0.05 level (2-tailed).

**. Correlation is significant at the 0.01 level (2-tailed).

Table 3-9: Linear regression equation between the characteristic factors of arm root, shoulder and torso (below the shoulder) and their variables.

Body Part	Control Items	Linear Regression Equation
Shoulder	SL(F)	6.247 + 0.234 x SW(T) - 0.075 x SW
Arm root	AAL(F)	5.682 - 0.17 x CG + 0.205 x WG +0.399 x AAPW - 0.020 :
	AAL(B)	5.215 + 0.304 x PAPW + 0.205 x WG
	SCD(B)	4.823 - 0.320 x CAL + 0.303 x AAL(B) + 0,503 x SWD
	ARW	-2.466 + 0.059 x CG + 0.069 x WG + 0.064 x ARG
Torso (below the shoulder)	SWD(B)	13.909 + 0.227 x CBL + 0.388 x CFL

3.4 Discussion and validation of the models

3.4.1 Comparing Classification Methods (Before and After Human Body Segmentation)

Many classification methods have been proposed, including clustering based on different classification indicators [192], [193] and cluster methods [68][194]. For example, the International Standardization Organization (ISO) standard [195] classifies male body shapes (as A, R, P, S, and C) using the chest-waist difference. The Chinese standard [196] classifies male body shapes (as Y, A, B, and C) using the chest-waist difference. In Japan, the difference between armpit circumference and waist circumference is used to classify male body types into ten body shapes (as E, EB, BB, B, AB, A, YA, Y, JY, and J) [197]. This means that body shape classification depends on a single variable. However, when classifying body shape, the above methods usually take a global view of the human body, which results in a final clustering result that easily ignores the characteristics of each part of the human body [52]. As shown in Figure 3-4, classification result based on the chest-waist difference or the difference between armpit circumference and waist circumference shows that the same shape (after classification) includes different levels of the shoulder, arm root and torso (below the shoulder) shapes. This classification method thus usually results in fitting problems and the final garment pattern may only fit a few people [198]. However, various parts of the body can be effectively classified using SCM. After combining information on the classified body parts, the final classification results include information on the

whole and part shape features of the human body. SCM effectively remedies the defects of current body shape classification methods, which do not reflect real body shape.

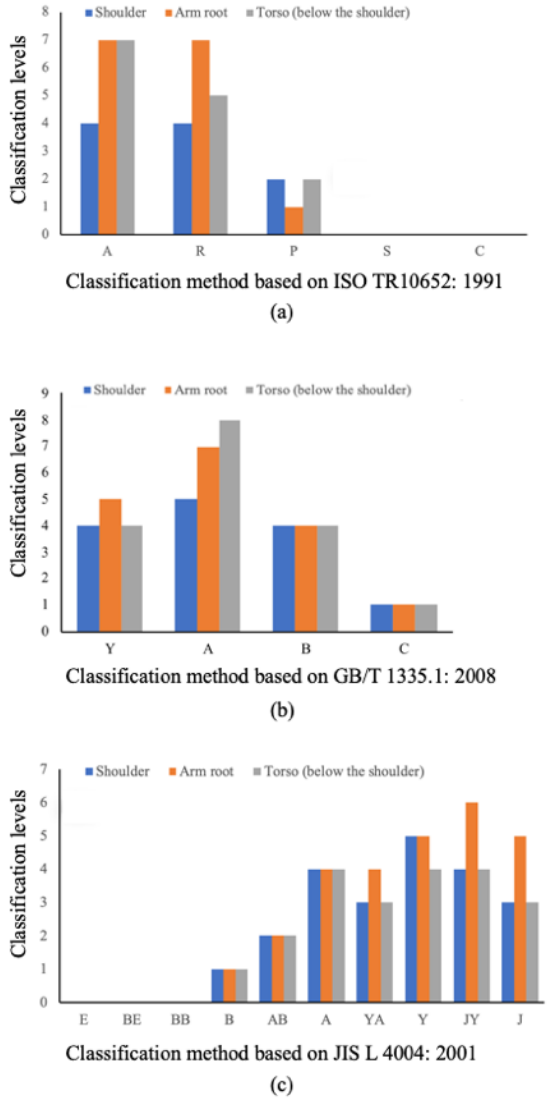

Figure 3-4: Relationship between global and segmented classification results.

3.4.2 Validation of regression effects between easy-to-measure and difficult-to-measure items

In our research, since the measurements will directly influence the results of the body shape classification, the accuracy of the difficult-to-measure items predicted from the easy-to-measure items are important. They must be consistent or have small errors with the data obtained from easy-to-measure items not to affect the accuracy of the body size classification results. Therefore, we validate the proposed regression model by whether

the output of the regression model and the data of easy-to-measure items are consistent. This validation is based on 5 new subjects of the human model. Tables 3-10 show the results provided by the regression models and easy-to-measure items.

The difference between the two results is represented by Model_Error, which is defined as follows.

Let the set of all results predicted by the model be $X = \{x_1, x_2, \dots, x_n\}$ and the set of all results from easy-to-measure items be $Y = \{y_1, y_2, \dots, y_n\}$. . The criterion definition of Model_Error as:

$$\text{Model\_Error}(X, Y) = \sqrt{\frac{1}{n}\sum_{i=1}^{n}(x_i - y_i)^2}$$

Table 3-10: The values of Model_Error for each measurement items.

Items	SL(F)	AAL(F)	AAL(B)	SCD(B)	ARW	SWD(B)
Model Error	0,8062	1,2262	1,3407	1,3104	1,0684	1,3481

In this equation, all results $x_i, y_i \in \{1,2 \dots,33\}$. The values of Model_Error for all the measurement items are listed in Table 3-10. All these errors do not exceed 1.35, which means that the errors for the measurements data are on average lower than 1.35 level of 33 (< 4.1%). Therefore, we can be confident that the proposed model is acceptable.

Conclusion

Based on current trends and developments in the apparel industry, the future of the industry will be intelligent production and mass customization for personalized clothing products. The body segmentation method proposed in this chapter satisfies the concept of mass production and individuation. In the present study, the young male upper body was divided into three parts: the shoulder, torso (below the shoulder) and arm root.

We first classify three body parts by feature measurements into different body shape classes by combining the factor analysis and K-means clustering (Section 3.3, Model

I). Five shoulder shapes, eight torso (below the shoulder) shapes, and four arm root shapes were obtained through this classification, and the intermediate values for each shape were calculated separately. The effectiveness of the new classification method was verified by comparing it with the classical classification methods. In addition, to be a user-friendly measure, relationships between easy-to-measure and difficult-to-measure items are established based on the designer's measurement knowledge and correlation analysis (Section 3.3.2).

Based on the above models, in Chapter 4, a 3D model database (Database II) based on body scans is constructed. The 3D model within the database should accurately reflect the shape of the whole human body and the corresponding features of the segmented body parts. In Chapter 5, the design knowledge base and the final personalized recommendation system will be set up, permitting to design a personalized garment pattern for the user.

Based on the method proposed in this study, the concepts of mass production and individualization can be satisfied simultaneously, enabling producers and consumers to create more reasonable body shapes according to their needs.

CHAPTER 4: 3D Human Upper Body Modelling

Introduction

In the modern apparel industry, three-dimension (3D) human body models, established from data measured by 3D body scanners, have become one of the fundamental elements for the design and fabrication of digital garments. However, the current 3D human body models used in the apparel industry are mostly rigid and lack semantic information on body positions and body parts. Therefore, it is difficult for designers to make accurate, fast and effective designs from these models. This chapter proposes a new parametric 3D human body model based on key position labelling and optimized body parts segmentation. Based on the relation between feature measurements and body part shapes (Model I), obtained from chapter 3, the key positions are labelled on the corresponding 3D body model obtained from 3D body scanning and segment the whole 3D body model into semantically interpretable body parts. In this way, the second database (Database II) has been created, enabling to identify features of all segmented body parts, whose combination corresponds to the whole body shape. Database II includes all 3D body models for various body shapes, labelled and segmented according to the results of Database I, which is mentioned in chapter 3. The adjusted 3D human body model contains important human semantic information on labelled key body position points and features on each body part. Finally, for a specific consumer, his/her personalized 3D body model can be obtained by taking a very few numbers of body measures on himself/herself, selecting the closest body parts from Database II, making an appropriate combination of the selected body parts, and adjusting parameters of all involved body parts.

In this study, we used the operations described previously for conducting parametric modelling of human body shapes. Figure 4-1 shows an overview of the proposed modelling method, a detailed description of the proposed method is presented in the following sections.

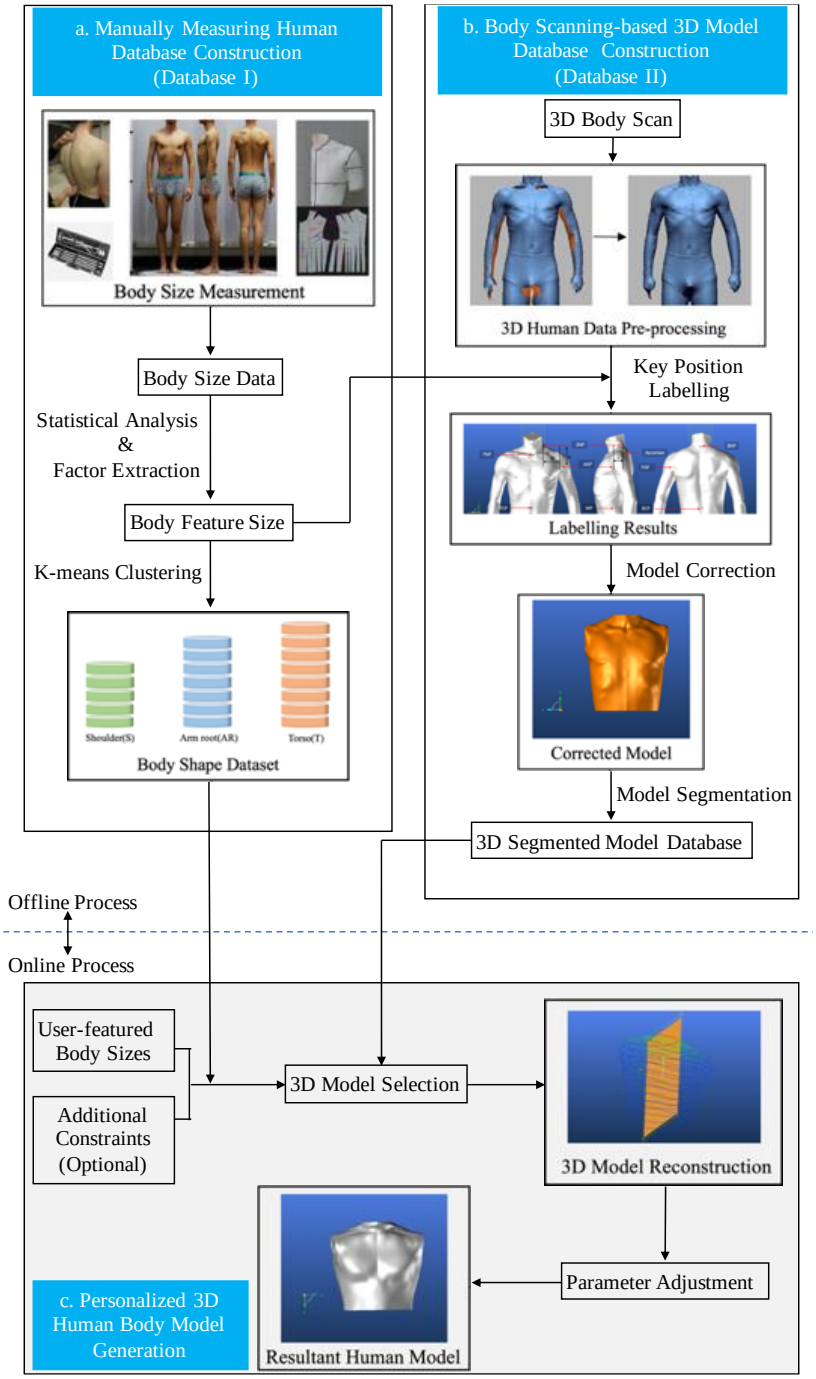

Figure 4-1. Overview of the proposed method.

4.1 3D human body model database construction (Database II)

For construction of the body scanning-based 3D model database, the required 3D model should be able to accurately reflect the characteristics of the whole human body shape and the corresponding segmented body parts. Therefore, all subjects involved in our experiments were scanned using a whole-body range laser scanner. The acquired 3D human body data were then preprocessed using reverse engineering modelling software, permitting filtering and hole filling of the 3D human body model. Second, by combining with the three-view of the human body obtained from the method of two-dimensional photogrammetry, we convert the feature point positions into coordinate positions in the three-dimensional space. Next, we map them onto a preprocessed three-dimensional human body model. Thus, the manually labelled feature points can be transformed into a 3D human model [88]. This step will significantly help the designers to design garments accurately and efficiently on the scanned three-dimensional human body model. The labelled three-dimensional human body model can also provide design references for the segmentation of the potential 3D human body model. Implicitly, human body structures (skeletons, muscles, etc.) can be considered in these labelled feature points on the revised 3D human model, which is initially a rigid geometric surface only. In addition, labelling the 3D human body model also corrects the preprocessed models. Finally, the labelled model is segmented (arm roots, shoulders, and torso [below the shoulders]) using the human body segmentation method mentioned in Section 2.2.2 and databases were constructed separately for each of the three human body parts based on the results of the previously segmented human body shape classification. This ensures that each segmented body part in the 3D model database corresponds to its correspondence in the manually created human body database.

4.1.1 3D human body data preprocessing

The 3D scan data are generally noisy and exhibit defects owing to the inaccessibility of hidden areas. A large hidden area, such as in the crotch and armpit, can result in large holes. Various data pre-processing operations, such as filtering and hole filling, were performed before reconstructing the model. The human model presented in this work is a curved surface defined by a network of basic morphological units on the scanned human body. The realistic rendering of the human model is ensured by the rational selection of these morphological units and human body feature points. The reverse engineering modelling software Geomagic Design X was used to generate CAD models from the scanned data of the subjects.

In this paper, the imported 3D scanned data were pre-processed using Geomagic Design X software as follows [88], [199], [200].

(1) Optimisation of the mesh structure: Apply the "POLYGONES" -> "assistant de reparation" command of Geomagic Design X to the scan model to optimise it.

(2) Hole repair: Apply "POLYGONES" -> "remplier les trous" -> "ajouter un pont" and "remplir le gouffre" command, to repair the holes of the model.

(3) Surface smoothing: Apply "POLYGONES" -> "Lissage" command, to smooth the model and remove surface noise.

(4) Removal of head data: As the head and leg data were seriously missing and not part of this study, the head and leg scan data were removed, as shown in Figure 4-2. Apply "POLYGONES" -> "Fractionner" -> "Selon un plan defini par l'utilisateur" command, to remove the head and leg data.

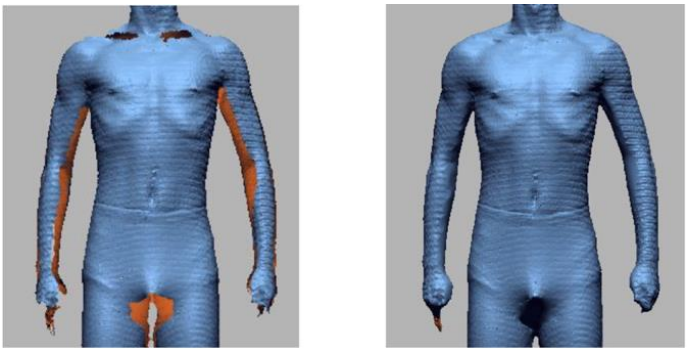

pre-treatment post-treatment

Figure 4-2: Comparison of 3D human body models with pre-treatment and post-treatment. The holes are filled automatically.

4.1.2 Human body model coordinate system setup

The human model is placed in a uniform world coordinate system in certain orientations to facilitate the reconstruction of 3D human body shapes. The main orientations of the human body are aligned with the axes. The six orientations of the human body are usually defined as up, down, left, right, front and back according to the anatomical standards of clothing. The ground on which the human body stands is defined as horizontal. In this paper, the scanner-derived human model is placed in the world coordinate system according to the orientation settings shown in Figure 4-3. The up and down (height) direction of the human body is aligned with the Z-axis, and the top is the positive direction; the left and right (width) directions are aligned with the Y-axis, and the left is the positive direction; the front and back (thickness) directions are aligned with the X-axis, and the front is the positive direction. The plane parallel to the XY plane is defined as the horizontal plane.

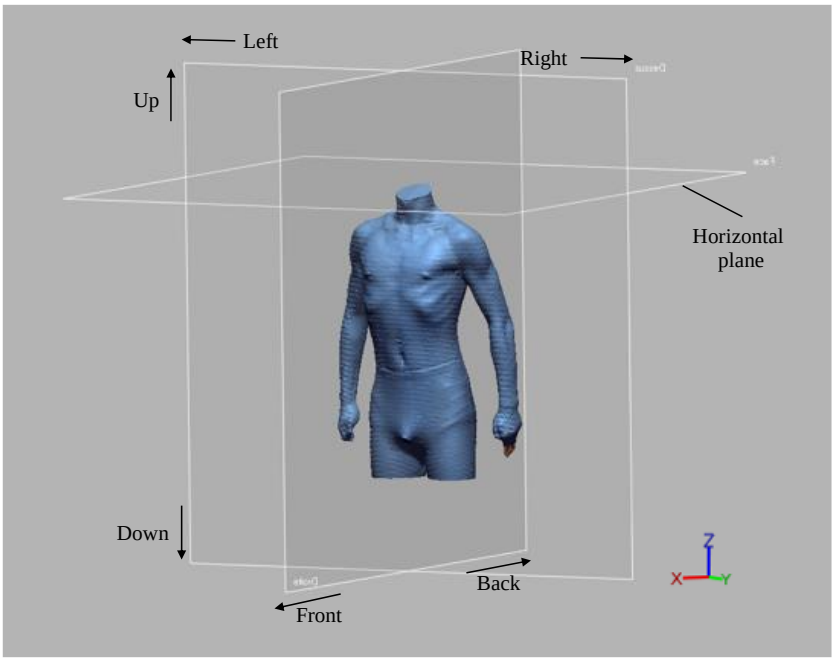

Figure 4-3: Relationship between the orientation of the human body and the coordinate axes.

4.1.3 Human feature information definition

In this paper, the information of anthropometric points, curves and surfaces on the 3D human body model is defined as the feature information of the human body. The human body is complex three-dimensional geometry, and the feature information can easily influence the shape of the human body model. The feature information's quantity and position optimize the human body model's descriptive and discriminative capabilities. Before a 3D human body model can be reconstructed, the reference points, curves and surfaces of the human body model must be defined. In this paper, the main feature information of the human body model is defined as the following types (Figure 4-4).

(1) Feature mesh: A three-dimensional mesh model solid of each part of the human body with geometric information as a triangular mesh model. Figure 4-4 shows that the mesh solid after removing the limbs is used as the feature mesh for subsequent reconstruction.

(2) Feature point: Feature points are the most basic human feature information. Most of the body's measurements are defined by feature points, and the geometric information is the coordinates of spatial points. In addition, the points calculated from

other feature information are also called feature points.

(3) Feature curve: It is the body surface curve, the projection contour curve of the feature grid, the convex wrap curve of the curve and other shape feature information. It can represent the intersection line between the feature section and the feature mesh, such as chest, waist and hip section curves, or the projected contour curve of the mesh entity, such as the minimum outer envelope curve of the upper and lower body of the human body, the front and side contour curves of the human body, etc. The geometric information is represented in Geomagic Design X as a 3D NURBS (Non-Uniform Rational B-Spline) curve.

(4) Feature vector: This refers to information about the body's orientation and the direction and distance between the body's feature points and can also be used to describe the direction of the feature plane (i.e. the normal vector of the plane). For example, the body length direction, frontal orientation and other orientation, the length and direction of the human shoulder slope, etc. The geometric information is the coordinates of the starting point of the vector and the direction and length of the vector.

(5) Feature plane: It is the datum or reference plane that needs to be defined when measuring the human body, such as the body's median plane; the body's bust, waist and hip circumference planes; the left and right arm root planes, etc. The geometric information is a point on the plane and the normal vector of the plane. The characteristic planes are mainly determined by the characteristic points and the characteristic vectors.

(6) Feature dimension: It is the dimensional information calculated based on feature points, feature vectors, feature planes, feature curves and feature grids by certain measurement methods or rules and is non-displayable feature information. Such as the distance between two feature points, X coordinate difference, Y coordinate difference; the length of the feature vector; the angle between two feature vectors; the length of the feature curve; the volume of the feature grid, etc.

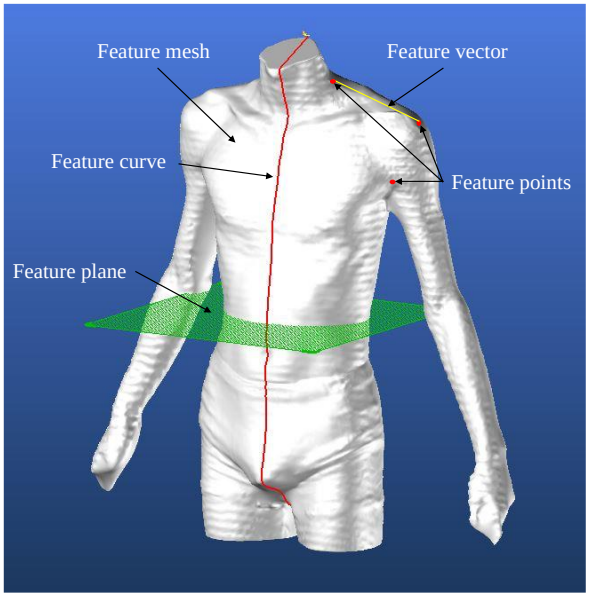

Figure 4-4: Classified representation of human body feature information.

4.1.4 Feature points labelling

4.1.4.1 Feature points definition

The determination of key feature points has been studied previously. An algorithm for locating the axillary fossa was developed by Wang and Lu [201][33]. The goal of the algorithm is to define the axillary point as the position where the arm begins to connect to the body trunk (armpit). Han et al. [202] proposed an algorithm for the automatic recognition of human landmarks, including axillary, lateral neck, and acromion points. The above algorithm can quickly find human feature points on a human model, but its accuracy is closely related to scanning effects when examining the human body. If the scanning effect of the human model is insufficient, the positions of the feature points are very different from those of a real human body. If these points are misplaced, the structure and semantics of the human body cannot be analyzed correctly; this can lead to inaccurate measurement results [203]. To solve this problem, the following operations were performed in this study.

4.1.4.2 Labelling operation process

To implement human-computer interactive modelling, we mark the positions of 10 human feature points on each subject by professional surveyors based on human skeletal features and the extraction results of feature measurement items before scanning. As shown in Table 4-1, these points are adequate to extract the key morphological contours of the male upper body. Combined with the three views of the human body, the ten feature anthropometric points are annotated on the human model by mapping them according to their positional relationship with each other, as shown in Figure 4-5. The operation is as follows:

Table 4-1: List of feature anthropometric points used in this study.

NO.	Body Feature Point	Abbreviation	Definition
1	Fossa Jugularis Point	FNP	The intersection of the line connecting the superior border of the right and left lateral clavicular terminal with the median sagittal plane.
2	Front Central Point	FCP	The intersection point of the waistline with the front central line.
3	Lateral Neck Root Point	SNP	At the lateral cervical triangle, the intersection of the anterior border of the trapezius muscle and the curve connecting the cervical fossa to the cervical point on the lateral part of the neck.
4	Waist Point	WP	The maximum point of lumbar concavity on the left side of the body.
5	Cervical	BNP	The point of the tip of the seventh cervical spine.
6	Back Central Point	BCP	The intersection point of the waistline with the back central line.
7	Anterior Axillary Point	AAP	The point superior to the anterior axillary fissure.
8	Acromion		The most lateral point of the outer edge of the scapula, usually equal to the shoulder height.
9	Posterior Axillary Point	PAP	The point at the upper end of the posterior axillary fissure.
10	Armpit point	AP	The point at the lower edge of the axillary fissure, with a wooden stick inserted to identify this point.

(1) By combining anthropometric definitions and expert experience, six landmarks (feature points) are marked on the real human body. These are the lateral neck root point, waist point, fossa jugularis point, cervical, front central point, and back central point. Before scanning, black marker stickers are labelled on the real human body, as shown in Figure 4-5. Labelled stickers assist the surveyor in finding these points quickly and accurately using 3D human body models.

(2) A three-view photograph of the human body was obtained using 2D photogrammetry techniques. The positions of the feature points were measured and calculated according to the scale marked in Figure 4-5 and the positions of the auxiliary

points. For example, the position of the front armpit point is derived from the position of the lateral neck root point. The width difference (W), height difference (H), and thickness difference (T) between the two points was measured. The lateral neck root point was used as the origin to establish a 3D coordinate system. By adjusting the values of the coordinate system, the relationship between the lateral neck root point and the anterior axillary point was mapped onto the 3D human body model to obtain the position of the anterior axillary point. In this experiment, the process was repeated twice using the lateral neck root point and the waist point as the coordinate origin to reduce the errors generated in the mapping process. The final coordinate values of the feature points were obtained as averages.

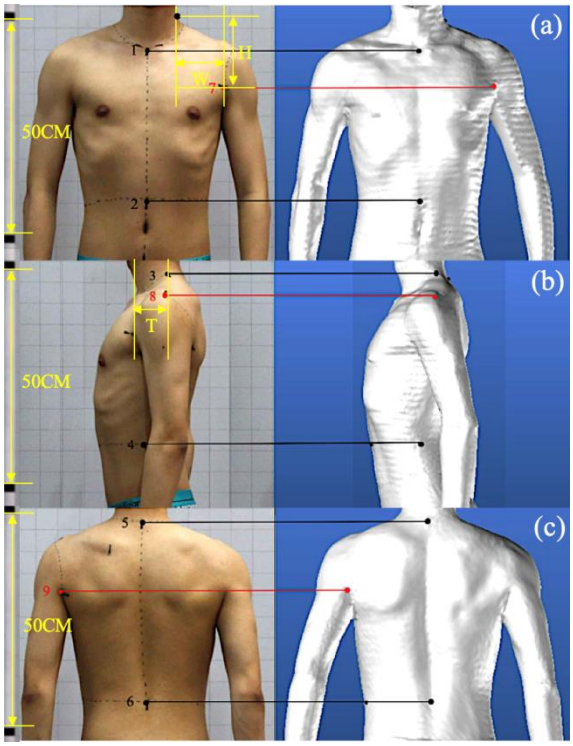

Figure 4-5: 10 feature anthropometric points correspondence for human body: (a) front view; (b) left side view; (c) back view. Both red and black dots denote the land markers used in our experiments. The black dots are the points marked before the 3D scan.

(3) Notably, the armpit point is relatively hidden. Its position cannot be determined directly from a three-view photograph and cannot be mapped from a three-view photograph to a 3D human body model directly. First, the actual height of the armpit

point and the intersection positions of the horizontal line of the armpit with the front-back centre line are first determined according to the definition and scale relationship manually, as shown in Figure 4-6(a). The distances D1 and D2 from the armpit point to the front-back centre line (excluding the dart volume) can then be measured from the paper flattened graph of the body, as shown in Figure 4-6 (a). The position of the armpit point was calculated by combining the cross-section of the horizontal armpit line on the 3D model with the values of D1 and D2, as shown in Figure 4-6 (b). Starting from the intersection of the horizontal cross-section where the axillary point is positioned with the front and back central lines, i.e. C1, C2, respectively. Draw curves with the same length as D1 and D2 along the body surface. If D1 and D2 cross at one point exactly, this is the armpit point position. This position is only an approximate position and is not necessarily accurate and requires continuous adjustment. This will be later described in this section 4.1.6.

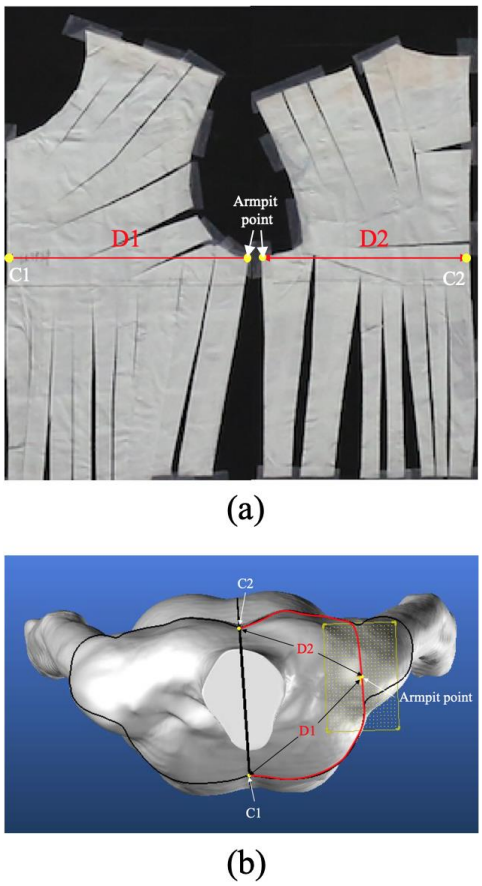

Figure 4-6: (a) Gypsum inner wall flatten graph. (b) Determination of the armpit point on a 3D human body model diagram.

4.1.5 Creation of feature curves

4.1.5.1 Feature curves definition

According to the feature items and feature points, the feature curves are drawn on the surface of the 3D human body, as shown in Figure 4-7(a). The drawing method followed an anthropometric definition, as shown in Table 4-2.

Table 4-2: List of upper body feature curves used in this study.

NO.	Body Feature Line	Abbreviation	Definition
1	Neck Base Girth	NBG	The horizontal circumference length through the lateral neck root point.
2	Shoulder Line	SL	Measure the straight line distance from the lateral neck root point to the shoulder crest point.
3	Upper Chest Girth	AG	The horizontal circumference length through the posterior point of the left and right axilla.
4	Chest Girth	CG	The horizontal circumference measured through the scapula, axilla, and nipple.
5	Minimum Waist Girth	WG	The horizontal circumference of the smallest part of the waist between the inferior border of the ribs and the superior border of the iliac crest.
6	Front centre Line	FCL	The length of the curve from the anterior neck point to the minimum waist circumference on the anterior centerline of the torso.
7	Back centre Line	BCL	The length of the curve from the posterior cervical point to the minimum waist circumference on the posterior centerline of the torso.
8	Lateral Line	LL	Solid length from the waist point to the armpit point.
9	Chest Arc Line	CAL	Solid length of body surface from right anterior axillary point to left anterior axillary point.
10	Back Arc Line	BAL	Solid length of body surface from right posterior axillary point to left posterior axillary point.

4.1.5.2 Operation process

To directly draw the arm root curve on a 3D human body model is unique and challenging. According to the anthropometric definition of arm root circumference, the circumference from the scapula through the anterior and posterior points of the axilla to the starting point. The arm root circumference curve is an irregular closed curve that does not lie in the same plane. Therefore, two different planes are created based on the feature points of the brachial root associated with the brachial root, as shown in Figure 4-7(b). First, we divide the arm root circumferential curve into anterior and posterior arm root curves. The anterior arm root curve is constructed on a red plane with the acromion, anterior axillary points, and armpit points. In contrast, the posterior arm root curve is constructed on a blue plane with the acromion, posterior axillary points, and armpit point, as shown in Figure 4-7(b). The principle is that the curve must pass

through three feature points on the same plane. The completed arm root curve (black curve) is still somewhat different from the real arm root curve of the human body. To obtain a more accurate arm root curve, the parameter values must be set separately. The parameter values are represented by equal lines perpendicular to the black curve. The parameter curves (yellow and green curves) were obtained by joining the other ends of all lines, as shown in Figure 4-7(b). The aim is to change the shape of the arm root curve by adjusting the parameters to obtain the same arm root curve as the real human body. In addition, to create a model closer to the real human body, it is also necessary to draw some human feature lines on the surface of the model, as shown in Figure 4-6(c).

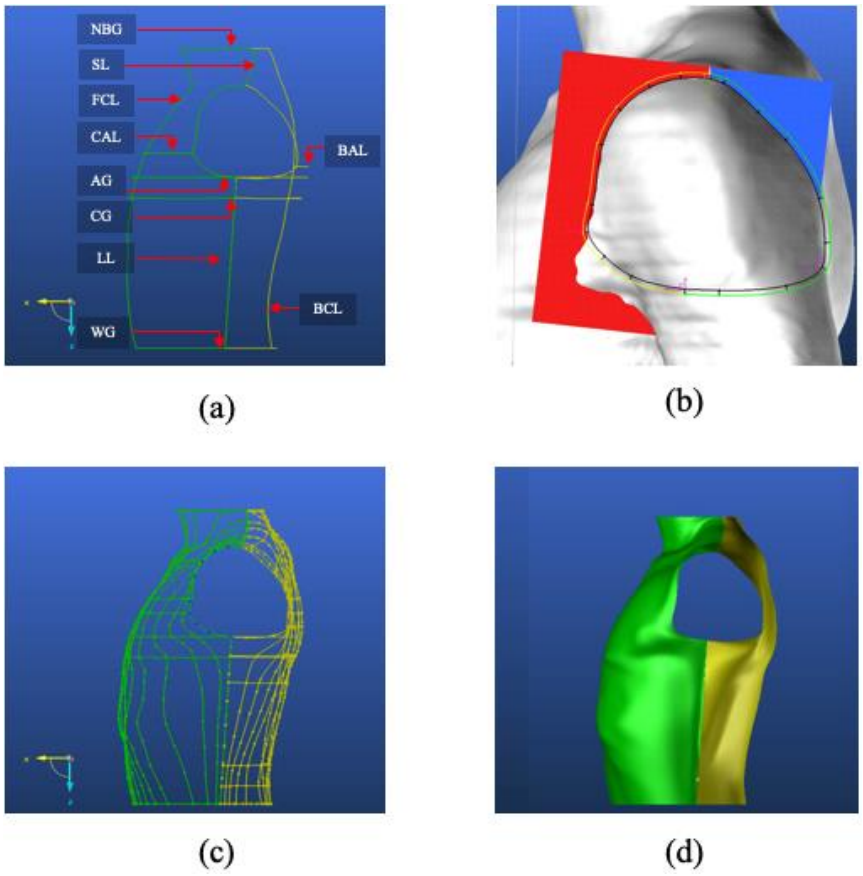

Figure 4-7: Human model reconstruction process using 10 feature anthropometric points and 10 feature curves.

4.1.6 3D surface model creation

The surface model generated from the feature curves is shown in Figure 4-7(d). The new surface model was meshed using the Design Concept 3D (DC3D) software. The surface model is also processed from 3D to 2D to obtain the 2D form of the surface model. The 2D morphology of the 3D model is compared with the part of the arm root curve (dark blue curve) based on the flattened graph of the human paper film, as shown in Figure 4-8(a). Usually, there are differences between the two arm root curves. In that case, they can be made similar by adjusting the parameter values that have been previously set. The overlapped results of the 2D morphology and the real arm root curve show the quality of the morphological similarity given by the method. As the parameters were adjusted, the shape of the 3D arm root changed accordingly, resulting in the revised left half of the human model shown in Figure 4-8(b). To make the body symmetrical, only the surface model from the left side is used to reconstruct the right surface model. Finally, two half surface models are stitched to a symmetrical one to create a unique, complete whole upper body surface model (see Figure 4-8(c)).

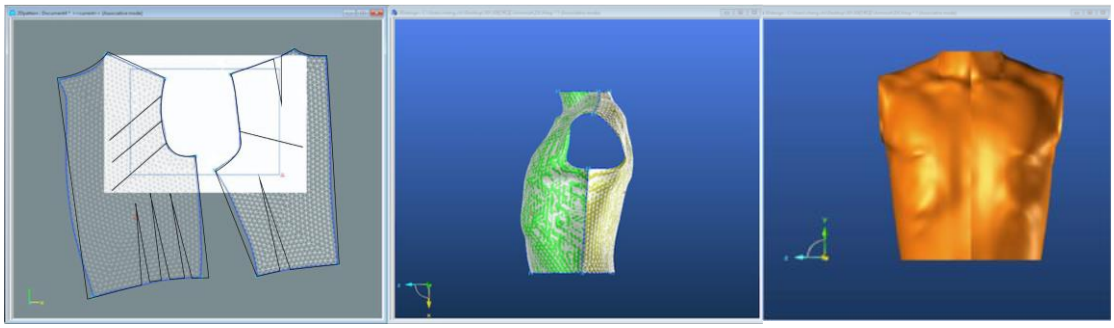

(a) (b) (c)

Figure 4-8: Parametric adaptation process of the arm root curve: (a) A comparison of the 2D morphology of the 3D model with the flattened graph of the human paper film; (b) Adapted arm root shape; (c) Result of 3D human model contour symmetrization.

4.1.7 3D human upper body model segmentation

To create the 3D model bases characterising the three body parts, the corrected models must be segmented manually, as shown in Figure 4-9. To maintain consistency between

the real human body and the 3D human body model, the segmentation method follows the same procedure described in Section 2.2.2. By segmenting the 3D human body model and combining them according to various specific requirements, we can effectively increase the variety of human models and make the final 3D human body model more accurate.

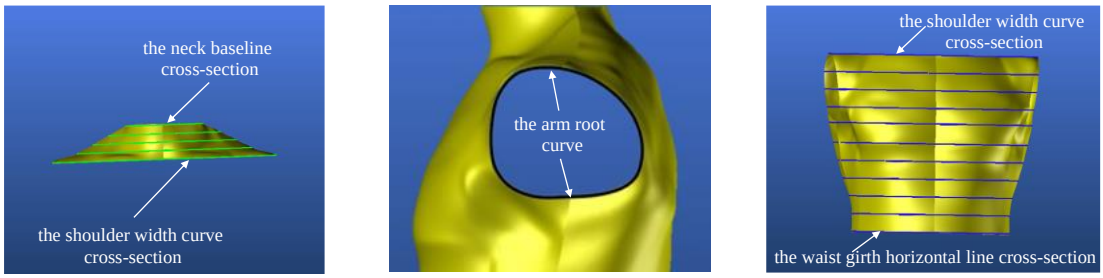

Shoulder part | Arm root part | Torso (below the shoulder) part

Figure 4-9: Segmented body part models and contour lines

4.2 Parametric 3D human body model generation (Model II)

As shown in Figure 4-10, for a specific consumer, the corresponding 3D body part models can be established by inputting a few human body features and matching them with the three databases of the shoulder, arm root, and torso. Then, these three identified body part models were combined and adjusted to obtain the final 3D human body model. The details of this are presented below.

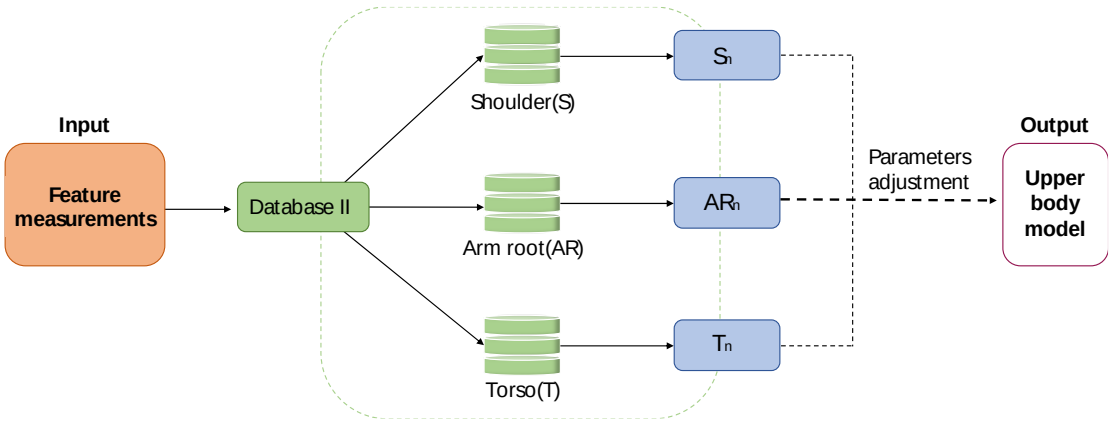

Figure 4-10: Overview of the optimized body parts segmentation modelling method.

4.2.1 Homothetic axe and distribution line creation

Before creating the homothetic axis and distribution line, the morphological contours were transferred by selecting another new space to create the new model. This operation involves transferring the shapes and coordinates of: the shoulder, the torso (below the shoulder), and the arm root (see Figure 4-11). Next, from the three existing body part model databases (shoulder, arm root, torso), we selected the models closest to the body features measured on the relevant features measured from the real body.

For the shoulder and torso below the shoulder, the homothetic axis is defined by the intersection of the sagittal and coronal planes. The sagittal plane was the body-symmetry plane (see Figure 4-11). The coronal plane, which is the body distribution plane, is perpendicular to the sagittal plane and separates the front and back parts of the upper body through two points of the chest contour. The front-to-back ratio is determined by the vertical line passing through the armpit point and perpendicular to the line joining these two points. The line joining these two points corresponds to the line of distribution. The line of symmetry is the line perpendicular to the intersection of the distribution line and the vertical line (see Figure 4-11).

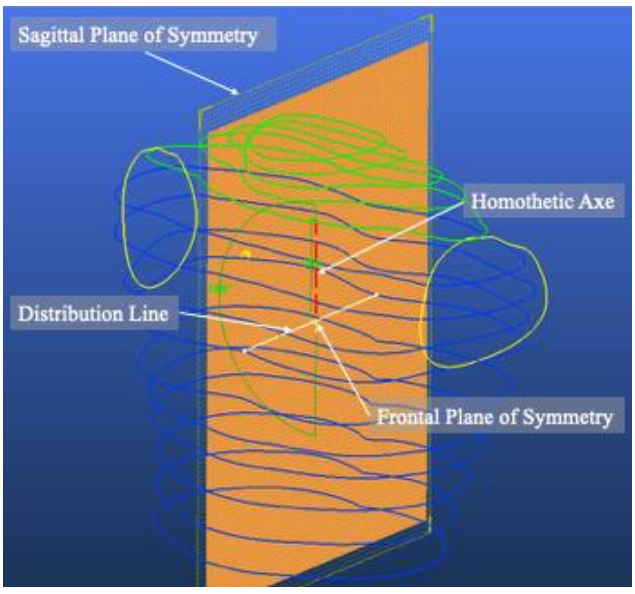

Figure 4-11: Homothetic axe and distribution plane.

4.2.2 Model volumes parameterization

The current human model is combined by selecting three segmented parts. The model of these three parts is only similar in body shape to the new subject but is different in dimension. This step aims to parameterise the volume of these three parts so that the final model is closer to the new subject. We set new contour values for the human model based on the new subject dimensions, as shown in Figure 4-12. The key curve was parameterised according to the key dimensions of the new subject. Moreover, the other curves between key curves were estimated by enlarging or reducing. The scale of enlargement and reduction is determined by calculating the ratio of the corresponding key curves between the new subject and the existing model.

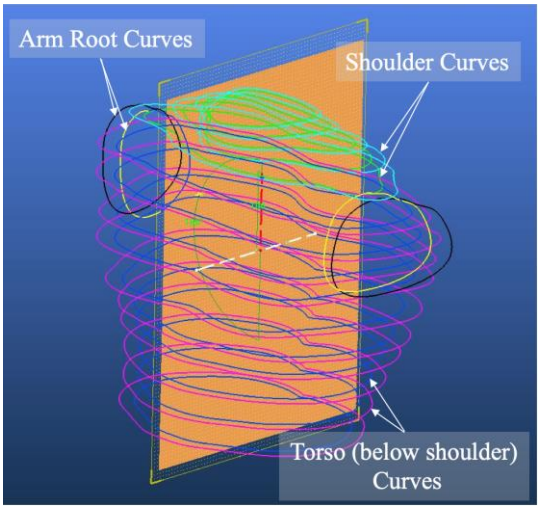

Figure 4-12: Human model volume parameterization process: Arm root contour curves include yellow curves (before adjustment) and black curves (after adjustment); shoulder contour curves include green curves (before adjustment) and light blue curves (after adjustment); below shoulder torso contour curves include blue curves (before adjustment) and pink curves (after adjustment).

4.2.3 Fusion relevant boundary curves

The fusion of the relevant boundary curves between two selected adjacent parts is an important problem to be solved. The relevant boundary curves between two selected adjacent parts are different, as shown in Figure 4-13, where green is the curve belonging to the shoulder and blue is the curve belonging to the torso (below the shoulder). In order to obtain the boundary curves that most closely resemble the real human body,

when fusing the two curves, the first thing that needs to be determined is that the key points on the boundary curves include the two acromions and the intersection of the boundary curves with the front and rear central lines respectively, i.e. the black points. Next, mark all the intersection points between the two boundary curves, i.e. the yellow points. Then, the auxiliary points for drawing the final boundary line are determined, i.e. the white points. The method to determine the position of the white point is to use the curvature calculation tool supplied with DC3D to find and mark the position of maximum curvature in each of the two boundary curves, i.e. the maximum curvature point. Then connect the corresponding maximum curvature points and mark a point in the middle of the line between the two corresponding maximum curvature points as an auxiliary point for drawing the final boundary line. Finally, the Spline (b-spline) tool [204, 205] in DC3D is used to connect all points in order to obtain the final boundary curve, i.e. the red curve.

About the arm root, there are no relevant boundary curves to fuse with the other two parts. Therefore, when determining the position of the arm root curve, it is necessary to align the four feature points contained on the arm root (acromion, anterior axillary point, posterior axillary point and armpit point) with these four points on the torso (below the shoulder). This can be done by adjusting the coordinate positions of the four points.

The final model is shown in Figure 4-14. Based on this method, consumers can design personalised models to meet their individual needs based on this classification system. Designers can also easily find the semantic information about human body features needed for their designs on this model. This method can satisfy both the concepts of mass production and personalisation.

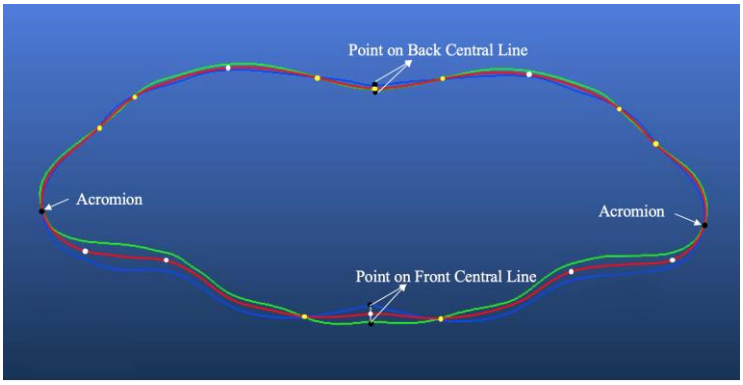

Figure 4-13. The final boundary curve drawing method.

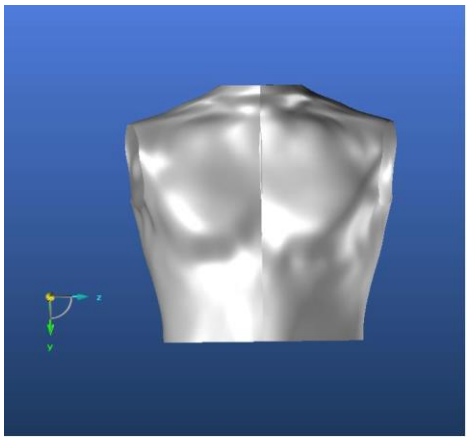

Figure 4-14. The final parametric human body model.

4.3 Discussion and validation of the model

So far, we have mainly introduced methods for correcting 3D human body models based on manual measurements and modelling methods for segmentation-optimized models. To prove the feasibility of these methods, in this section, we evaluate the corrected and reconstructed models separately, in terms of the qualitative and quantitative results, and then provide further discussion. All models were well aligned in Geomagic Design X before the comparison.

4.3.1 Evaluation of the corrected model

Figure 4-15 shows a comparison of the corrected model with the original model. The overlap of the original model (grey in Figure 4-15) with the corrected model (yellow in Figure 4-15) shows the quality of morphological similarity given by our method, as shown in Figure 4-15. The colour bars range from 2.0000 (red) to -2.0000 (blue) in Figure 4-15. The reconstructed model has a similar geometry to that of the original scanned model. Moreover, the corrected model had suitable repair of the arm root area. Reconstruction errors in essential areas, such as the chest, waist, and shoulders, are quite small. In addition, all reconstructed human models have the same topology as the original models, which significantly facilitates the subsequent processing of the garment design. Figure 4-16 shows the overlap between the original scanned model and

corrected model. For example, the shape of the corrected arm root curve (black curve) is significantly repaired relative to the shape of the arm root curve of the original scanned model (blue curve).

Real Scan

Corrected Model

(a)

Three views of real scan and corrected model overlap.

(b)

Three views of real scan and corrected model comparison.

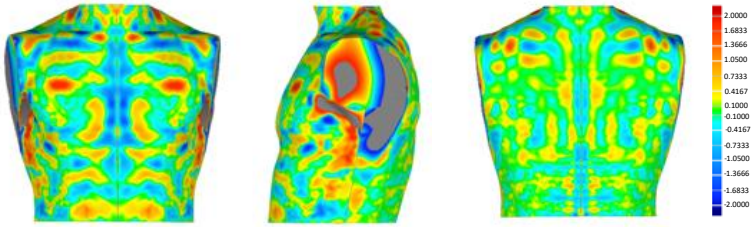

Figure 4-15: Results of male human model correction. The original scanned model is on the left of the first row, and the corrected model is right. (a) gives the results of the overlap between the two models; (b) gives the results of the geometric error analysis between the corrected model and the original scanned model. The color bars range from -2.0000 (blue) to 2.0000 (red) in mm. Green indicates that there is almost no error between the real scans and corrected results.

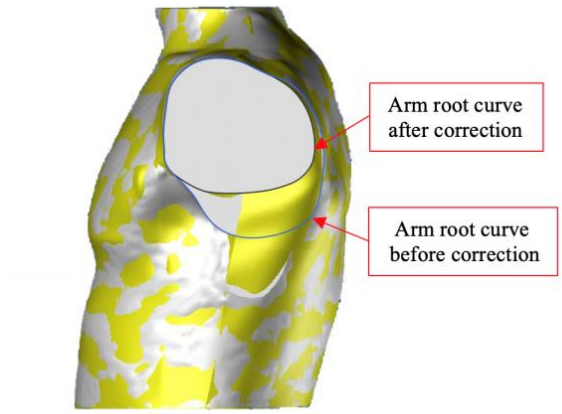

Figure 4-16: Correction results of the arm root area.

From the perspective of quantitative analysis, feature items were measured on 3D human models before and after correction and each of the three body parts shape classification results were compared to demonstrate that manual measurements can effectively be corrected for 3D human models. The accuracy of arm root classification before correction was 42.3% and the accuracy after correction was 87.9% (Table 4-3). The accuracy of shoulder classification before correction was 58% and the accuracy after correction was 85% (Table 4-3). The accuracy of torso (below the shoulder) classification before correction was 68.1% and the accuracy after correction was 87.9% (as in Table 4-3). A comparison of the classification results demonstrated that correction of the scanned 3D human model based on manual measurements and expert experience can significantly improve the accuracy of 3D human models, especially for the hidden areas of the human body (i.e. arm roots).

Table 4-3: Classification accuracy of three body parts.

Body parts		Classification based on 3D model before correction									Classification based on 3D model after correction								
	Existing groups	T1	T2	T3	T4	T5	T6	T7	T8	Classification accuracy(%)	T1	T2	T3	T4	T5	T6	T7	T8	Classification accuracy(%)
Torso (Below the Shoulder)	T1	1	0	0	0	0	0	0	0	100	1	0	0	0	0	0	0	0	100
	T2	0	4	0	0	0	0	5	0	44.4	0	7	0	0	0	0	2	0	77.8
	T3	0	0	1	2	0	0	0	0	25	0	0	3	1	0	0	0	0	75
	T4	0	0	1	1	0	0	0	0	100	0	0	0	1	0	0	0	0	100
	T5	1	0	0	0	1	0	0	0	100	0	0	0	0	1	0	0	0	100
	T6	0	2	0	0	0	4	2	0	50	0	0	0	0	0	6	2	0	75
	T7	0	0	0	1	0	0	1	1	33.3	0	0	0	0	0	0	2	1	66.7
	T8	0	1	0	0	0	0	2	4	66.7	0	1	0	0	0	0	0	5	83.3
	Total	-	-	-	-	-	-	-	-	64.9	-	-	-	-	-	-	-	-	84.7
	Existing groups	AR1		AR2		AR3		AR4		Classification accuracy(%)	AR1		AR2		AR3		AR4		Classification accuracy(%)
Arm root	AR1	4		3		0		0		23.5	13		3		0		0		76.5
	AR2	0		2		0		0		12.5	2		9		0		0		75
	AR3	0		0		1		0		33.3	0		0		3		0		100
	AR4	0		0		0		1		100	0		0		0		1		100
	Total	-		-		-		-		42.3	-		-		-		-		87.9
	Existing groups	S1		S2		S3				Classification accuracy(%)	S1		S2		S3				Classification accuracy(%)
Shoulder	S1	5		0		2				62.5	7		0		1				87.5
	S2	0		6		0				54.5	0		9		0				81.8
	S3	3		0		8				57.1	2		0		12				85.7
	Total	-		-		-				58	-		-		-				85

Note：Unit, number of people; Red font numbers indicate effective classification.

4.3.2 Evaluation of the segmentation-optimised model

To verify that the parametric modelling method proposed in this paper is suitable for different body shapes. Three samples with large differences in body shape have been selected by designers and surveyors experience for validation, namely slim body shape, normal body shape and plump body shape. Figure 4-17 compares the reconstructed model using the segmentation optimisation method for the human body with the model which is obtained by adjusting the dimensions of the template model for the Asian body shape supplied in CLO 3D software (A 3D fashion design software that supports virtual garment visualization as a fashion-forward simulation technique), all adjusted sizes are the real sizes of the corresponding subjects. The corrected model is aligned with the segmentation-optimised model and the template model of the corresponding dimensions, respectively. The overlap results show that our method yields a much higher morphological similarity than the template model. For normal body shape, the colour bars range from 24.9977 (red) to -24.9977 (blue) and from 55.2077(red) to -55.2077 (blue) in Figure 4-17. For plump body shape, the colour bars range from 19.5007 (red) to -19.5007 (blue) and from 32.0499(red) to -32.0499 (blue) in Figure 4-17. For slim body shape, the colour bars range from 25.3998 (red) to -25.3998(blue) and from 40.5999(red) to -40.5999 (blue) in Figure 4-17. This proves that the segmentation optimised human body model is more similar to the corresponding

scanned human body model. This also proves that the modelling method proposed in this study is superior to the template-based modelling method, no matter for which body shape.

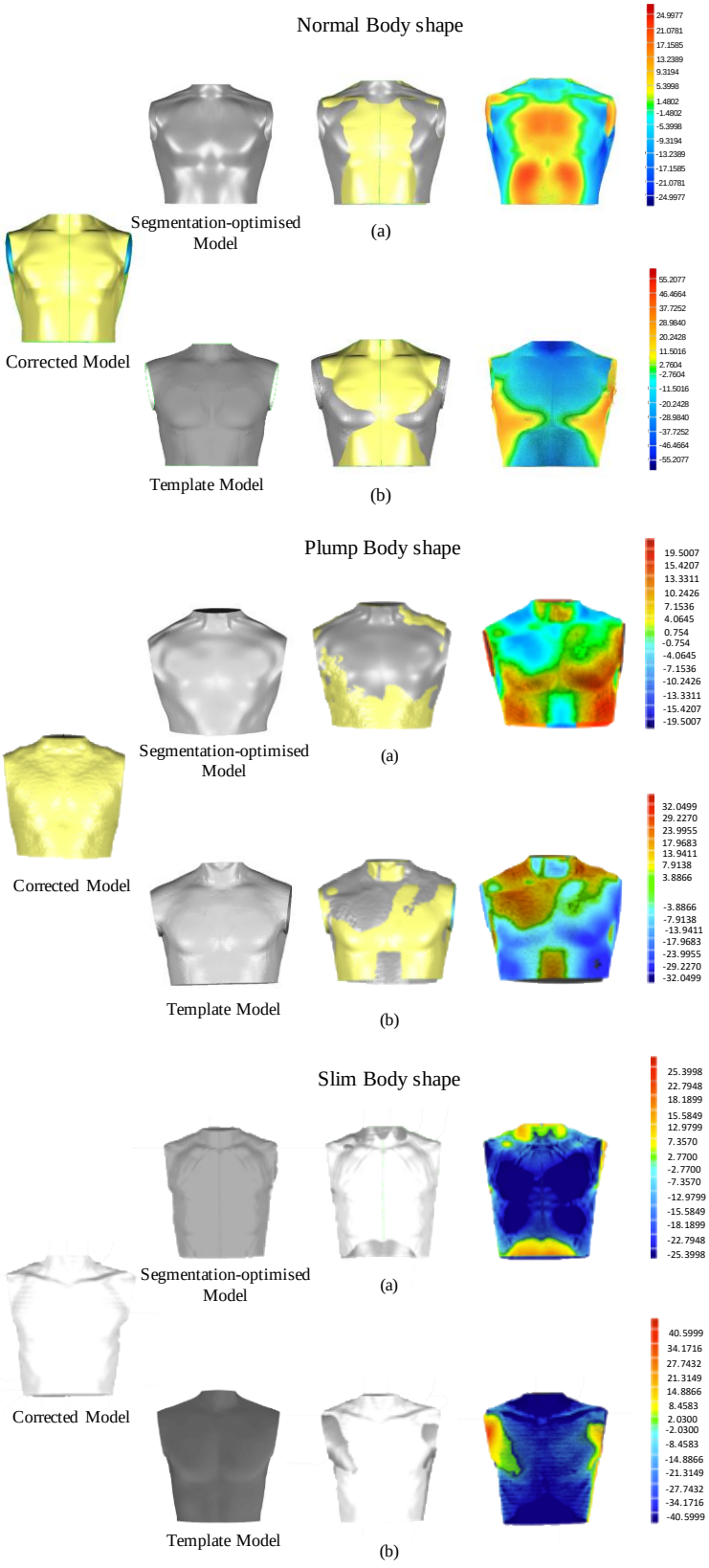

Figure 4-17: Comparison of segmentation-optimized modelling results and template modelling results. In (a) and (b), the results of the segmentation-optimized and template models are shown in the left section, respectively, the overlap with the corrected model is shown in the middle section, and the geometric errors are shown in the right section, described the gap between the two models and the target model, respectively. The unit of measurement in the color plot is mm.

Conclusion

In the current apparel industry, the existing scanning-based 3D human body models are primarily rigid surfaces and lack a semantic interpretation on body structures and body compositions. Therefore, designers cannot find relevant body positions for accurately and efficiently making garments on these 3D human models. In this situation, this chapter proposes a new parametric 3D human body modelling approach by using professional designer's knowledge for key position labelling and body parts segmentation. First, expert experience-based manual measurements are used for acquiring more accurate and interpretable human body data in order to identify different levels of the three segmented body parts, i.e. arm roots, shoulders and torso. Manual measurements and design knowledge are successfully used to improve the defects of the scanning-based 3D human body model and label the key body positions on it. From a comprehensive quantitative analysis, we find that the accuracy of the hidden areas (caused by human-self occlusion) of the 3D human body model (e.g. arm roots) related to the real human body has been improved by 45.6% after correction. The accuracy of the shoulders and torso also improved by 27% and 19.8% respectively. Second, the corrected human models for these three segmented body parts can be combined to obtain a complete model of the upper body. The model contains the body part features and labelling information for the feature points within each body part area. In general, the proposed modeling procedure can largely improve the accuracy and interpretability of the scanning-based 3D human models, making them more available for garment designers. The effectiveness of this procedure has been visually and quantitatively

validated by the effects of the human body reconstruction.

In the chapter 5, the feasibility of these corrected 3D human models in the apparel industry will be further explored by developing a number of relevant garment design processes.

CHAPTER 5: Parametric Garment Pattern-making

Introduction

Garment pattern-making is one of the most important parts of the apparel industry. However, traditional pattern-making is an experience-based work, very time-consuming, and ignores the body shape difference. This chapter proposes a parametric design method of garment pattern based on body dimensions acquired from a body scanner and body features (body feature points and three segmented body part shape classification) identified by designers according to their professional knowledge. From the above parametric 3D human body modelling method (Model II), we generate a 3D human upper body model which is semantically interpretable (feature points labelling). The 3D personalized basic pattern is drawn on the parametric model based on these feature points. By using three-dimensional to two-dimensional (3D-to-2D) flattening technology, a 2D flatten graph of the 3D personalized basic pattern of the interpretable model is obtained and slightly adjusted to the form suitable for industrial production, i.e., PBP, and the PBP database (Database III) is built. In addition, there are three models that need to be built, including a basic pattern parametric model (Model III) (characterizing the relations between the basic pattern and its key influencing human dimensions (chest girth and back length)), a regression model (Model IV) which enables to infer from basic pattern to PBP for three body parts based on the one-to-one correspondence of key points between the PBPs and the basic patterns, and a personalized shirt pattern parametric model (Model V) (characterizing the structural relations between the personalized shirt pattern (PBP_{Shirt}) and PBP).

Finally, we construct a men's shirt pattern recommendation system oriented to personalized fit. The initial input items of the recommendation system are the body dimension constraint parameters, including chest girth, back length, and the body

feature dimensions used to determine each body part shape, as well as three shirt style constraint parameters (slim, regular, and loose). Using Model III, the corresponding basic pattern can be generated through the user's chest girth and back length. Body feature measurements determine the three body parts shapes. Then, Model IV is used to generate the PBP for the corresponding body parts shape. Based on the shirt style chosen by the user, Mode V is used to generate the PBP_{Shirt} from the PBP. The output of the recommendation system is a fit oriented PBP_{Shirt}. Moreover, if the PBP_{Shirt} is unsatisfactory after a virtual try-on, four adjustable parameters (front side-seam dart, back side-seam dart, waist dart, and garment bodice length) are designed to adjust the PBP_{Shirt} generated by the proposed recommendation system. The proposed recommendation system combines the designer's knowledge of manual measurement of the human body, traditional 2D pattern-making methods, and 3D-to-2D flattening technology to generate personalized shirt patterns automatically and quickly, thus significantly improving pattern-making efficiency. A detailed description of the proposed method is presented in the following sections.

5.1 3D basic pattern design and 2D basic pattern flattening

5.1.1 Types of basic patterns

The basic pattern is relatively easy to fit all shapes and sizes, simplifies the creation of the pattern and is the basis for all design work. The basic pattern for menswear is mainly for the upper body, which is predominantly on the left side of the body, so only the left side of the body is drawn for pattern making. The basic pattern is drawn based on the chest, as this is the easiest to draw, conforms to the body shape and provides the best shape. The details are determined by the proportions of the chest measurement, a method known as the bust measurement system. The prototype is semi-fitted with just the right amount of space to allow movement without compromising function. There is additional space to accommodate the length and width of the design and the contours

of the design lines. The main advantage is that both chest darts and shoulder darts are clearly defined, which makes it easier to understand how the darts should be deployed and the design developed.

The basic pattern can be divided according to the pattern-making method into the proportional method, the short measure method, and the combination method [16].

(1) The proportional method involves measuring the wearer's chest, back and arm lengths and using the chest as a base for calculating the pattern dimensions of other parts of the body. The correlation between the chest and other body parts (such as collar width or back width) varies from one individual to another. The main consideration in setting the formula is the average correlation and hence the suitability of the formula.

(2) The short measure method, i.e. drawing the dimensions of each part of the human body after taking precise measurements. As the paper pattern is drawn using individual measurements, it is possible to obtain a good fitting basic pattern if the drawing is correct. However, as the human body is soft and prone to measurement errors, it is important to have the correct measurement data in addition to the correct mapping theory.

(3) The combination method, i.e. the combination of the proportional method and the short measure. This method has been used in schools in Japan for a long time.

5.1.2 Personalized basic pattern (men) database construction (Database III)

After generating a personalized parametric 3D human body model (in Chapter 4), a 3D basic pattern can be designed on the 3D human body model. The top garment pattern is a basic pattern that covers the upper body of the human body and reflects the body shape information. It is a simplification and flat approximation of the complex body surface. It corresponds structurally to the feature points, curves and surfaces of the human body. Therefore, the basic pattern structure lines (left part only) are drawn on the model first, based on the correspondence between the basic pattern parts and the

body following the body wearing the basic pattern, as shown in Figure 5-1 (a). Then, using the 3D-to-2D flattening technology generates the 2D flattened graph of the basic pattern, as shown in Figure 5-1 (b). Finally, the 2D flattened graph is slightly modified to meet the requirements for industrial production, i.e., PBP, as shown in Figure 5-1 (c). The PBP obtained by this method will be used for overlapping comparison with the New Bunka basic pattern for the corresponding subject.

In addition, the design of the 3D basic pattern must include several darts to generate a 2D flattened graph [206]. The dart locations of the basic pattern are determined according to the structural features of the human body, the common structure of garments in the design and the location of the common darts and partition lines. After the location of each feature points on the 3D basic pattern have been determined, the basic pattern drawn according to the proportional method is measured to obtain the lengths of the darts. Then, the equal lengths of the darts are drawn on the 3D basic pattern, as shown in Figure 5-1 (b).

Figure 5-1: The PBP making process: (a) Drawing the basic pattern structure lines; (b) Generating 2D flattened graph of basic pattern; (c) Making the PBP.

5.2 Parametric modelling of the personalized basic patterns (men) (Model IV)

To research the method of personalized parametric garment pattern-making for different styles on the PBP, this chapter takes the personalized parametric pattern-making for the men's shirts body as an example, focusing on the calculation model, plotting method, and programming of the front and back piece pattern structure of the

basic pattern and PBP*shirt*, as well as the regression model from basic pattern to PBP.

5.2.1 Basic pattern parametric pattern-making method (Model III)

5.2.1.1 Calculation model of the basic pattern

In the structural making of the New Bunka Men's upper body basic pattern [12], the key variables include chest girth and back length, as shown in Figure 5-2. After the calculation based on these key variables and the structural relationships inherent in the garment pattern, the values of the other secondary parameters are determined. Table 5-1 shows the expressions of the secondary parameters based on the key parameters. Regarding the darts, the New Bunka Men's upper body basic pattern contains the front chest dart, the back scapular dart, and the waist darts (a, b, c, d, e). The front chest dart and back scapular dart can be obtained by using the formulas in Table 5-1. The volumes of waist darts are assigned as shown in Table 5-2.

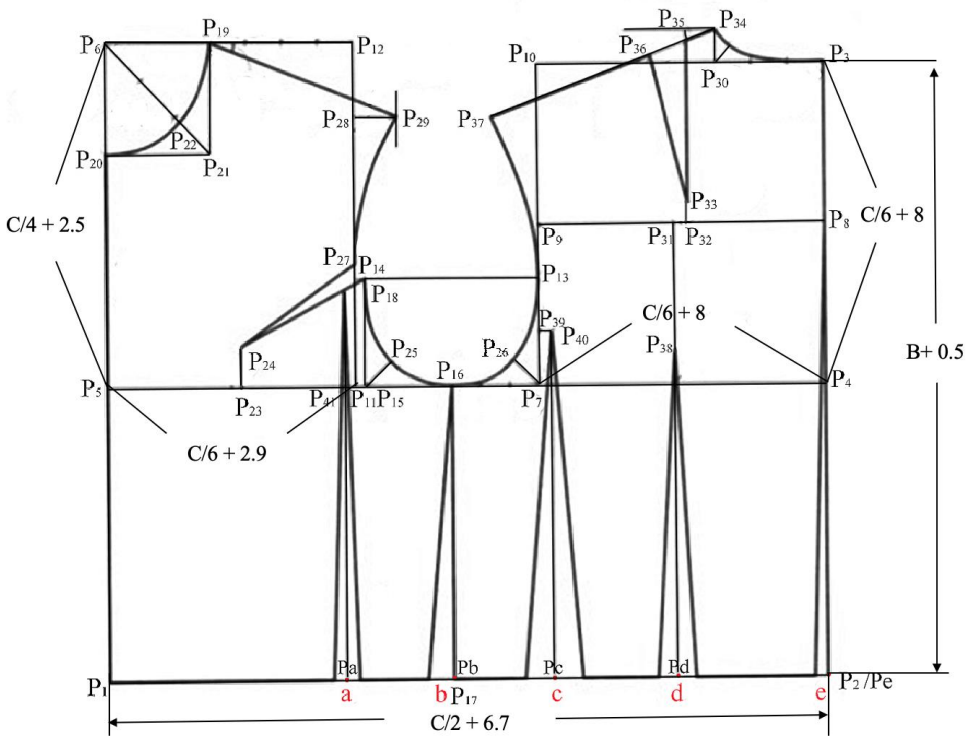

Figure 5-2: Structure of New Bunka men's basic pattern. C stands for chest girth and B stands for back length. Red font a, b, c, d, e are waist darts.

Table 5-1: Structural relationship between dimensions of New Bunka men's basic pattern.

	No.	Line	Dimensioning formula
Basic Lines	1	P1P2, P4P5	C/2+6,7
	2	P2P3	B+0,5
	3	P3P4, P7P10	C/6+8,5
	4	P1P5, P2P4, P16P17	B-(C/6+8)
	5	P4P7, P8P9, P3P10	C/6+5,8
	6	P3P8, P9P10, P4P8, P7P9	(C/6+8,5)/2
	7	P5P6, P11P12	C/4+2,5
	8	P5P11, P6P12	C/6+2,9
	9	P11P15, P14P18	0,7
	10	P7P15, P13P18	C/6-2,7
	11	P7P13, P15P18, P11P14	(C/6+8,5)/3
Contour Lines	12	P6P19, P20P21	C/16+1,9
	13	P6P20, P19P21	C/16+2,4
	14	P6P22	2/3* $\sqrt{(C/16+1,9)^2+(C/16+2,4)^2}$ +0,5
	15	P12P19	5C/48+1
	16	P28P29	1/4*(5C/48+1)+0,5
	17	P5P23	1/2* (C/6+2,9)+0,7
	18	P23P24	(C/6+8,5)/6-1
	19	P24P27, P18P24	P14P24=P18P24
	20	P15P25, P7P26	1/6* (C/6-2,7)+0,5
	21	P3P30	C/16+2,2
	22	P9P31	1/2* (C/6+5,8)+0,5
	23	P31P32	1
	24	P32P33	1,5
	25	P30P34	1/3* (C/16+2,2)-0,3
	26	P35P36	C/32
	27	P19P29	cos22∘*(5/4*(5C/48+1)+1/2)
	28	P34P37	cos22∘*(5/4*(5C/48+1)+1/2)+C/32
	29	P12P28	tan22∘*(5/4*(5C/48+1)+1/2)
	30	P31P38	(C/6+8,5)/2+-2,5
	31	P7P39	(C/6+8,5)/6
	32	P39P40	1
	33	P11P41	0,8
Angle	34	∠ P25P15P16	45∘
	35	∠ P39P7P16	45∘
	36	∠ P12P19P29	22∘
	37	∠ P42P34P37	21∘

Note: C stands for chest girth and B stands for back length. All units are in cm.

Table 5-2: Distribution of waist dart volume of New Bunka men's basic pattern.

Total dart volume	a	b	c	d	e
100%	16%	16%	36%	24%	8%
4	0,64	0,64	1,44	0,96	0,32
5	0,80	0,80	1,80	1,20	0,40
6	0,96	0,96	2,16	1,44	0,48
7	1,12	1,12	2,52	1,68	0,56
8	1,28	1,28	2,88	1,92	0,64
9	1,44	1,44	3,24	2,16	0,72
10	1,60	1,60	3,60	2,40	0,80
11	1,76	1,76	3,96	2,64	0,88
12	1,92	1,92	4,32	2,88	0,96
13	2,08	2,08	4,68	3,12	1,04
14	2,24	2,24	5,04	3,36	1,12
15	2,40	2,40	5,40	3,60	1,20

Note: All units are in cm.

5.2.1.2 Coordinates value measurement

After being drawn, the intersections of the front and back center lines with the waistline are used as the coordinate original points respectively (P1 and P2 in the New Bunka Men's upper body basic pattern in Figure 5-2). The relative coordinates of each key point of the front and back pieces are calculated. The coordinates of the key points of the New Bunka Men's upper body basic pattern are shown in Table 5-3.

Table 5-3: Coordinates of the key points of New Bunka men's basic pattern.

Point	Coordinate	
	X	Y
P1	0	0
P2	C/2+6,7	0
P3	C/2+6,7	B+0,5
P4	C/2+6,7	B-(C/6+8)
P5	0	B-(C/6+8)
P6	0	B+C/12-5
P7	C/3+0,9	B-(C/6+8)
P8	C/2+6,7	B-C/12-3,75
P9	C/3+0,9	B-C/12-3,75
P10	C/3+0,9	B+0,5
P11	C/6+2,9	B-(C/6+8)
P12	C/6+2,9	B+C/12-5
P13	C/3+0,9	B-C/9-62/12
P14	C/6+2,9	B-C/9-62/12
P15	C/6+3,6	B-(C/6+8)
P16	C/4+2,25	B-(C/6+8)
P17	C/4+2,25	0
P18	C/6+3,6	B-C/9-62/12
P19	C/16+1,9	B+C/12-5
P20	0	B+C/48-7,4
P21	C/16+1,9	B+C/48-7,4
P22	C/16+1,9-(5C+76)/40 *(1/3-1/2* $\sqrt{(C/16+1,9)^2+(C/16+2,4)^2}$	B+C/48-7,4+(5C+192)/80 *(1/3-1/2* $\sqrt{(C/16+1,9)^2+(C/16+2,4)^2}$
P23	C/12+2,15	B-(C/6+8)
P24	C/12+2,15	B-5C/36-91/12
P25	C/6+3,6+cos45∘*(1/6* (C/6-2,7)+0,5)	B-(C/6+8)+sin45∘*(1/6* (C/6-2,7)+0,5)
P26	C/3+0,9-cos45∘*(1/6* (C/6-2,7)+0,5)	B-(C/6+8)+sin45∘*(1/6* (C/6-2,7)+0,5)
P27	C/6+2,9	$\sqrt{(C/12+1,45)^2+(C/36+29/12)^2-(C/12+3/4)^2}$ + B-5C/36-91/12
P28	C/6+2,9	B+C/12-5-tan22∘*(5/4*(5C/48+1)+1/2)
P29	37C/192+3,65	B+C/12-5-tan22∘*(5/4*(5C/48+1)+1/2)
P30	7C/16+4,5	B+0,5
P31	5C/12+3,3	B-C/12-3,75
P32	5C/12+4,3	B-C/12-3,75
P33	5C/12+4,3	B-C/12-2,25
P34	7C/16+4,5	B+C/48+28/30
P35	5C/12+4,3	C/48+13/30-tan21∘*(C/48+1/5)
P36	5C/12+4,3-cos21∘*C/32	C/48+13/30-tan21∘*(C/48+1/5)-sin21∘*C/32
P37	7C/16+4,5-cos21∘*(cos22∘*(5/4*(5C/48+1)+1/2)+C/32)	B+C/48+28/30-sin21∘*(cos22∘*(5/4*(5C/48+1)+1/2)+C/32)
P38	5C/12+3,3	B-C/6+10,5
P39	C/3+0,9	B-5C/36-79/12
P40	C/3+1,9	B-5C/36-79/12
P41	C/6+2,1	B-(C/6+8)

Note: C stands for chest girth and B stands for back length.

5.2.2 A regression model enabling to infer from Basic pattern to personalized basic pattern

From the geometric perspective, a garment pattern can be considered as a set of geometric elements, including points, lines, and curves [207]. In this study, the points are considered as the basic elements to construct a basic pattern. By connecting the points, the outline of the basic pattern can be obtained. Therefore, the first step to adjust the basic pattern is to adjust the coordinate position of the key points that build the basic pattern. The 2D coordinate systems for the front and back pieces have been established separately by using the FCP and BCP as the origin, as shown in Figure 5-3. The coordinates of the corresponding points on the basic pattern and the PBP are measured separately. According to the position of the coordinate points, a linear regression model of the key points on the PBP and the corresponding key points on the basic model are developed. To make the final obtained personalized basic pattern which is oriented to fit, the body parts feature differences should be considered. The basic pattern is also considered as a combination of three parts in this study based on upper body shape segmentation results. The basic pattern is made of points, straight lines, and curves. Therefore, in this study, the segmentation of the basic pattern should consider the key feature points contained in each part and the coordinate position of the key feature points, as shown in Figure 5-4. Since there is a one-to-one relationship between the body shape and the basic pattern, body part shape differences are considered when the linear regression model is built.

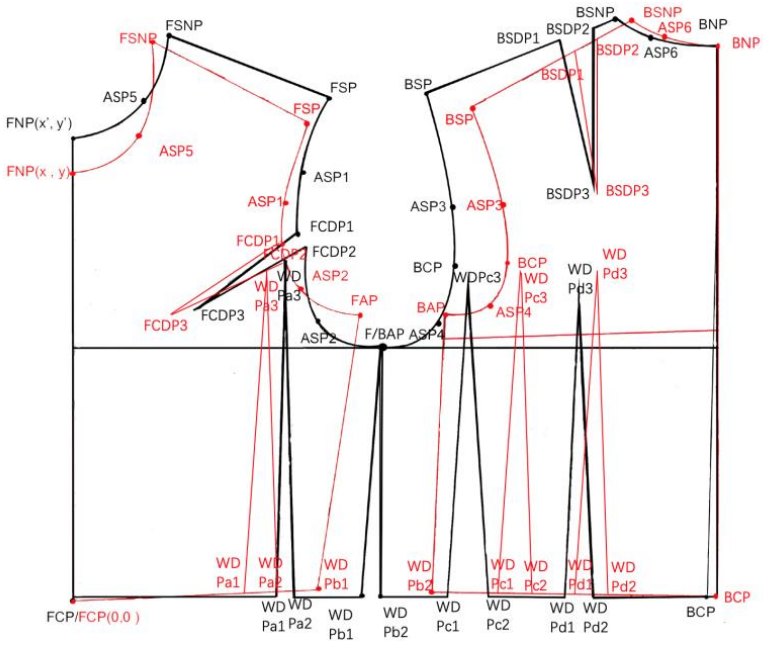

Figure 5-3: Correspondence points on the New Bunka basic pattern (Black) and PBP (Red).

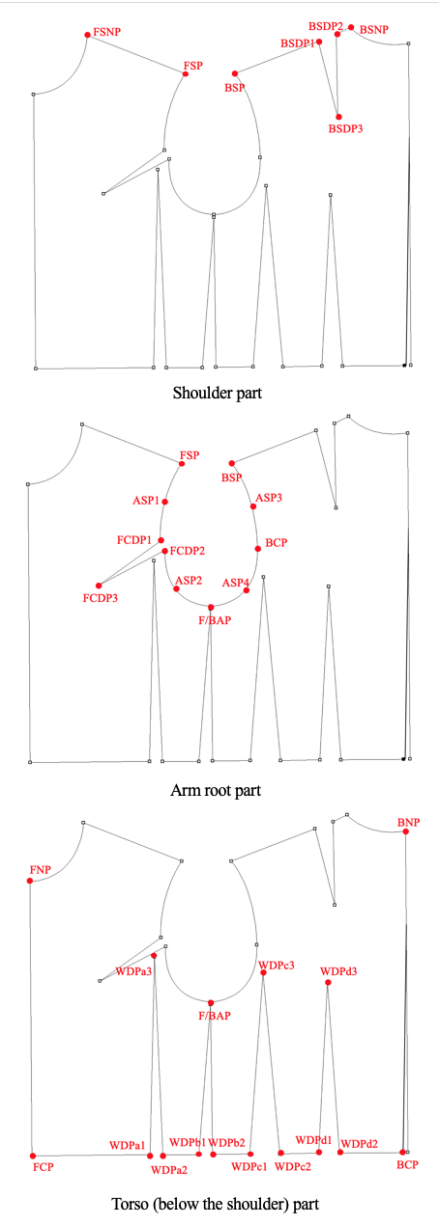

Figure 5-4: Key feature points on garment pattern.

About shoulder part, the key points on the front shoulder are FSNP and FSP, and the points on the back shoulder are BSP, BSDP1, BSDP2, BSDP3, and BSNP, as shown in Figure 5-4. The coordinates of these seven key points are measured on the PBP and the basic pattern, respectively. The linear regression models are built based on the shoulder shape classification results and the coordinate values, as shown in Figure 5-5.

As above, the key points about arm root part on the front arm root are FSP, ASP1, FCDP1, FCDP2, FCDP3, ASP2, and FAP, and the points on the back arm root are BSP, ASP3, BCP, ASP4, and BAP, as shown in Fiure 5-4. The coordinates of these twelve

key points are measured on the PBP and the basic pattern, respectively. The linear regression models are built based on the arm root shape classification results and the coordinate values. The key points about torso (below the shoulder) part on the front piece are FNP, FCP, WDPa1, WDPa2, WDPa3, FAP, and WDPb1, and the points on the back piece are BNP, BCP, WDPb2, WDPc1, WDPc2, WDPc3, WDPd1, WDPd2, and WDPd3, as shown in Figure 5-4. The coordinates of these fourteen key points are measured on the PBP and the basic pattern, respectively. The linear regression models are built based on the torso (below the shoulder) shape classification results and the coordinate values.

According to the regression models, the coordinates of the points on the PBP can be predicted from the coordinates of the points on the basic pattern.

Figure 5-5: Key feature points linear regression models on shoulder.

Shoulder shape	S1		S2		S3	
Coordinates	X	Y	X	Y	X	Y
FSP	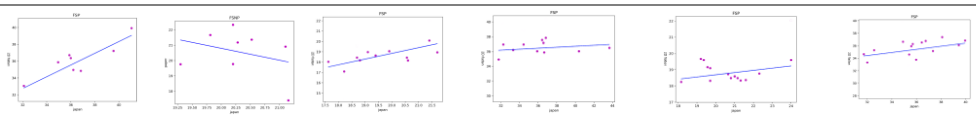					
FSNP	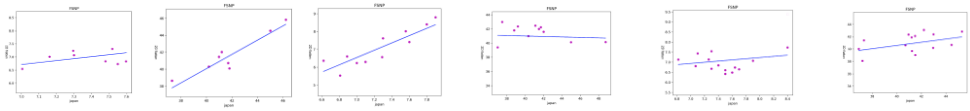					
BSP	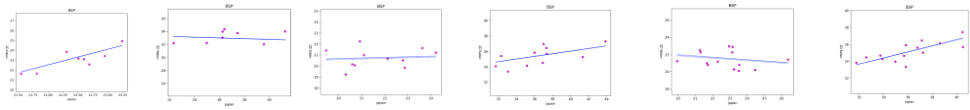					
BSNP	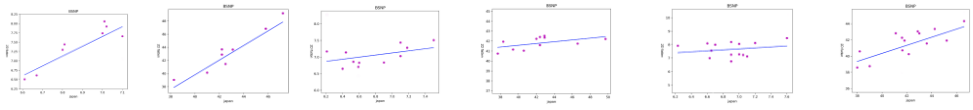					
BSDP1	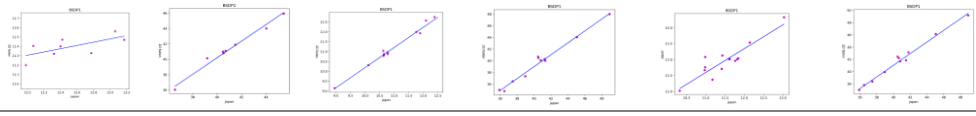					
BSDP2	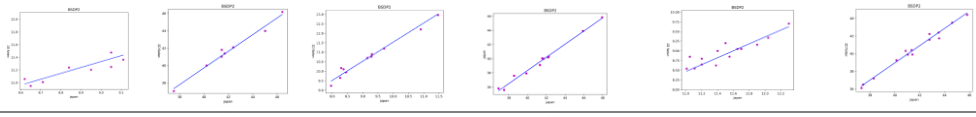					
BSDP3	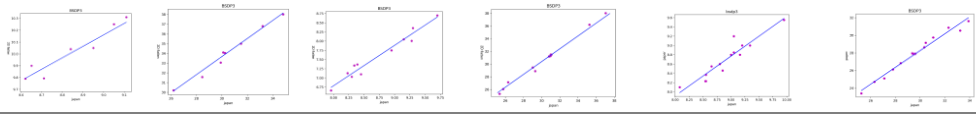					

5.2.3 Personalized basic pattern plotting method

After obtaining the final coordinates of each key point, the matpoltlib package of Python is used to draw straight lines on the basic pattern [178], [208], [209]. Drawing curves on the PBP outline is relatively complicated. In this paper, the Bézier curve model [210][211][212] is used to accurately draw the armhole curves (FSP-ASP1-FCDP1, FCDP2-ASP2-FAP, BSP-ASP3-BCP-ASP4-BAP), the front collar girth curve (FSNP-ASP5-FNP), and the back collar girth curve (BSNP-ASP6-BNP) (see Figure 5-3). The Bézier curve model is:

$$B(t) = \sum_{i=0}^{n} \binom{n}{i} (1-t)^{n-i} t^{i} = \binom{n}{0} P_0 (1-t)^{n} t^{0} \binom{n}{1} + P_1 (1-t)^{n-1} t^{1} + \cdots$$
$$+ \binom{n}{n-1} P_{n-1} (1-t)^{1} t^{n-1} + \binom{n}{n} P_n (1-t)^{0} t^{n}, t \in [0,1]$$

Where,

P_i are the control points on the Bézier curve, P0 is the starting point, Pn is the end point, and n is the order label of the points, starting from 0, and i is the order of the points, indicating the i-th point in the label, from 0 to n;

t represents the length of a point on the line segment from the starting point divided by the length of the line segment and takes the value of [0, 1], representing the change from 0 to 1.

The function Bézier curve (x, y) is written in Python based on the general formula of the Bézier curve. The input x is an array of horizontal coordinates of all points, and y is an array of vertical coordinates of all points. In this chapter, when drawing the cuff curve, four auxiliary points are used to determine the shape; when drawing the back and front collar curve, one auxiliary point is used to determine the shape separately.

In this study, a function program for PBP parametric pattern-making is written, named def PBP (C, B). The initial parameters in the function represent the chest girth and back length dimensions, respectively. When this program is running, the def PBP is called directly in the Command Window. The values of the initial parameters are entered to obtain the corresponding PBP directly.

5.3 Parametric modelling of the personalized men's shirt pattern (Model V)

5.3.1 Types of men's shirt style

The earliest shirts were discovered in Egypt around 3000 BC, showing that the shirt was made up of three simple pattern pieces: the lower front piece, the lower back piece and the upper front piece attached to the upper back piece, which was attached to the sleeve at the shoulder [213][214]. Since this time, although the shape of the shirt pattern has developed and changed, the basic shape of the shirt pattern is still very similar [215][216]. Over the last hundred years, the style and shape of the shirt have evolved, for example, from loose fits that allow for more movement with wide shoulders and a wider chest to slimmer fits that are narrower from the shoulders to the chest and waist, providing the wearer with a slimmer look. In addition, a wide variety of combinations of cuffs, sleeve lengths, collar and collar frame styles, coupled with decorative buttonhole plackets, shirts have developed into a large market in the apparel industry. Figure 5-6 shows some details of the front and back of the shirt.

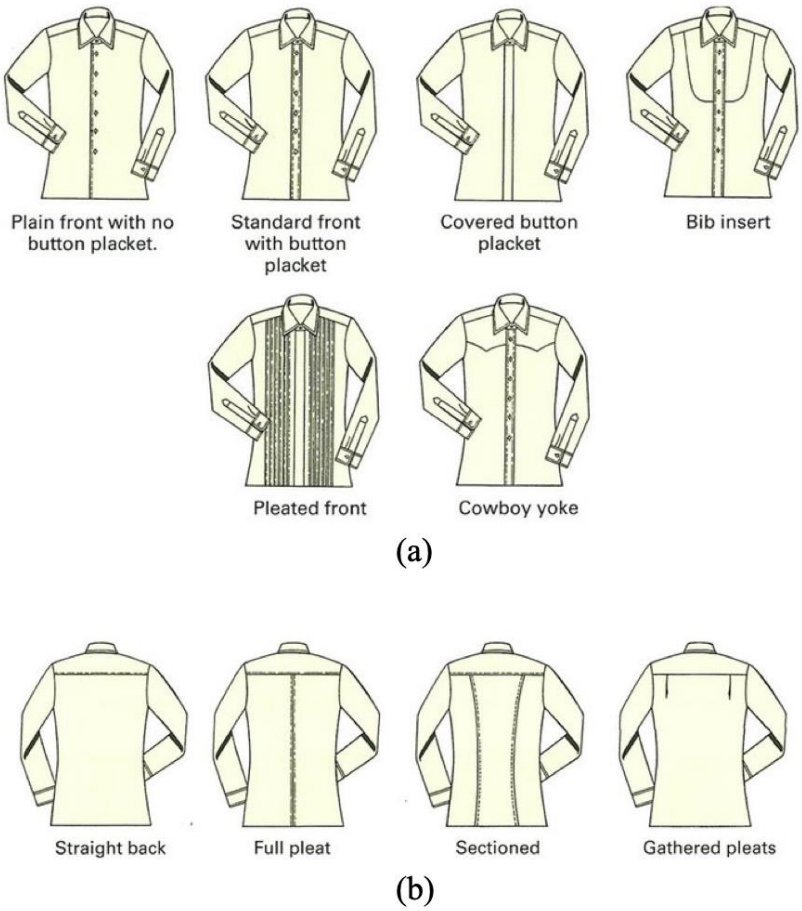

Figures 5-6: (a) Detail of the front of the shirt illustrated. (b) Detail of the back of the shirt illustrated [214].

With the upgrading of consumption and aesthetics, consumers are increasingly focused on individuality, comfort and fit. The men's tailored apparel market shows huge potential for consumer growth, especially among young men, where shirts are among the most popular categories. Therefore, this study uses the shirt as a carrier. The shirt is more complete in terms of structural design, unlike the T-shirt with fewer structural variables to study and the suit with more variables involved. Shirts are a necessary clothing category for the workplace, especially for men's shirts, which have a large market demand. It has often been the topic of study in many researches [131], [217]–[219]. The style of the shirt, which represents the specific contour and shape of the shirt around the torso, is usually classified as slim, regular fit and loose.

5.3.2 Men’s shirt pattern parametric pattern-making method

5.3.2.1 Relationship between shirt pattern and basic pattern

The PBP obtained in this study can be directly applied to generate different styles of shirt patterns, including slim, regular, and loose. The principle is based on the prototyping method, where the structured lines are lengthened, shortened, expanded, and contracted according to the PBP to generate the garment patterns for different styles, as shown in Figure 5-7. Although the pattern of men's shirts includes the front and back pieces, collar, and sleeves [215], [216], this study focuses on improving the fit of the garment, so we mainly consider the generation of the front and back pieces of the garment. The generated shirt pattern is named PBP$_{Shirt}$. The structured relationship between the PBP and the PBP$_{Shirt}$ is shown in Table 5-4.

The pattern structure analysis shows that differences of the shirt styles depend on two factors: the waist dart of the back piece and the dart of the side seam. After the parametric pattern is built, if the user is not satisfied with the style effect, the adjustable input (dart ease allowance) and appearance parameter (garment length) can be modified to quickly produce a personalized shirt pattern. The expressions can be given a definite value for each user's specific dimension and requirement so that one person can have one garment pattern.

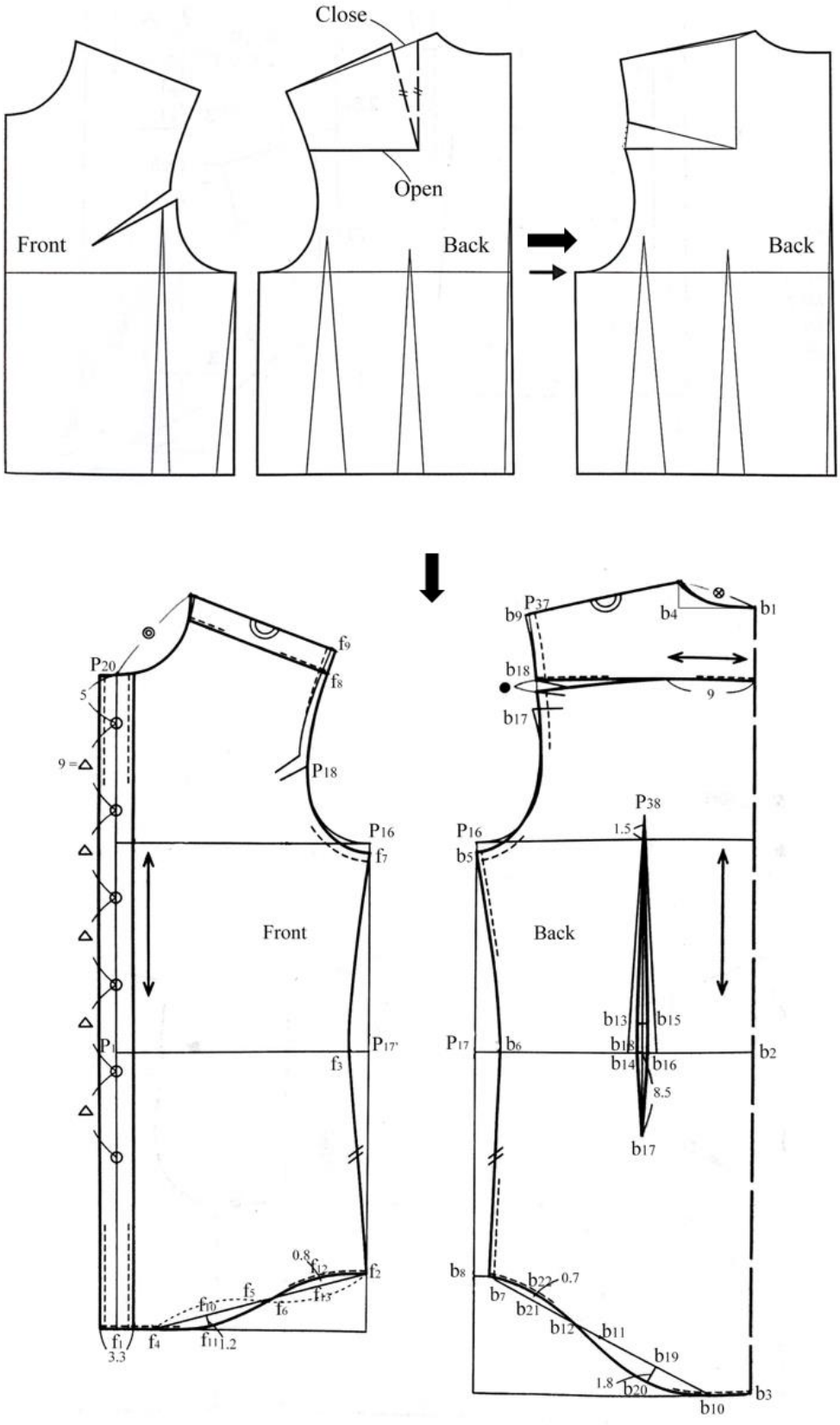

Figure 5-7: Men's shirt body pattern making method based on PBP pattern.

Table 5-4. Rules for changing from PBP to men's shirt bodices.

Garment pattern	Line	Rule changes	Garment pattern	Line	Rule changes
Back	b1b2	B+0,5	Front	f1P1	29
	b2b3	35		f1f4	2
	b1b4	N/5-0,5		f5f6	1,5
	b5P16	1		f4f5, f2f5	1/2* f2f4
	b6P17	2,5		f4f10	1/2* f5f4
	b8P17	23		f6f13	1/2* f6f2
	b7b8	1,5		f10f11	1,2
	b3b10	4		f12f13	0,8
	b10b11	1/2* b7b10		f7P16	1
	b11b12	3		f3P17'	2
	b13b14, b15b16	5		f8f9	2,5
	b13b15, b14b16	1			
	b17 b18	8,5			
	b11b19	1/2* b11b10			
	b20b19	1,8			
	b21b7	1/2* b7b12			
	b21b22	0,7			
	•	2/5*b17b18			

Note: N stands for neck girth and B stands for back length. All units are in cm.

5.3.2.2 Personalized shirt pattern plotting method

According to the final coordinates of each key point on the basic pattern and the changing rules, the matpoltlib package of Python is used to draw straight lines on the shirt pattern. Moreover, the Bézier curve model is used to accurately draw the armhole curves, front collar girth, back collar girth, front and back hem curves (see Figure 5-7). In this study, a function program for PBP*Shirt* parametric pattern-making is written, named def PBP*Shirt* (PBP). The initial parameters in the function represent the basic pattern plotting based on chest girth and back length dimensions. When this program is running, both the def PBP and def PBP*Shirt* are called directly in the Command Window. The values of the initial parameters are entered to obtain the corresponding PBP*Shirt* directly.

5.4 Garment fitting evaluation

The fit of a garment has a significant impact on whether a customer chooses the garment [220][221]. The evaluation of garment fit can be very useful for clothing buyers if there is no actual designer involved. In this case, this section presents an application based

on a garment virtual try-on strain map to evaluate the fit of a garment pattern derived from the recommendation system proposed in this study.

For a specific user, a personalized human body model based on chapter 4 is used for the garment virtual try-on. Next, a garment pattern is recommended for this user based on the parametric pattern-making method presented in Chapter 5. Then, the garment is tried on and evaluated virtually in 2D-to-3D using CLO 3D software [125][222]. The steps are as follows.

(1) Import user-specific 3D personalized human body models (without limbs) (Figure 5-8(a)) and personalized garment patterns (front pieces, back pieces, button plackets) (Figure 5-8(b)) respectively, and determine the coordinate orientation and scale of the 3D personalized human body model and personalized garment patterns when importing.

(2) Then, the garment patterns are assembled on the personalized human body model (Fig. 5-8(c)). Next, the assembled patterns are sewn together to form a 3D virtual garment (Figure 5-8(d)).

(3) Finally, the pressure of the digital garment is measured by a strain map (Figure 5-8(e)).

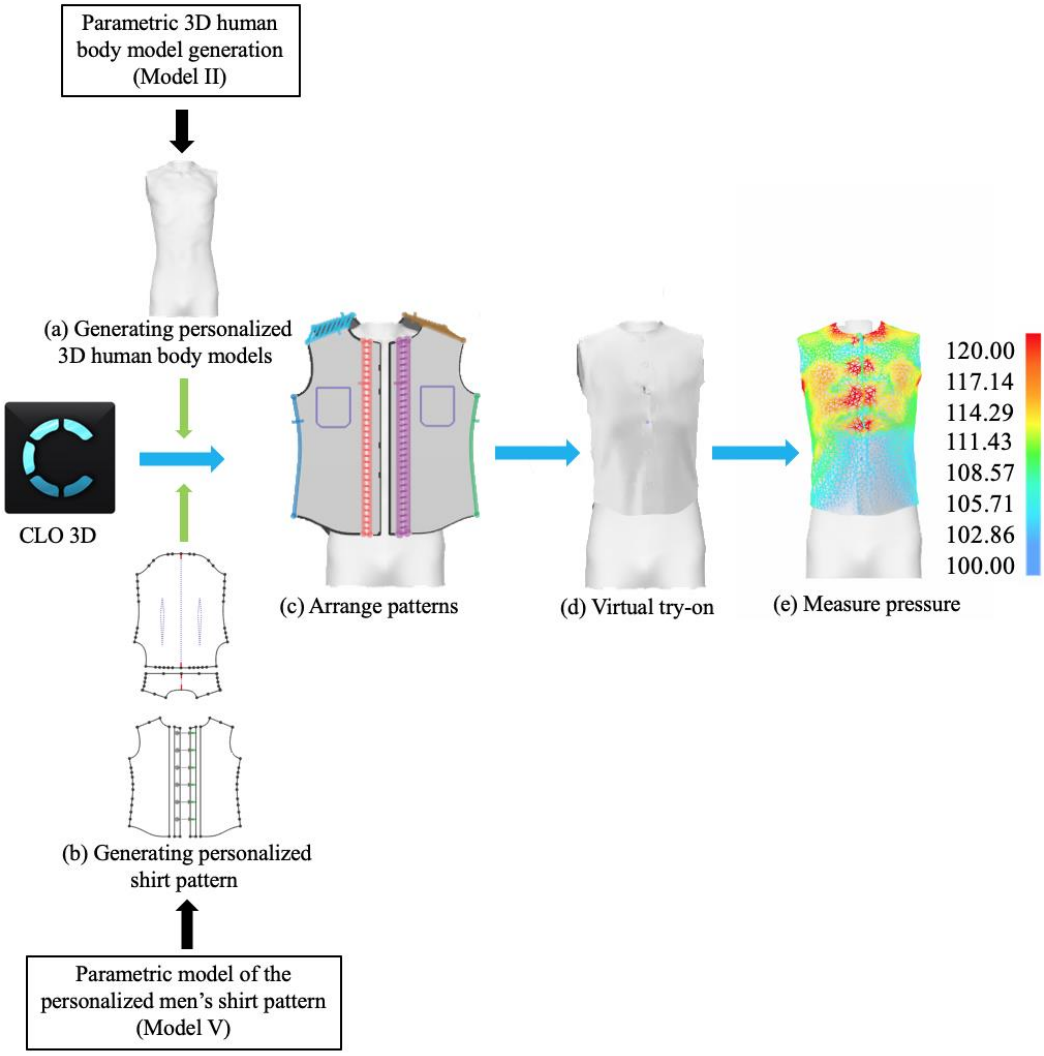

Figure 5-8: 2D-to-3D virtual try-on process.

Before evaluating the virtual garment, the user takes a few minutes to understand the method and purpose of the evaluation based on the designer's knowledge. During the evaluation process, the user observes a strain map of the virtual try-on. This observation involves a static view from different angles (front, back, left, right, top and bottom). The fit evaluation of the garment virtual try-on is achieved mainly through the results of the strain map in four areas (chest, back, shoulders, arm roots).

During the fit evaluation process, if the user feels that the design result of the recommended garment pattern is not what he/she expected, he/she can adjust it by adjusting the amount of ease allowance. This procedure is repeated until satisfaction with the result is obtained. Otherwise, the recommended design solution is accepted.

5.5 Fit-Oriented personalized shirt pattern Recommendation System

Based on integrating the above databases and models, the general framework of a fit-oriented personalized men's shirt pattern recommendation system is proposed, as shown in Figure 5-9. The system is an intelligent recommendation system for users with feedback and adjustment functions.

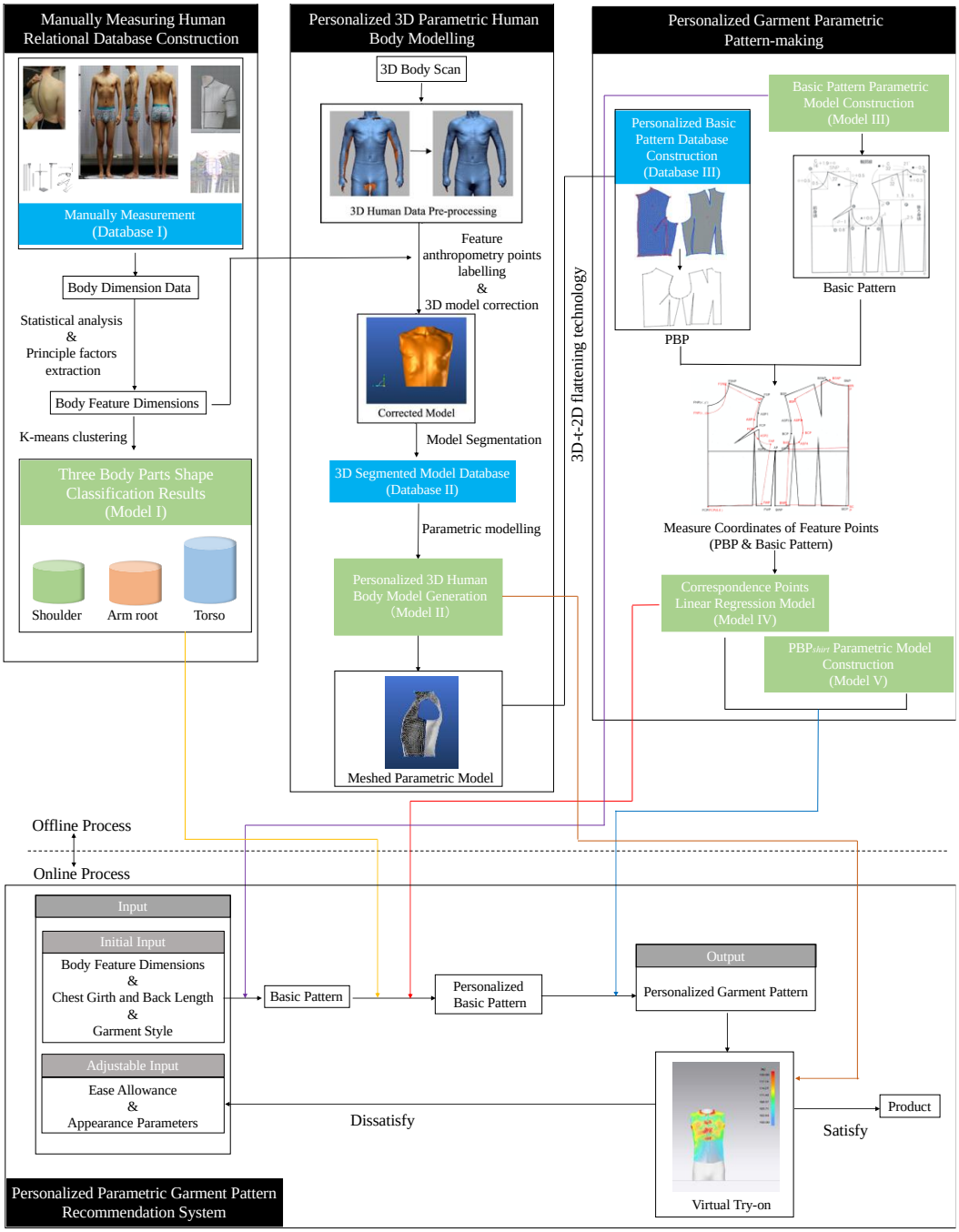

Figure 5-9: Overview of the proposed recommendation system.

5.5.1 Design of the system framework

The system consists of three databases and five models. The three databases include a human body database (Database I), a database of corrected 3D human body parts (Database II) and a personalized basic pattern (PBP) database (Database III). The five models include a relational model between feature measurement items and body shape (Model I), a parametric model for generating personalized 3D human body (Model II), a relational model between key body dimensions (bust and back length) and basic patterns (Model III), a relational model between basic patterns and PBP corresponding to key points (Model IV), and a relational model between PBP and PBP*shirt* (Model V). The input of the recommendation system is a user interface. The initial input items of the recommendation system are the body dimension constraint parameters (chest girth, back length), and the body feature dimensions (SW, SL(F), FSA for shoulder shape; AAL(F), AAL(B), SCD(B), ARW for arm root shape; PAPH, WG, SWD(B), CAL, UBAIA, BAL, LCIA for torso shape) used to determine each body part shape, as well as three shirt style constraint parameters (slim, regular, and loose), used to determine the style of the final recommended shirt's pattern. Using Model I, the user's body part shapes are identified in Database I based on the input feature measurements. The identified body part shapes will be applied to Model II and Model IV. Based on the results of the determining body shape, the corresponding 3D human body model template is found in Database II. Through Model II, a personalized 3D human body model corresponding to the user is generated. The personalized 3D human body model will be applied in two ways: one for the fit evaluation of the final recommended shirt's pattern (virtual try-on) and one to complement the database III (3D-to-2D flattening technique). Using Model III, it is obtained that the corresponding basic pattern can be generated from the user's chest girth and back length. The body feature measurements determine the shape of the three body parts. Then, model IV is used to generate PBP for the corresponding body part shapes. Depending on the shirt style selected by the user, model V is used to generate a PBP*shirt* from the PBP. The output of the

recommendation system is a fit oriented PBP*shirt*. Moreover, if the PBP*shirt* is unsatisfactory after a virtual try-on, four adjustable parameters (front side-seam dart, back side-seam dart, waist dart, and garment bodice length) are designed to adjust the PBP*shirt* generated by the proposed recommendation system. The user will use the strain map of the virtual try-on to determine if the design suits a specific body. If the user is satisfied with the design, it is then delivered to the production unit for real garment production. Otherwise, the user will obtain a new design solution by adjusting the parameters.

The proposed recommendation system combines the designer's knowledge of manual measurements of the human body, traditional 2D pattern-making methods and 3D-to-2D flattening techniques to automatically and quickly generate personalized shirt patterns, thus significantly improving the efficiency of pattern-making. The proposed recommendation system allows the development of a new feedback work cycle of recommendation - 3D visualization - evaluation - adjustment, which will be repeated until the user is satisfied with the body shape and the recommended shirt's pattern. By successively adding new body shape samples and design cases, the database can become more and more enriched, and recommendation satisfaction will increase.

In the next section, we describe the principles of the functional modules used in the recommendation system and the inference process from the initial input parameters to the recommended shirt's pattern, the evaluation of the recommended shirt's pattern and the adjustment of the recommended shirt's pattern based on the fit evaluation results.

5.5.2 Inference procedure for personalized shirt pattern recommendation

In the general process of garment pattern-making, the suggested inference procedure consists of the following six steps.

Step 1: Identify the specific consumer's body shape BS (S+AR+T) based on Model I in Section 3.

Step 2: Based on the identified body shape BS (S+AR+T), find the corresponding 3D human body model template 3DTBS (S+AR+T) in Database II.

Step 3: Generate a specific consumer personalized human body model 3DPBS based on Model II in Section 4.

Step 4: Based on Model III in Section 5, generate a specific consumer's basic pattern BP.

Step 5: Based on Model IV and BP in Section 5, generate a specific consumer's personalized basic pattern PBP.

Step 6: Based on Model V and PBP in Section 5, generate a specific consumer personalized shirt pattern PBP*shirt.*

5.6 Discussion and validation of the model

So far, we have mainly introduced a regression model to obtain PBP by adjusting the basic pattern, and parametric modelling methods for the shirt pattern. To prove the feasibility of these methods, in this section, we evaluate the PBP and PBP*shirt* obtained through these two models separately, in terms of qualitative and quantitative results, and then provide further discussion.

5.6.1 PBP's parametric pattern-making effect

To test the effect of the parametric pattern-making method proposed in the application in this chapter, the chest girth and back length of three people with large differences in body shapes were measured and recorded as an example. Then, these dimensions are input into Python, and the functions written previously are called. The final generated PBPs are shown in Figure 5-10. Figure 5-10 shows a comparison of the strain maps of the virtual try-on [219][223] effect of the PBP and New Bunka basic pattern. The strain map shows the degree of deformation that occurred after the garment is worn on the virtual model. The area of color zone represents garment fit level. If the area shown is red, the garment is stretched by more than 120%. This indicates that the garment strains

the body more than the body can handle. The orange to yellow area indicates that the garment is stretched between 110% and 120%. This means that although the garment feels tight to the body when worn, it is tolerable. The green area indicates that the garment is in a normal condition. This means that the body does not put pressure on the garment, and the person wearing the garment feels comfortable and unrestrained. The light to dark blue area indicates that the garment is stretched between 110% and 100%. This means that there is more space between the garment and the body. Therefore, the fit of the garment is not proper even though there is no tightness. Overall, the fit evaluation standard for judging garments by using the strain map should be that the red area, the orange to yellow area, and the light to dark blue area on the strain map are only represented in small or no ratio, while the green area is represented in a larger or even all of them.

By comparison, it can be observed in Figure 5-10 that the PBP significantly improves the fit of the New Bunka basic pattern. The shoulder fit of subject A is significantly improved in PBP. Subject B's shoulder, arm root, and chest fit are significantly improved in PBP. The shoulder and arm root fit of subject C is significantly improved in PBP. As is shown in Table 5-5, in the same way, the distribution ratio of the New Bunka basic pattern and PBP of 33 subjects are measured. The red areas on the strain maps of the 33 subjects decrease by an average of 5.6%, the orange to yellow areas decrease by an average of 8.7%, the light to dark blue areas decrease by an average of 15.8%, and the green areas increase by an average of 29.3%. This shows that the PBP has a better fit than the New Bunka basic pattern.

Subject A

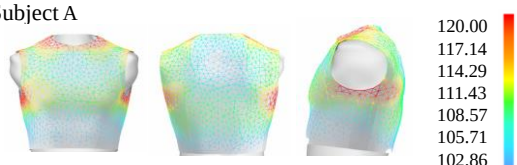

New Bunka

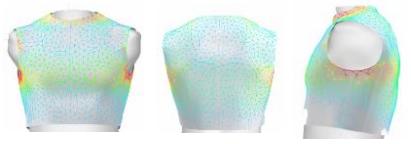

PBP

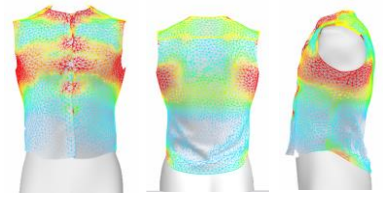

New Bunka Shirt

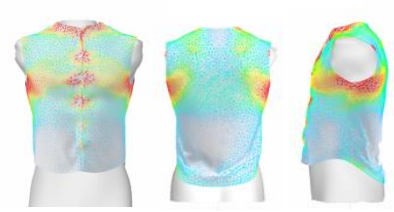

PBP*Shirt*

Subject B

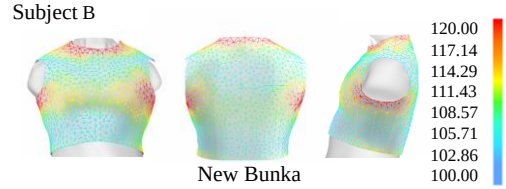

New Bunka

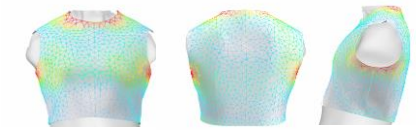

PBP

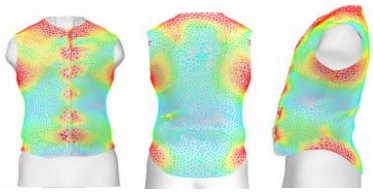

New Bunka Shirt

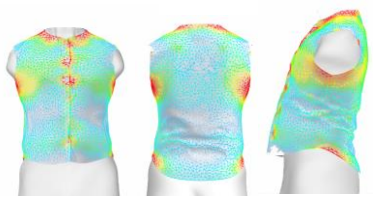

PBP*Shirt*

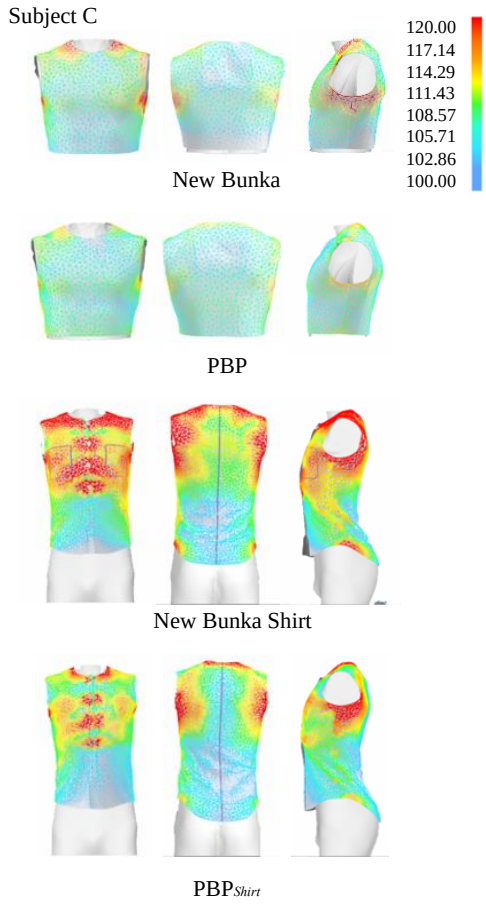

Figure 5-10: Virtual try-on strain map for three subjects with different body shapes.

Table 5-5: Comparison of the strain map.

Subject	Garment pattern	Strain map distribution ratio			
		Red	Orang-Yellow	Green	Light-Dark Blue
A	New Bunka basic pattern	8,9%	15,8%	19,6%	55,6%
	PBP	3,8%	6,5%	46,8%	42,5%
	New Bunka shirt pattern	17,4%	26,4%	14,9%	41,3%
	PBP*shirt*	9,8%	15,7%	38,9%	35,4%
B	New Bunka basic pattern	12,7%	22,0%	17,5%	47,6%
	PBP	5,4%	9,1%	44,7%	40,3%
	New Bunka shirt pattern	19,7%	25,4%	13,3%	41,6%
	PBP*shirt*	7,2%	11,3%	46,1%	35,2%
C	New Bunka basic pattern	4,6%	8,1%	26,7%	60,4%
	PBP	0,0%	5,7%	66,7%	27,6%
	New Bunka shirt pattern	22,1%	31,2%	19,7%	26,9%
	PBP*shirt*	9,3%	20,0%	39,2%	32,1%
All Subjects Average	New Bunka basic pattern	9,2%	14,8%	22,4%	53,5%
	PBP	3,6%	6,7%	51,7%	37,7%
	New Bunka shirt pattern	19,1%	29,4%	15,1%	36,3%
	PBP*shirt*	8,8%	19,1%	41,9%	30,1%

5.6.2 PBP*shirt* parametric pattern-making effect

The PBP*shirt* proposed in this paper are obtained by using the prototype making method

based on the PBP. To test the effectiveness of this method in the application, PBP_{shirt} is made based on the PBP that are obtained in the previous section. Taking the slim fit style as an example, the finally generated PBP_{shirt} are shown in Figure 5-10. By comparing the strain maps of the virtual try-on effect of the PBP_{shirt} and the New Bunka shirt version [29], it can be seen that the PBP_{shirt} fit better than the New Bunka shirt pattern. As is shown in Table 5-5, compared to the New Bunka shirt pattern, the red areas on the strain maps of the 33 subjects decrease by an average of 10.3%, the orange to yellow areas decrease by an average of 10.3%, the light to dark blue areas decrease by an average of 6.2%, and the green areas increase by an average of 26.8%. This shows that the PBP_{shirt} has a better fit than the New Bunka shirt pattern.

Although there is an increase in the light to dark blue areas of subjects like subject C, the increments are not large. Based on the virtual try-on view and designer's experience, this level of increment is not enough to cause the shirt to be excessively loose and thus can be accepted.

5.6.3 PBP_{shirt} in different styles

Shirt patterns of the three styles (slim fit, regular, loose fit) are verified simultaneously in CLO 3D. As an example, the results of subject C are shown in Figure 5-11.

As is shown in Figure 5-11, it can be seen from the strain map presentation that all three styles of shirt show an overall good garment fit. From the slim fit style to the loose fit style, the amount of folds due to stress (not fit) decreases, and the amount of natural draping folds increases. The volume of the garment body becomes larger. At the same time, the position and dimension of the neckline, shoulder line, and sleeve holes remain the same. Therefore, the PBP_{shirt} parametric pattern-making method can be applied to different shirt styles, from slim to lose, with assured high-level garment fit.

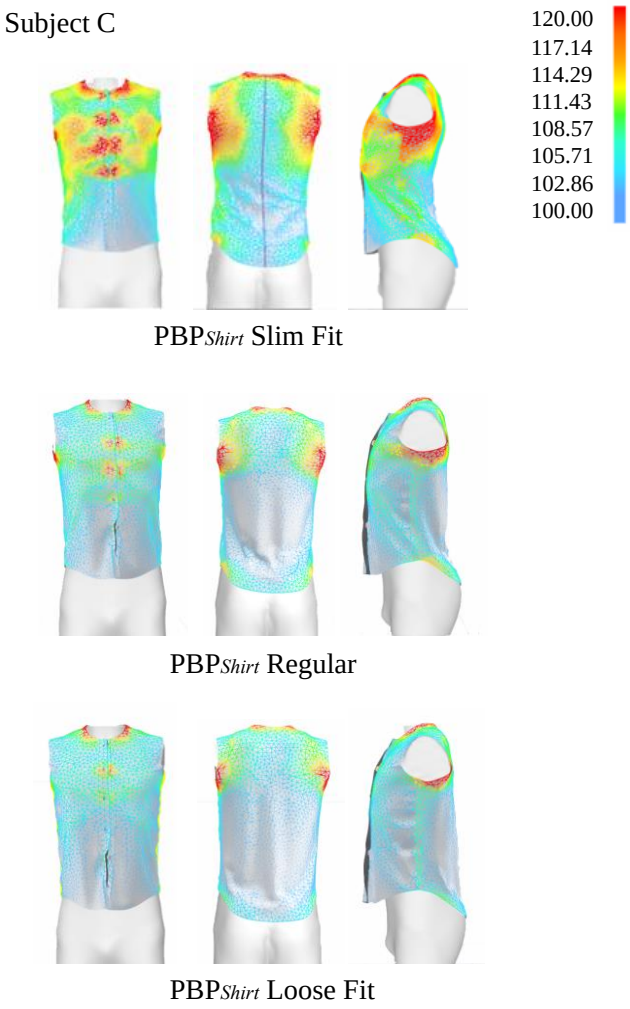

Figure 5-11: Virtual try-on strain map for three styles of shirts.

5.6.4 The efficiency of parametric pattern-making

Using parametric garment pattern-making can remove the repeated data calculations and drawings made by the designer after adjusting the parameters. After comparing the results of the above garment pattern-making, it is found that during the pattern-making process, the change of parameter value will cause changes in the relevant structural lines of the pattern. If the pattern is drawn manually, the designer needs to calculate and adjust the new pattern again according to the new parameter values, which increases the designer's workload considerably. Through parametric pattern-making, the position of the feature points and the corresponding structure lines can be automatically adjusted according to the input parameters. Another outstanding effect of using parametric

pattern making is that designers can easily handle complex curves in a garment pattern. Designers do not need to calculate the relationship of the structure and position of complex curves because the program can automatically draw complex curves according to the internal structure of the garment and the value of the parameters, which significantly improves the efficiency and accuracy of the pattern design, while in manual pattern making, designers need to recalculate the structure and position of complex curves when the parameter values change. There is no guarantee of the accuracy of the final curve.

Conclusion

In the current apparel industry, the existing parametric garment pattern-making models have only considered the differences in human body dimensions. They lack consideration of body shape differences. Therefore, users cannot find suitable clothes often. In this situation, this chapter proposes a personalized garment pattern recommendation system which oriented to fit by integrating the designer's knowledge and 3D measurement. The final generated garment pattern considers the influence of body dimension and body part shape, and the user's requirement of style. The proposed recommendation system can rapidly, accurately, and automatically generate PBP_{shirt} by a linear regression model (from basic pattern to PBP) and parametric model based on the prototype making method (from PBP to PBP_{shirt}). From a comprehensive quantitative analysis, we find that the average of the PBP fit areas has been improved by 29.3% compared with the New Bunka basic pattern. The average of the PBP_{shirt} fit areas has been increased by 26.8% compared with the New Bunka shirt pattern. Meanwhile, the average of PBP and PBP_{shirt} unfit areas (red areas, orange to yellow areas, light to dark blue areas) have been decreased in different degrees. In addition, the proposed method saves plenty of time for designers, and the cost of the shirt's development reduces distinctly. Even users with no pattern-making knowledge can also develop professional shirt patterns by using the proposed system.

In the future work, the feasibility of the parametric garment pattern-making model in the apparel industry will be further explored by developing different garment pattern design processes. Also, the proposed modelling procedure will be extended from the men's top garment to their lower garment and female garment.

GENERAL CONCLUSION AND PROSPECT

In the current clothing market, personalization is increasingly required by consumers. Achieving low-cost, fast-response，fit-oriented personalized garment design is then key to the success of many apparel companies. In this context, the development of a personalized recommendation system based on designer knowledge is extremely important. This is because it can effectively reduce the complexity of the designer's work and effectively respond to the different needs of the consumer (body shape, style, fit, etc.) through a range of options and evaluations. In this thesis, based on the designer's knowledge, an intelligent recommendation system is proposed for users who lack professional garment making knowledge, which is used to help them determine the best-fit design solution in terms of personalized body shape.

The general structure of the proposed recommendation system is outlined in Figure 6-1. It is based on the designer's knowledge (knowledge of anthropometry and knowledge of pattern design) and consists of five models and associated rules (from model 1 to model 5) that allow the body shape of the target population to be classified and the relationship between the body shape and the garment pattern to be described. These models are built by learning data obtained from a set of physical (manual anthropometry, 3D anthropometry, and technical parameters of the pattern-making). Linear regression constitutes the main computational tool of these modelling procedures. The overall knowledge structure of garment pattern-making is composed by integrating previously models. In addition, the proposed recommendation system has a feedback and adjustment mechanism. This feedback mechanism enables human-computer interaction by fit evaluation of the recommended 3D virtual garment on a specific consumer human body model. If the 3D virtual try-on of the current recommended design solution does not satisfy the designer, a new design solution will be obtained by adjusting the set

parameters. The recommended recommendation cycle, i.e. design recommendation - personalized garment pattern generation - virtual try-on - fit evaluation - parameter adjustment, will be repeated until the user is satisfied. The proposed recommendation system has been validated by performing the pattern recommendation on all subjects.

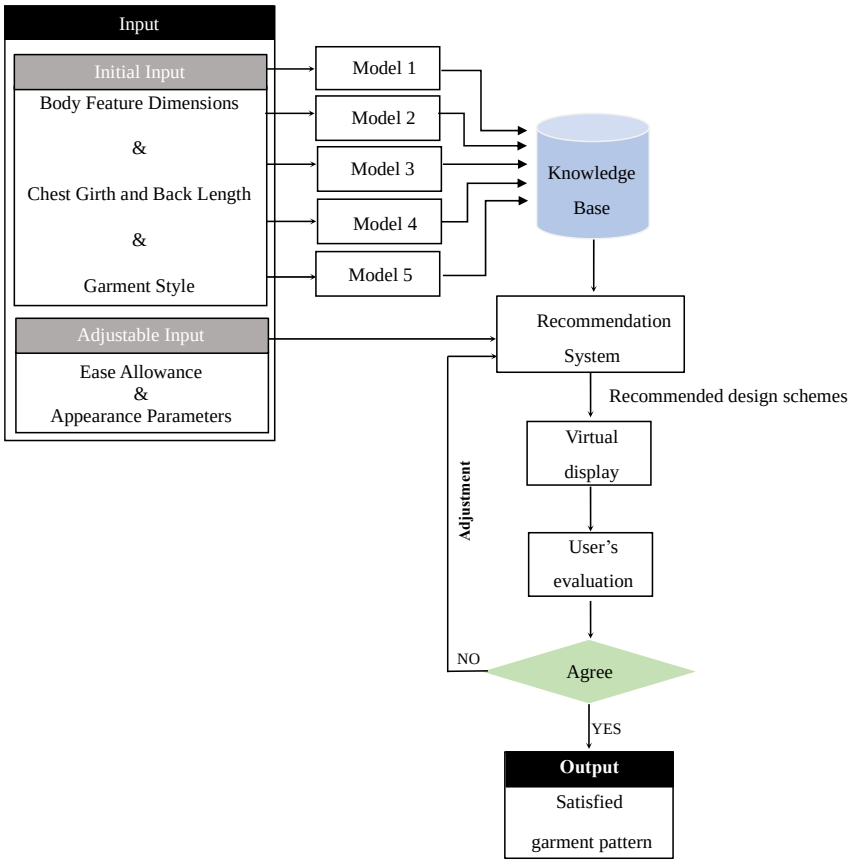

Figure 6-1: The general scheme of this thesis

The main contributions of this thesis can be summarized as follows.

1) The upper body shape is classified by combining professional anthropometric knowledge, manual measurement methods and human segmentation methods. The proposed method is more accurate and interpretable than classical body measurements based classification methods. It takes into account human body differences more comprehensively.

2) The current study proposes a method using manual measurements to assist 3D measurements. By comparing classification results of 3D human models before and after correction, we verified that manual measurement can effectively correct 3D

human models and play an auxiliary role in 3D human measurement. This method provides a meaningful solution to the problem that 3D body scan cannot capture data on hidden areas. This innovation is significant for building personalized 3D human models.

3) The proposed parametric human body modelling method can combine the corrected human models for these three segmented body parts to obtain a complete model of the upper body. The model contains the body part features and labelling information for the feature points within each body part area. In general, the proposed modeling procedure can largely improve the accuracy and interpretability of the scanning-based 3D human models, making them more available for garment designers.

4) This research work proposes a personalized garment pattern recommendation system which oriented to fit by integrating the designer's knowledge and 3D measurement. The final generated garment pattern considers the influence of body dimension and body part shape, and the user's requirement of style. In addition, the proposed method saves plenty of time for designers, and the cost of the shirt's development reduces distinctly. Even users with no pattern-making knowledge can also develop professional shirt patterns by using this proposed system.

5) Classical recommendation systems only offer recommended products to users without considering whether they accept them or not. The proposed feedback mechanism can be adapted to the user's requirements and fed back into the knowledge base. This knowledge base will be gradually enhanced by the addition of new design cases.

The current work can be improved and refined in many ways. In future research, we expect to make more efforts in the following directions.

1) The " Human " is the main subject of garments. In order to achieve a better personalized design of garments, it is necessary to do the best possible to suit human requirements for fit, comfort and health in garment design. Theoretically, the "person - clothing - environment" should be fully considered. However, for simplicity, we only

consider the human layer in these works of thesis. In fact, there are many other layers such as physical indicators (skin color and facial features), socio-cultural factors (mood and occupation), natural environmental factors (seasons, temperature, humidity) and the social environment (e.g. political and economic).

2) Currently, our participants are limited to young Chinese men and we only examined the upper body in the current study. Further studies should apply the results of this study to the whole body and should target children, women, and men of varying ages. For 3D human models built with semantic knowledge, accurate and automatic localization of human feature points and accurate identification and classification of new models are still academic challenges that need to be solved urgently. This is especially true for models with obscure body part shape index features, which requires further in-depth research.

3) In the proposed parametric human body modelling, only the upper body modelling of males was focused on. In the future, the proposed modelling procedure will be extended from the men's upper bodies to their lower bodies and female populations.

4) Due to the very limited amount of data in our study, we can only build data-based models. The knowledge-base is only for the specific type of garment products for specific target groups. To deal with more data in an open environment, we need to improve the relevant models to make them more flexible and resolve data conflicts effectively.

5) In this study, the recommended design solutions were displayed using the corresponding virtual products, allowing significant savings in design time and costs. However, there is still a gap between real and virtual garments. Therefore, we need to control the relationship between real and virtual try-on displays to obtain more accurate evaluation results.

BIBLIOGRAPHY

[1] G. L. Hersey, *The evolution of allure: sexual selection from the Medici Venus to the Incredible Hulk*, vol. 34, no. 07. Cambridge, MA: MIT Press, 1997.

[2] M. N. Wetmore, Vitruvius, and M. H. Morgan, *Vitruvius: The Ten Books on Architecture*, vol. 9, no. 15. Dover, 1916.

[3] E. I. Levin, "Dental esthetics and the golden proportion," *J. Prosthet. Dent.*, vol. 40, no. 3, pp. 244–252, 1978, doi: 10.1016/0022-3913(78)90028-8.

[4] E. Sunderland, *Anthropometry: the Individual and the Population*, vol. 32, no. 7. Cambridge University Press, 1995.

[5] D. B. Chaffin and G. Andersson, "Occupational Biomechanics. New York: John and Wiley Sons." Inc, 1984.

[6] N. Zakaria and D. Gupta, *Anthropometry, apparel sizing and design*. Woodhead Publishing, 2019.

[7] I. F. Leong, J. J. Fang, and M. J. Tsai, "A feature-based anthropometry for garment industry," *Int. J. Cloth. Sci. Technol.*, vol. 25, no. 1, pp. 6–23, 2013, doi: 10.1108/09556221311292183.

[8] D. Gupta, "Anthropometry and the design and production of apparel: An overview," *Anthr. Appar. Sizing Des.*, pp. 34–66, 2014, doi: 10.1533/9780857096890.1.34.

[9] J.-M. Surville and S. Herichi, "HOAXY Body Shapes and Fashion Formula," in *International conference on 3D body scanning technologies, Lugano, Switzerland*, 2010, pp. 249–258, doi: 10.15221/10.249.

[10] D. V Knudson, *Fundamentals of biomechanics*, vol. 183. Springer, 2007.

[11] JIS L0111-1983, *Glossary of Terms Used in Body Measurements for Clothes*. 1983.

[12] Yumiko ITO, *Bunka Fashion System Lecture (9) Fashion Design [M]*. Bunka Publishing Bureau, 2006.

[13] Y. J. Wang, P. Y. Mok, Y. Li, and Y. L. Kwok, "Body measurements of Chinese males in dynamic postures and application," *Appl. Ergon.*, vol. 42, no. 6, pp. 900–912, 2011, doi: 10.1016/j.apergo.2011.02.006.

[14] A. Beazley, “Size and fit: procedures in undertaking a survey of body measurements,” *J. Fash. Mark. Manag.*, vol. 2, no. 1, pp. 55–85, 1997, doi: 10.1108/eb022519.

[15] M. Xia, “Shape analysis of bust slice using elliptic Fourier,” *J. Text. Res*, vol. 35, no. 7, pp. 106–116, 2014.

[16] MIYOSHI Mashiko, *Clothing Modelling Learning[M]*. Beijing China Textile Apparel Press, 2006.

[17] M. Sung and H. Makabe, “A comparison of the body type between Korean and Japanese young female adults,” *J. Japan Res. Assoc. Text. End-Uses*, vol. 45, no. 6, pp. 28–35, 2004, doi: 10.11419/senshoshi1960.45.408.

[18] G. E. Yan and L. I. U. Guolian, “Study on photogrammetric measurement of body in apparel industry,” *J. Text. Res.*, vol. 9721, 2007.

[19] Y. L. Lin and M. J. J. Wang, “Automatic feature extraction from front and side images,” in *2008 IEEE International Conference on Industrial Engineering and Engineering Management, IEEM 2008*, 2008, pp. 1949–1953, doi: 10.1109/IEEM.2008.4738212.

[20] P. Meunier and S. Yin, “Performance of a 2D image-based anthropometric measurement and clothing sizing system,” *Appl. Ergon.*, vol. 31, no. 5, pp. 445–451, 2000, doi: 10.1016/S0003-6870(00)00023-5.

[21] C. Hung, C. P. Witana, and R. S. Goonetilleke, “Anthropometric measurements from photographic images,” *Proc. 7th Int. Conf. Work with Comput. Syst.*, vol. 29, no. 20, pp. 764–769, 2004, [Online]. Available: http://www.ielm.ust.hk/dfaculty/ravi/papers/wwcs2004_1.pdf.

[22] M. J. R. Gittoes, I. N. Bezodis, and C. Wilson, “An image-based approach to obtaining anthropometric measurements for inertia modeling,” *J. Appl. Biomech.*, vol. 25, no. 3, pp. 265–270, 2009, doi: 10.1123/jab.25.3.265.

[23] P. S. Herianto and A. Darmawan, “Development of digital anthropometric circumferential measurement system based on two dimensional images,” in *The 11th Asia Pacific Industrial Engineering and Management Systems Conference, Melaka*, 2010, pp. 7–10.

[24] H. K. Song and S. P. Ashdown, “Female Apparel Consumers’ Understanding of Body Size and Shape: Relationship Among Body Measurements, Fit Satisfaction, and Body Cathexis,” *Cloth. Text. Res. J.*, vol. 31, no. 3, pp. 143–156, 2013, doi:

10.1177/0887302X13493127.

[25] C. M. Chen, “Analysis of upper physical characteristics based on angle measurements,” *Text. Res. J.*, vol. 81, no. 3, pp. 301–310, 2011, doi: 10.1177/0040517510380781.

[26] Zhu Jiangtao, “Human Body 3D Reconstruction and Size Measurement Based on Kinect [D],” Hangzhou Dianzi University, 2015.

[27] H. Takasaki, “Moiré Topography,” *Appl. Opt.*, vol. 12, no. 4, pp. 845–850, 1973, doi: 10.1364/AO.12.000845.

[28] F. Cottle, “Statistical Human Body Form Classification: Methodology Development and Application,” Sep. 2021.

[29] P. Hariharan, *Basics of interferometry*. Elsevier, 2010.

[30] Z. Hu, Z. Xiao, X. Tao, and J. Yang, “Noncontact body measurement for 3-dimensional garment design,” *JOURNAL-DALIAN Inst. Light Ind.*, vol. 20, no. 1, pp. 44–48, 2001.

[31] Y. Gan, D. Chen, and S. Meng, “Recent development of non-touch 3D body measurement,” *J. Text. Res.*, vol. 26, no. 3, p. 145, 2005.

[32] L. Guo, X. Chen, B. Liu, and T. Liu, “3D-object reconstruction based on fusion of depth images by Kinect sensor,” *J. Appl. Opt.*, vol. 35, no. 5, pp. 811–816, 2014.

[33] J.-M. Lu and M.-J. J. Wang, “Automated anthropometric data collection using 3D whole body scanners,” *Expert Syst. Appl.*, vol. 35, no. 1–2, pp. 407–414, 2008.

[34] J. Tong, J. Zhou, L. Liu, Z. Pan, and H. Yan, “Scanning 3d full human bodies using kinects,” *IEEE Trans. Vis. Comput. Graph.*, vol. 18, no. 4, pp. 643–650, 2012.

[35] Y. Chen, G. Dang, Z.-Q. Cheng, and K. Xu, “Fast capture of personalized avatar using two Kinects,” *J. Manuf. Syst.*, vol. 33, no. 1, pp. 233–240, 2014.

[36] A. Weiss, D. Hirshberg, and M. J. Black, “Home 3D body scans from noisy image and range data,” in *2011 International Conference on Computer Vision*, 2011, pp. 1951–1958.

[37] H. A. M. Daanen and F. B. Ter Haar, “3D whole body scanners revisited,” *Displays*, vol. 34, no. 4, pp. 270–275, 2013, doi: https://doi.org/10.1016/j.displa.2013.08.011.

[38]“http://www.nuctech.com/fr/SitePages/ThDetailPage.aspx?nk=PAS&k=DABHAG.” .

[39] E. Özbay and A. Çinar, “A voxelize structured refinement method for registration of point clouds from Kinect sensors,” *Eng. Sci. Technol. an Int. J.*, vol. 22, no. 2, pp. 555–568, 2019, doi: https://doi.org/10.1016/j.jestch.2018.09.012.

[40] M. Aharchi and M. A. Kbir, “A review on 3D reconstruction techniques from 2D images,” in *The Proceedings of the Third International Conference on Smart City Applications*, 2019, pp. 510–522.

[41] S.-J. Hwang, “Three dimensional body scanning systems with potential for use in the apparel industry,” *A Pap. Submitt. to Grad. Fac. North Carolina State Univ. Partial Fulfillment Requir. Degree Dr. Philos. Text. Technol. Manag. Raleigh*, 2001.

[42] P. R. M. Jones, G. M. West, D. H. Harris, and J. B. Read, “The Loughborough anthropometric shadow scanner (LASS),” *Endeavour*, vol. 13, no. 4, pp. 162–168, 1989.

[43] J. Gu, T. Chang, I. Mak, S. Gopalsamy, H. C. Shen, and M. M.-F. Yuen, “A 3D reconstruction system for human body modeling,” in *International Workshop on Capture Techniques for Virtual Environments*, 1998, pp. 229–241.

[44] Y. Huang, X. Li, and P. Chen, “Calibration method for line-structured light multi-vision sensor based on combined target,” *EURASIP J. Wirel. Commun. Netw.*, vol. 2013, no. 1, p. 92, 2013, doi: 10.1186/1687-1499-2013-92.

[45] E. Paquet, K. Robinette, and M. Rioux, “Management of three-dimensional and anthropometric databases: Alexandria and Cleopatra,” *J. Electron. Imaging*, vol. 9, no. 4, pp. 421–431, 2000.

[46] R. P. Pargas, N. J. Staples, and J. S. Davis, “Automatic measurement extraction for apparel from a three-dimensional body scan,” *Opt. Lasers Eng.*, vol. 28, no. 2, pp. 157–172, 1997.

[47] D. Protopsaltou, C. Luible, M. Arevalo, and N. Magnenat-Thalmann, “A body and garment creation method for an Internet based virtual fitting room.,” in *Advances in modelling, animation and rendering*, Springer, 2002, pp. 105–122.

[48] F. Cordier, H. Seo, and N. Magnenat-Thalmann, “Made-to-measure

technologies for an online clothing store," *IEEE Comput. Graph. Appl.*, vol. 23, no. 1, pp. 38–48, 2003.

[49] E. Goldsberry, S. Shim, and N. Reich, "Women 55 years and older: Part I: Current body measurements as contrasted to the PS 42-70 data," *Cloth. Text. Res. J.*, vol. 14, no. 2, pp. 108–120, 1996.

[50] E. Goldsberry, S. Shim, and N. Reich, "Women 55 years and older: Part II. Overall satisfaction and dissatisfaction with the fit of ready-to-wear," *Cloth. Text. Res. J.*, vol. 14, no. 2, pp. 121–132, 1996.

[51] Fengqin Xia, "Research of Somatotype Based on the Sagittal Plane Silhouette of Human Body [D]," Donghua University, 2017.

[52] L. J. Connell, P. V Ulrich, E. L. Brannon, M. Alexander, and A. B. Presley, "Body shape assessment scale: instrument development foranalyzing female figures," *Cloth. Text. Res. J.*, vol. 24, no. 2, pp. 80–95, 2006.

[53] E. Newcomb and C. Istook, "Confronting stereotypes: apparel fit preferences of Mexican-American women," *J. Fash. Mark. Manag. An Int. J.*, 2011.

[54] R. W. Marklin, K. A. Saginus, P. Seeley, and S. H. Freier, "Comparison of anthropometry of US electric utility field-workers with North American general populations," *Hum. Factors*, vol. 52, no. 6, pp. 643–662, 2010.

[55] K. Okabe, N. Yamana, and K. Yamamoto, "Figure evaluation of the adult females silhouette and relation between the figure and the dress silhouette," *JOURNAL-JAPAN Res. Assoc. Text. END USES*, vol. 36, p. 45, 1995.

[56] N. Zakaria, "Body shape analysis and identification of key dimensions for apparel sizing systems," in *Anthropometry, apparel sizing and design*, Elsevier, 2014, pp. 95–119.

[57] C. Y. Huang, "Study on classification of body shape and size grading on young women of Quanzhou District," in *Advanced Materials Research*, 2014, vol. 989, pp. 5319–5322.

[58] N. Hasler, C. Stoll, M. Sunkel, B. Rosenhahn, and H.-P. Seidel, "A Statistical Model of Human Pose and Body Shape," *Comput. Graph. Forum*, vol. 28, no. 2, pp. 337–346, Apr. 2009, doi: https://doi.org/10.1111/j.1467-8659.2009.01373.x.

[59] N. Y. Krakauer and J. C. Krakauer, "A New Body Shape Index Predicts Mortality Hazard Independently of Body Mass Index," PLoS One, vol. 7, no. 7, p.e39504, Jul.2012, [Online]. Available:

https://doi.org/10.1371/journal.pone.0039504.

[60] N. TSUNAWAKE, Y. TAHARA, K. YUKAWA, T. KATSUURA, H. HARADA, and Y. / KIKUCHI, “Classification of Body Shape of Male Athletes by Factor Analysis,” *Ann. Physiol. Anthropol.*, vol. 13, no. 6, pp. 383–392, 1994, doi: 10.2114/ahs1983.13.383.

[61] Y. L. Choi and Y. J. Nam, “Classification of upper lateral body shapes for the apparel industry,” *Hum. Factors Ergon. Manuf. Serv. Ind.*, vol. 20, no. 5, pp. 378–390, Sep. 2010, doi: https://doi.org/10.1002/hfm.20188.

[62] P. Cheng, D. Chen, and J. Wang, “Clustering of the body shape of the adult male by using principal component analysis and genetic algorithm–BP neural network,” *Soft Comput.*, vol. 24, no. 17, pp. 13219–13237, 2020, doi: 10.1007/s00500-020-04735-9.

[63] N. Kim, H. K. Song, S. Kim, and W. Do, “An Effective Research Method to Predict Human Body Type Using an Artificial Neural Network and a Discriminant Analysis,” *Fibers Polym.*, vol. 19, no. 8, pp. 1781–1789, 2018, doi: 10.1007/s12221-018-7901-0.

[64] C. L. Istook, “FEMALE FIGURE IDENTIFICATION TECHNIQUE (FFIT) FOR APPAREL PART II: DEVELOPMENT OF SHAPE SORTING SOFTWARE.”

[65] M.-J. Chung, H.-F. Lin, and M.-J. J. Wang, “The development of sizing systems for Taiwanese elementary-and high-school students,” *Int. J. Ind. Ergon.*, vol. 37, no. 8, pp. 707–716, 2007.

[66] A. Petrova and S. P. Ashdown, “Three-dimensional body scan data analysis: Body size and shape dependence of ease values for pants’ fit,” *Cloth. Text. Res. J.*, vol. 26, no. 3, pp. 227–252, 2008.

[67] D. Gupta, “Anthropometric study of young indian men for garment sizing,” *Res. J. Text. Appar.*, 2010.

[68] A. Vuruskan and E. Bulgun, “Identification of female body shapes based on numerical evaluations,” *Int. J. Cloth. Sci. Technol.*, 2011.

[69] R. Hrženjak, K. Doležal, and D. Ujević, “Sizing system for girls aged 13–20 years based on body types,” *Text. Res. J.*, vol. 85, no. 12, pp. 1293–1304, 2015.

[70] W. Lee and H. Imaoka, “Classification of body shape characteristics of

women's torsos using angles," *Int. J. Cloth. Sci. Technol.*, 2010.

[71] J. Sun, S. Ni, L. Ye, and F. Zou, "Classification and automatic identification of females's body shape based on body-surface angles [D]," Zhejiang Sci-Tech University, 2013.

[72] S. Ni, J. Jin, C. Pang, and F. Zou, "Research of young female somatotype based on longitudinal profile corves," *J. Text. Res.*, vol. 35, no. 8, pp. 87–93, 2014.

[73] Q. M. Wang, "Female body classification in Jiangsu and Zhejiang based on cross-sectional area of body," *J. Text. Res.*, vol. 37, no. 5, pp. 131–135, 2016.

[74] Y. Yao, J. Ma, H. Wu, Q. M. Li, and F. Y. Zou, "Young female body shape classification and prototype patterns based on wavelet coefficient," *J Text Res*, vol. 38, pp. 119–123, 2017.

[75] H.-Y. Lee, K. Hong, and E. A. Kim, "Measurement protocol of women's nude breasts using a 3D scanning technique," *Appl. Ergon.*, vol. 35, no. 4, pp. 353–359, 2004.

[76] L. Chang, X. Zhang, and J. Qi, "Research on subdividing of female breast shapes based on 3-D body measurement," *J. Text. Res.*, vol. 27, no. 12, p. 21, 2006.

[77] H. K. Song and S. P. Ashdown, "Categorization of lower body shapes for adult females based on multiple view analysis," *Text. Res. J.*, vol. 81, no. 9, pp. 914–931, 2011.

[78] H. K. Song and S. P. Ashdown, "Development of automated custom-made pants driven by body shape," *Cloth. Text. Res. J.*, vol. 30, no. 4, pp. 315–329, 2012.

[79] M. Alexander, G. R. Pisut, and A. Ivanescu, "Investigating women's plus-size body measurements and hip shape variation based on SizeUSA data," *Int. J. Fash. Des. Technol. Educ.*, vol. 5, no. 1, pp. 3–12, 2012.

[80] J. Wang, X. Li, and L. Pan, "Waist hip somatotype and classification of young women in Northeast China," *J. Text. Res*, vol. 39, no. 4, pp. 106–110, 2018.

[81] P. Li, B. Corner, and S. Paquette, "Shape analysis of female torsos based on discrete cosine transform," *Int. J. Cloth. Sci. Technol.*, 2015.

[82] M. K. Yoon, Y. J. Nam, and W. Kim, "Classifying male upper lateral somatotypes using space vectors," *Int. J. Cloth. Sci. Technol.*, 2016.

[83] S. Wang, Y. Xu, and H. Wang, “Finite element modelling of Chinese male office workers’ necks using 3D body measurements,” *J. Text. Inst.*, vol. 108, no. 5, pp. 766–775, 2017.

[84] J. ZHANG and H. WANG, “Study of womens’ shoulder based on 3-D body measurement [J],” *J. Text. Res.*, vol. 5, 2011.

[85] J. F. Jin, C. F. Pang, W. J. Chen, X. L. Ye, and F. Y. Zou, “Study on subdivision of young male’s shoulder shapes and cross-section curve,” *J Text Res*, vol. 37, no. 8, pp. 100–106, 2016.

[86] Q. Fuzhou, H. Jin, and H. Yongkun, “A virtual human modeling method based on Chinese anthropometry data,” *Comput. Eng. Sci.*, vol. 37, no. 4, pp. 783–789, 2015.

[87] L. Xidao, Y. Long, X. Yuxiang, W. U. Lingda, and W. E. N. Jun, “Advances in study of 3D modeling,” *Comput. Sci.*, vol. 35, no. 2, pp. 208–210, 2008.

[88] C. Chi, X. Zeng, P. Bruniaux, and G. Tartare, “A study on segmentation and refinement of key human body parts by integrating manual measurements,” *Ergonomics*, no. just-accepted, pp. 1–39, 2021, doi: 10.1080/00140139.2021.1963489.

[89] K. M. Robinette, S. Blackwell, H. Daanen, M. Boehmer, and S. Fleming, “Civilian american and european surface anthropometry resource (caesar), final report. volume 1. summary,” Sytronics Inc Dayton Oh, 2002.

[90] K. He, A. Mao, J. Luo, and G. Li, “Rapid 3D Human Body Modeling and Skinning Animation Based on Single Kinect,” *J. Fiber Bioeng. Informatics*, vol. 8, no. 3, pp. 413–421, 2015.

[91] A. Weiss, D. Hirshberg, and M. J. Black, “Home 3D body scans from a single Kinect,” in *Consumer Depth Cameras for Computer Vision*, Springer, 2013, pp. 99–117.

[92] J. Wu, H. Yuan, and X. Li, “A novel method for comfort assessment in a supine sleep position using three-dimensional scanning technology,” *Int. J. Ind. Ergon.*, vol. 67, pp. 104–113, Sep. 2018, doi: 10.1016/j.ergon.2018.05.012.

[93] U. Clarenz, M. Griebel, M. Rumpf, M. A. Schweitzer, and A. Telea, “Feature sensitive multiscale editing on surfaces,” *Vis. Comput.*, vol. 20, no. 5, pp. 329–343, 2004.

[94] G. C. Sharp, S. W. Lee, and D. K. Wehe, “ICP registration using invariant

features," *IEEE Trans. Pattern Anal. Mach. Intell.*, vol. 24, no. 1, pp. 90–102, 2002.

[95] Z. Yanjuan, "Registration of scattered cloud data," *J. Comput. aided Des. Comput. Graph.*, vol. 18, no. 4, p. 475, 2006.

[96] L. Yong, F. Xiaoli, and S. Huichao, "Research on three-dimensional anthropometric methods," *J. Text. Res.*, vol. 22, no. 04, pp. 61–62, 2001.

[97] P. Li and P. R. M. Jones, "Anthropometry-Based Surface Modeling of the Human Torso," in *International Design Engineering Technical Conferences and Computers and Information in Engineering Conference*, 1994, vol. 13805, pp. 469–474.

[98] L. Yong, "A Review of Three-Dimensional Human Modeling," *J. Text. Res.*, vol. 23, no. 5, pp. 80–81, 2002.

[99] D. Almeida-Galárraga, A. Ros-Felip, V. Álvarez-Sánchez, F. Marco-Martinez, and L. Serrano-Mateo, "Kinematics based physical modelling and experimental analysis of the shoulder joint complex," *Ing. e Investig.*, vol. 37, no. 3, pp. 115–123, 2017.

[100] K. Case, J. M. Porter, D.-C. Xiao, and S. Acar, "Modelling the human body for ergonomic CAD," 1997.

[101] S.-Y. Baek and K. Lee, "Parametric human body shape modeling framework for human-centered product design," *Comput. Des.*, vol. 44, no. 1, pp. 56–67, 2012.

[102] Y. Zhao, Y. Mo, M. Sun, Y. Zhu, and C. Yang, "Comparison of three-dimensional reconstruction approaches for anthropometry in apparel design," *J. Text. Inst.*, 2019.

[103] S. Zhu, P. Y. Mok, and Y. L. Kwok, "An efficient human model customization method based on orthogonal-view monocular photos," *Comput. Des.*, vol. 45, no. 11, pp. 1314–1332, 2013.

[104] G. Pavlakos, L. Zhu, X. Zhou, and K. Daniilidis, "Learning to estimate 3D human pose and shape from a single color image," in *Proceedings of the IEEE Conference on Computer Vision and Pattern Recognition*, 2018, pp. 459–468.

[105] N. Kolotouros, G. Pavlakos, and K. Daniilidis, "Convolutional mesh regression for single-image human shape reconstruction," in *Proceedings of the IEEE/CVF Conference on Computer Vision and Pattern Recognition*, 2019, pp 4501–4510.

[106] H. Seo, F. Cordier, L. Philippon, and N. Magnenat-Thalmann, "Interactive

modelling of mpeg-4 deformable human body models," in *Deformable Avatars*, Springer, 2001, pp. 120–131.

[107] M. Kasap and N. Magnenat-Thalmann, "Parameterized human body model for real-time applications," in *2007 International Conference on Cyberworlds (CW'07)*, 2007, pp. 160–167.

[108] D. Zhang and Z. Miao, "3D Human shpae reconstruction from photographs based template model," in *2008 9th International Conference on Signal Processing*, 2008, pp. 1465–1468.

[109] T.-H. Kwok, K.-Y. Yeung, and C. C. L. Wang, "Volumetric template fitting for human body reconstruction from incomplete data," *J. Manuf. Syst.*, vol. 33, no. 4, pp. 678–689, 2014.

[110] H. Seo and N. Magnenat-Thalmann, "An automatic modeling of human bodies from sizing parameters," in *Proceedings of the 2003 symposium on Interactive 3D graphics*, 2003, pp. 19–26.

[111] H. Seo and N. Magnenat-Thalmann, "An example-based approach to human body manipulation," *Graph. Models*, vol. 66, no. 1, pp. 1–23, 2004.

[112] B.-Y. Koo, E.-J. Park, D.-K. Choi, J. J. Kim, and M.-H. Choi, "Example-based statistical framework for parametric modeling of human body shapes," *Comput. Ind.*, vol. 73, pp. 23–38, 2015.

[113] Y. Zhang, J. Zheng, and N. Magnenat-Thalmann, "Example-guided anthropometric human body modeling," *Vis. Comput.*, vol. 31, no. 12, pp. 1615–1631, 2015.

[114] Y. Zeng, J. Fu, and H. Chao, "3d human body reshaping with anthropometric modeling," in *International Conference on Internet Multimedia Computing and Service*, 2017, pp. 96–107.

[115] D. Malhotra *et al.*, "Linear viscoelastic and microstructural properties of native male human skin and in vitro 3D reconstructed skin models," *J. Mech. Behav. Biomed. Mater.*, vol. 90, pp. 644–654, 2019.

[116] E. Aksan, M. Kaufmann, and O. Hilliges, "Structured prediction helps 3d human motion modelling," in *Proceedings of the IEEE/CVF International Conference on Computer Vision*, 2019, pp. 7144–7153.

[117] A. Malti, “On the exact recovery conditions of 3D human motion from 2D landmark motion with sparse articulated motion,” *Comput. Vis. Image Underst.*, vol. 202, p. 103072, 2021.

[118] M. Kouchi and M. Mochimaru, “Errors in landmarking and the evaluation of the accuracy of traditional and 3D anthropometry,” *Appl. Ergon.*, vol. 42, no. 3, pp. 518–527, 2011.

[119] S. B. Heymsfield, B. Bourgeois, B. K. Ng, M. J. Sommer, X. Li, and J. A. Shepherd, “Digital anthropometry: a critical review,” *Eur. J. Clin. Nutr.*, vol. 72, no. 5, pp. 680–687, 2018.

[120] A. Kuehnapfel, P. Ahnert, M. Loeffler, A. Broda, and M. Scholz, “Reliability of 3D laser-based anthropometry and comparison with classical anthropometry,” *Sci. Rep.*, vol. 6, no. 1, pp. 1–11, 2016.

[121] Y. L. Choi, Y. Nam, K. M. Choi, and M. H. Cui, “A method for garment pattern generation by flattening 3D body scan data,” in *International Conference on Digital Human Modeling*, 2007, pp. 803–812.

[122] J. Su, G. Liu, and B. Xu, “Development of individualized pattern prototype based on classification of body features,” *Int. J. Cloth. Sci. Technol.*, 2015.

[123] J. Su, Y. Ke, B. Gu, and C. Kuang, “A method to develop a personalized pattern of pant from 3D scanning data,” *Proc. 3dbody. tech*, pp. 121–129, 2017.

[124] Q. ZHOU, L. HE, and R. LI, “Research on the Application of Personalized Customized Virtual Design Method in Clothing,” *DEStech Trans. Comput. Sci. Eng.*, no. cii, 2017.

[125] K. Liu, J. Wang, C. Zhu, and Y. Hong, “Development of upper cycling clothes using 3D-to-2D flattening technology and evaluation of dynamic wear comfort from the aspect of clothing pressure,” *Int. J. Cloth. Sci. Technol.*, 2016.

[126] K. Liu *et al.*, “3D interactive garment pattern-making technology,” *Comput. Des.*, vol. 104, pp. 113–124, 2018.

[127] B. Gu, G. Liu, and B. Xu, “Individualizing women’s suit patterns using body measurements from two-dimensional images,” *Text. Res. J.*, vol. 87, no. 6, pp. 669–681, 2017.

[128] T. J. Kang and S. M. Kim, “Optimized garment pattern generation based on three-dimensional anthropometric measurement,” *Int. J. Cloth. Sci. Technol.*,

2000.

[129] K. Liu, J. Wang, and Y. Hong, “Wearing comfort analysis from aspect of numerical garment pressure using 3D virtual-reality and data mining technology,” *Int. J. Cloth. Sci. Technol.*, 2017.

[130] Y. Xiu and Z.-K. Wan, “A survey on pattern-making technologies in Garment CAD,” in *IEEE Conference Anthology*, 2013, pp. 1–6.

[131] C. AP, J. Fan, and W. Yu, “Men’s Shirt Pattern Design Part Ⅱ: Prediction of Pattern Parameters from 3D Body Measurements,” *Sen’I Gakkaishi*, vol. 59, no. 8, pp. 328–333, 2003.

[132] K. Liu, J. Wang, E. Kamalha, V. Li, and X. Zeng, “Construction of a prediction model for body dimensions used in garment pattern making based on anthropometric data learning,” *J. Text. Inst.*, vol. 108, no. 12, pp. 2107–2114, 2017.

[133] Z. Wang, J. Wang, Y. Xing, Y. Yang, and K. Liu, “Estimating human body dimensions using RBF artificial neural networks technology and its application in Activewear pattern making,” *Appl. Sci.*, vol. 9, no. 6, p. 1140, 2019.

[134] S. Thomassey and P. Bruniaux, “A template of ease allowance for garments based on a 3D reverse methodology,” *Int. J. Ind. Ergon.*, vol. 43, no. 5, pp. 406–416, 2013.

[135] Y. Hong, X. Zeng, P. Bruniaux, and K. Liu, “Interactive virtual try-on based three-dimensional garment block design for disabled people of scoliosis type,” *Text. Res. J.*, vol. 87, no. 10, pp. 1261–1274, 2017.

[136] H. Lee, K. Hong, and Y. Lee, “Development of 3D patterns for functional outdoor pants based on skin length deformation during movement,” *Int. J. Cloth. Sci. Technol.*, 2017.

[137] K. Liu *et al.*, “Parametric design of garment flat based on body dimension,” *Int. J. Ind. Ergon.*, vol. 65, pp. 46–59, 2018.

[138] L. Cui, “The Establishment of Blouse’S Parameter Constraint Database Based on Pattern Automatic Generation,” in *2016 2nd International Conference on Advances in Energy, Environment and Chemical Engineering (AEECE 2016)*, 2016, pp. 1–4.

[139] I.-F. Leong, J.-J. Fang, and M.-J. Tsai, “Automatic body feature extraction from a marker-less scanned human body,” *Comput. Des.*, vol. 39, no. 7, pp.

568–582, 2007.

[140] K. Liu, X. Zeng, P. Bruniaux, J. Wang, E. Kamalha, and X. Tao, “Fit evaluation of virtual garment try-on by learning from digital pressure data,” *Knowledge-Based Syst.*, vol. 133, pp. 174–182, 2017.

[141] F. XIA, G. WU, H. XIE, and Y. ZHONG, “Classification of body shape based on longitudinal section curve[J],” *J. Text. Res.*, vol. 38, no. 06, pp. 86–91, 2017.

[142] K. Kim, N. Innami, M. Takatera, T. Narita, M. Kanazawa, and Y. Kitazawa, “Individualized male dress shirt adjustments using a novel method for measuring shoulder shape,” *Int. J. Cloth. Sci. Technol.*, 2017.

[143] J. Fan, W. Yu, and L. Hunter, *Clothing appearance and fit: Science and technology*. Woodhead publishing, 2004.

[144] L. Shen and J. Huck, “Bodice pattern development using somatographic and physical data,” *Int. J. Cloth. Sci. Technol.*, 1993.

[145] S. Efrat, “The development of a method for generating patterns for garments that conform to the shape of the human body.,” 1982.

[146] M. Nagamachi, “Kansei engineering,” in *Handbook of human factors and ergonomics methods*, CRC Press, 2004, pp. 794–799.

[147] L. Ou *et al.*, “A cross-cultural comparison of colour emotion for two-colour combinations,” *Color Res. Appl.*, vol. 37, no. 1, pp. 23–43, 2012.

[148] Y. Huang, C.-H. Chen, and L. P. Khoo, “Kansei clustering for emotional design using a combined design structure matrix,” *Int. J. Ind. Ergon.*, vol. 42, no. 5, pp. 416–427, 2012.

[149] Y. Na, “Fashion design styles recommended by consumers’ sensibility and emotion,” *Hum. Factors Ergon. Manuf. Serv. Ind.*, vol. 19, no. 2, pp. 158–167, 2009.

[150] S. Bensaid, J.-F. Osselin, L. Schacher, and D. Adolphe, “The effect of pattern construction on the tactile feeling evaluated through sensory analysis,” *J. Text. Inst.*, vol. 97, no. 2, pp. 137–145, 2006.

[151] Y. Wang and Y. Chen, “Application of the principle of psychological perceptions to student uniform design,” *J. Text. Res.*, vol. 28, no. 3, p. 96, 2007.

[152] E. Shin and F. Baytar, “Apparel fit and size concerns and intentions to use

virtual try-on: Impacts of body satisfaction and images of models' bodies," *Cloth. Text. Res. J.*, vol. 32, no. 1, pp. 20–33, 2014.

[153] K. Wolff, P. Herholz, and O. Sorkine-Hornung, "Reflection Symmetry in Textured Sewing Patterns," 2019.

[154] J. Lee, Y. Nam, M. H. Cui, K. M. Choi, and Y. L. Choi, "Fit evaluation of 3D virtual garment," in *International Conference on Usability and Internationalization*, 2007, pp. 550–558.

[155] Y. Lu, G. Song, and J. Li, "A novel approach for fit analysis of thermal protective clothing using three-dimensional body scanning," *Appl. Ergon.*, vol. 45, no. 6, pp. 1439–1446, 2014.

[156] X. Tao and P. Bruniaux, "Toward advanced three-dimensional modeling of garment prototype from draping technique," *Int. J. Cloth. Sci. Technol.*, 2013.

[157] X. Zhang, K. W. Yeung, and Y. Li, "Numerical simulation of 3D dynamic garment pressure," *Text. Res. J.*, vol. 72, no. 3, pp. 245–252, 2002.

[158] G. Wang and H. Liu, "Survey of personalized recommendation system," *Jisuanji Gongcheng yu Yingyong(Computer Eng. Appl.*, vol. 48, no. 7, pp. 66–76, 2012.

[159] F. O. Isinkaye, Y. O. Folajimi, and B. A. Ojokoh, "Recommendation systems: Principles, methods and evaluation," *Egypt. informatics J.*, vol. 16, no. 3, pp. 261–273, 2015.

[160] N. Manouselis and C. Costopoulou, "Analysis and classification of multi-criteria recommender systems," *World Wide Web*, vol. 10, no. 4, pp. 415–441, 2007.

[161] T. B. Lalitha and P. S. Sreeja, "Recommendation System Based on Machine Learning and Deep Learning in Varied Perspectives: A Systematic Review BT - Information and Communication Technology for Competitive Strategies (ICTCS 2020)," 2021, pp. 419–432.

[162] N. Wang, H. Zhao, X. Zhu, and N. Li, "The review of recommendation system," in *International Conference on Geo-Informatics in Sustainable Ecosystem and Society*, 2018, pp. 332–342.

[163] C. Guan, S. Qin, W. Ling, and G. Ding, "Apparel recommendation system evolution: an empirical review," *Int. J. Cloth. Sci. Technol.*, 2016.

[164] P. Volino, F. Cordier, and N. Magnenat-Thalmann, "From early virtual

garment simulation to interactive fashion design," *Comput. Des.*, vol. 37, no. 6, pp. 593–608, 2005.

[165] "'http://www.therightsize.com.'" .

[166] Q. I. Yang and Z. H. U. Xin-juan, "An apparel recommended system based on data mining [J]," *J. Xi'an Polytech. Univ.*, vol. 4, 2010.

[167] P. Y. Mok, J. Xu, X. X. Wang, J. T. Fan, Y. L. Kwok, and J. H. Xin, "An IGA-based design support system for realistic and practical fashion designs," *Comput. Des.*, vol. 45, no. 11, pp. 1442–1458, 2013.

[168] R. S. W. Masters, "Knowledge, knerves and know-how: The role of explicit versus implicit knowledge in the breakdown of a complex motor skill under pressure," *Br. J. Psychol.*, vol. 83, no. 3, pp. 343–358, 1992.

[169] A. Pascual-Leone, J. Grafman, and M. Hallett, "Modulation of cortical motor output maps during development of implicit and explicit knowledge," *Science (80-.).*, vol. 263, no. 5151, pp. 1287–1289, 1994.

[170] N. C. Ellis, "At the interface: Dynamic interactions of explicit and implicit language knowledge," *Stud. Second Lang. Acquis.*, vol. 27, no. 2, pp. 305–352, 2005.

[171] A. R. Puerta, J. W. Egar, S. W. Tu, and M. A. Musen, "A multiple-method knowledge-acquisition shell for the automatic generation of knowledge-acquisition tools," *Knowl. Acquis.*, vol. 4, no. 2, pp. 171–196, 1992.

[172] H. Chao, A. Luximon, and K.-W. Yeung, "Functional 3D human model design: a pilot study based on surface anthropometry and infrared thermography," *Comput. Aided. Des. Appl.*, vol. 12, no. 4, pp. 475–484, 2015.

[173] I. Dāboliņa, A. Viļumsone, J. Dāboliņš, E. Strazdiene, and E. Lapkovska, "Usability of 3D anthropometrical data in CAD/CAM patterns," *Int. J. Fash. Des. Technol. Educ.*, vol. 11, no. 1, pp. 41–52, 2018.

[174] M. Javadi Toghchi *et al.*, "Virtual Mannequin Simulation for Customized Electromagnetic Shielding Maternity Garment Manufacturing," *Designs*, vol. 3, no. 4, p. 53, 2019.

[175] M. Zeraatkar and K. Khalili, "A Fast and Low-Cost Human Body 3D Scanner Using 100 Cameras," *J. Imaging*, vol. 6, no. 4, p. 21, 2020.

[176] Y. Hong, P. Bruniaux, X. Zeng, K. Liu, Y. Chen, and M. Dong, "Virtual reality-based collaborative design method for designing customized garment

for disabled people with scoliosis," *Int. J. Cloth. Sci. Technol.*, 2017.

[177] E. Marsac, K. Kim, and M. Takatera, "Japanese–French tastes in simulated women's sportswear t-shirts," *Int. J. Cloth. Sci. Technol.*, 2018.

[178] K. C. Greder, J. Pei, and J. Shin, "Design in 3D: a computational fashion design protocol," *Int. J. Cloth. Sci. Technol.*, 2020.

[179] K. Ju and Y. Jeong, "Usage & education of the CLO 3D virtual clothing program in the development office & academic," *Fash. Inf. Technol.*, vol. 13, pp. 51–59, 2016.

[180] P. Kline, *An easy guide to factor analysis*. Routledge, 2014.

[181] C. D. Dziuban and E. C. Shirkey, "When is a correlation matrix appropriate for factor analysis? Some decision rules.," *Psychol. Bull.*, vol. 81, no. 6, p. 358, 1974.

[182] P. Hammond *et al.*, "3D analysis of facial morphology," *Am. J. Med. Genet. Part A*, vol. 126, no. 4, pp. 339–348, 2004.

[183] J. Lei, X. You, and M. Abdel-Mottaleb, "Automatic ear landmark localization, segmentation, and pose classification in range images," *IEEE Trans. Syst. Man, Cybern. Syst.*, vol. 46, no. 2, pp. 165–176, 2015.

[184] S. C. Peres, R. K. Mehta, and P. Ritchey, "Assessing ergonomic risks of software: Development of the SEAT," *Appl. Ergon.*, vol. 59, pp. 377–386, 2017.

[185] S. Karamizadeh, S. M. Abdullah, A. A. Manaf, M. Zamani, and A. Hooman, "An overview of principal component analysis," *J. Signal Inf. Process.*, vol. 4, no. 3B, p. 173, 2013.

[186] J. Lee Rodgers and W. A. Nicewander, "Thirteen ways to look at the correlation coefficient," *Am. Stat.*, vol. 42, no. 1, pp. 59–66, 1988.

[187] S. M. Stigler, "Francis Galton's account of the invention of correlation," *Stat. Sci.*, pp. 73–79, 1989.

[188] Y.-C. Lee and M.-J. Wang, "Taiwanese adult foot shape classification using 3D scanning data," *Ergonomics*, vol. 58, no. 3, pp. 513–523, 2015.

[189] J. Schiller, R. Srinivasan, and M. Spiegel, *Probability and statistics*. McGraw-Hill Education, 2012.

[190] X. Yan and X. Su, *Linear regression analysis: theory and computing*. World Scientific, 2009.

[191] G. Grégoire, “Multiple linear regression,” *Eur. Astron. Soc. Publ. Ser.*, vol. 66, pp. 45–72, 2014.

[192] T. Olds, N. Daniell, J. Petkov, and A. David Stewart, “Somatotyping using 3D anthropometry: a cluster analysis,” *J. Sports Sci.*, vol. 31, no. 9, pp. 936–944, 2013.

[193] A. Stewart, R. Ledingham, and H. Williams, “Variability in body size and shape of UK offshore workers: A cluster analysis approach,” *Appl. Ergon.*, vol. 58, pp. 265–272, 2017.

[194] K. Liu, J. Wang, X. Tao, X. Zeng, P. Bruniaux, and E. Kamalha, “Fuzzy classification of young women’s lower body based on anthropometric measurement,” *Int. J. Ind. Ergon.*, vol. 55, pp. 60–68, 2016.

[195] *ISO/TR 10652:1991. Standard sizing systems for clothes. Geneva: ISO.* .

[196] *The State administration of quality Supervision, inspection and quarantine of the PRC. The People’s Republic of China’s national standard clothing size men: clothing size men. China Standard Press (2009).* .

[197] *Japanese Industrial Standards Committee (2001) “Sizing Systems for Men’s Garments JIS L 4004 2001 JATRA/JSA.”* .

[198] M. Alexander, L. J. Connell, and A. B. Presley, “Clothing fit preferences of young female adult consumers,” *Int. J. Cloth. Sci. Technol.*, 2005.

[199] B. HAMAD, M. HAMAD, S. THOMASSEY, and P. BRUNIAUX, “3D adaptive morphotype mannequin for target population,” *J. Ergon.*, vol. 8, no. 2, p. 9, 2018.

[200] C. Siyuan, W. Xiaokang, and Y. Xuerong, “Application of 3D human body scanning technology in individualized design,” *Exp. Technol. Manag.*, p. 5, 2018.

[201] C. C. L. Wang, T. K. K. Chang, and M. M. F. Yuen, “From laser-scanned data to feature human model: a system based on fuzzy logic concept,” *Comput. Des.*, vol. 35, no. 3, pp. 241–253, 2003.

[202] H. Han and Y. Nam, “Automatic body landmark identification for various body figures,” *Int. J. Ind. Ergon.*, vol. 41, no. 6, pp. 592–606, 2011.

[203] S. Wuhrer, Z. Ben Azouz, and C. Shu, “Semi-automatic prediction of landmarks on human models in varying poses,” in *2010 Canadian Conference on Computer and Robot Vision*, 2010, pp. 136–142.

[204] D.-J. Yoo, “Three-dimensional surface reconstruction of human bone using a B-spline based interpolation approach,” *Comput. Des.*, vol. 43, no. 8, pp. 934–947, 2011.

[205] S.-W. Hsiao and R.-Q. Chen, “A study of surface reconstruction for 3D mannequins based on feature curves,” *Comput. Des.*, vol. 45, no. 11, pp. 1426–1441, 2013.

[206] S. Kim and C. K. Park, “Basic garment pattern generation using geometric modeling method,” *Int. J. Cloth. Sci. Technol.*, 2007.

[207] C.-J. He, B.-A. Ying, X.-F. Wang, and J. Qi, “Construction and Application of Clothing Pattern Design Model Based on Directed Graph Method,” *J. Fiber Bioeng. Informatics*, vol. 14, no. 1, pp. 41–51, 2021.

[208] W. Wang, G. Zhang, L. Yang, and W. Wang, “Research on garment pattern design based on fractal graphics,” *EURASIP J. Image Video Process.*, vol. 2019, no. 1, pp. 1–15, 2019.

[209] Y. Wang, “Digitalization of Garment Design Based on CorelDRAW Software,” 2020.

[210] B. Gu and G. Liu, “Research on Structural Design of Pants and Pattern Generation System.,” *J. Multimed.*, vol. 8, no. 6, 2013.

[211] Y. Gu and Y. Shi, “Research on automatic method of curves drawing in garment CAD pattern system,” *Comput. Sci. Appl.*, vol. 9, no. 1, pp. 9–18, 2019.

[212] H. Liu, G. Jiang, Z. Dong, F. Xia, and H. Cong, “The size prediction and auto-generation of garment template,” *Int. J. Cloth. Sci. Technol.*, 2020.

[213] N. Rothstein, M. Ginsburg, A. Hart, V. D. Mendes, and P. Barnard, *Four hundred years of fashion*. Victoria and Albert Museum London, 1984.

[214] F. T. Fung, L. Hes, and V. Bajzik, “Review of Men’s Shirt Pattern Development for the Last 100 Years,” *Vlákna a Text. (Fibres Text.*, vol. 27, no. 3, 2020.

[215] D. M. Brough, “Neo-dandy: wearability, design innovation and the formal white dress shirt for men.” Queensland University of Technology, 2008.

[216] C. W. Cunnington and P. Cunnington, *The history of underclothes*. Courier Corporation, 1992.

[217] D. Sindicich and C. Black, “An assessment of fit and sizing of men’s business

clothing," *J. Fash. Mark. Manag. An Int. J.*, 2011.

[218] A. P. Chan, J. Fan, and W. M. Yu, "Prediction of men's shirt pattern based on 3D body measurements," *Int. J. Cloth. Sci. Technol.*, 2005.

[219] J. Yan and V. E. Kuzmichev, "A virtual e-bespoke men's shirt based on new body measurements and method of pattern drafting," *Text. Res. J.*, vol. 90, no. 19–20, pp. 2223–2244, 2020.

[220] H. Kim and M. L. Damhorst, "The relationship of body-related self-discrepancy to body dissatisfaction, apparel involvement, concerns with fit and size of garments, and purchase intentions in online apparel shopping," *Cloth. Text. Res. J.*, vol. 28, no. 4, pp. 239–254, 2010.

[221] K. DesMarteau, "CAD: Let the fit revolution begin," *Bobbin*, vol. 42, no. 2, p. 42, 2000.

[222] X. Tao, X. Chen, X. Zeng, and L. Koehl, "A customized garment collaborative design process by using virtual reality and sensory evaluation on garment fit," *Comput. Ind. Eng.*, vol. 115, pp. 683–695, 2018.

[223] D. Hidellaarachchi, H. Gunatilake, S. Perera, D. Sandaruwan, and M. Weerasinghe, "Towards a virtual garment fitting model for male upper body for online marketplace," in *2018 18th International Conference on Advances in ICT for Emerging Regions (ICTer)*, 2018, pp. 322–331.

PUBLISHED AND SUBMITTED PAPERS

[1] Chi C, Zeng X, Bruniaux P, et al. A study on segmentation and refinement of key human body parts by integrating manual measurements [J]. Ergonomics, 2021: 1-18.

[2] Chi C, Zeng X, Bruniaux P, et al. Arm root shape classification of young male based on artificial anthropometry[C]//Developments of Artificial Intelligence Technologies in Computation and Robotics: Proceedings of the 14th International FLINS Conference (FLINS 2020). 2020: 622-630.

[3] Chi C, Zeng X, Bruniaux P, et al. Application of human feature curves in 3D human model hole repair [C]// Proceedings of the 14th Textile Bioengineering and Informatics Symposium (TBIS 2021) .

[4] Chi C, Zeng X, Bruniaux P, et al. A new parametric 3D human body modelling approach by using key position labelling and body parts segmentation (accepted by Textile Research Journal).

[5] Chi C, Zeng X, Bruniaux P, et al. An intelligent recommendation system for personalized parametric garment patterns by integrating designer's knowledge and 3D body measurements (submitted to International Journal of Clothing Science and Technology).

Résumé Étendu en Français

Avec le développement rapide de l'économie, de plus en plus de consommateurs exigent la personnalisation des produits. Les entreprises de l'habillement ont besoin de toute urgence d'un nouveau modèle de production pour répondre à cette exigence. Grâce à ce modèle, toutes les activités du processus complet de conception et de production des produits seront davantage axées sur les besoins des consommateurs. La personnalisation de masse peut satisfaire les exigences d'une population spécifique, fournir des produits ou des services adaptables et réaliser le processus de personnalisation rapide à faible coût. Cependant, la complexité des exigences des consommateurs a entraîné une difficulté accrue dans la conception des vêtements. Par exemple, la variation croissante de la taille corporelle parmi les différents groupes de consommateurs fait que les vêtements produits selon le système actuel de dimensionnement des vêtements de prêt-à-porter ne sont pas parfaitement ajustés. Pour résoudre ce problème, il faut employer davantage de designers dans les entreprises de l'habillement ou actualiser les méthodes et processus de conception actuels. Cependant, l'emploi de designers plus expérimentés augmenterait considérablement les coûts. Par conséquent, la modification de la méthode et du processus de conception actuels est un moyen efficace de résoudre les difficultés des entreprises modernes de l'habillement.

Pour adapter la conception des produits, des environnements et des systèmes aux utilisateurs cibles, il faut d'abord tenir compte des caractéristiques corporelles de ces derniers. Dans l'industrie de l'habillement, la forme du corps est étroitement associée à la fabrication et à l'ajustement des vêtements. Le point de départ de la fabrication de vêtements confortables est de comprendre et de caractériser de manière exhaustive les différences de forme du corps humain. Actuellement, la plupart des recherches sur la morphologie sont basées sur des données obtenues à partir de modèles humains 3D. Cependant, la plupart des modèles humains 3D utilisés dans l'industrie de l'habillement

sont des modèles de surface géométriques rigides en position debout et ne tiennent pas compte de facteurs tels que la structure du squelette, la composition du corps (os, graisse et muscles) et la déformation du corps associée à l'élasticité de la peau et aux mouvements du corps. Si ces facteurs ne sont pas intégrés dans les modèles humains 3D, les produits fabriqués sur cette base peuvent ne pas convenir aux consommateurs. En outre, dans une posture debout naturelle, il est difficile d'obtenir des données sur les zones cachées (par exemple, les racines des bras, l'aine, l'entrejambe) à partir d'un scan 3D. De ce fait, le modèle corporel 3D généré ne reflète pas exactement la forme réelle du corps humain. Il est donc important de proposer une méthode de correction des modèles humains 3D pour résoudre les problèmes ci-dessus.

En outre, la création de patrons de vêtements est un élément clé pour satisfaire la personnalisation des vêtements. Cependant, qu'il s'agisse d'un patronage traditionnel réalisé manuellement ou par un logiciel de conception assistée par ordinateur (CAO), les modélistes doivent posséder un grand nombre de connaissances professionnelles et de compétences pour créer rapidement un patron de vêtement parfaitement adapté. Cependant, ces méthodes présentent également les inconvénients suivants : (1) le processus d'apprentissage est particulièrement long et difficile à promouvoir, et le processus de fabrication prend beaucoup de temps, ce qui limite l'amélioration de l'efficacité de la production. Bien que le logiciel de création de patrons de vêtements par CAO puisse effectuer la gradation automatiquement, ce qui améliore l'efficacité de la production, il ne convient que pour une gradation générale des spécifications des dimensions standards. Il ne peut pas ajuster automatiquement les modifications des dimensions individuelles. Les vêtements produits sur la base de spécifications de dimensions standards ne peuvent pas satisfaire les exigences des consommateurs en matière d'ajustement ; (2) une fois que le style du vêtement change, le dessin de la structure du vêtement doit être redessiné ou ajusté manuellement, et les concepteurs inexpérimentés sont incapables de répondre rapidement aux ajustements des patrons de vêtements. Par conséquent, il est très utile pour l'industrie de l'habillement de savoir

comment développer des produits vestimentaires sans designers et modélistes expérimentés. En effet, l'industrie de l'habillement peut réduire sa dépendance à l'égard des stylistes et des modélistes :

- Dans la recherche sur la forme du corps humain, cette thèse propose une méthode de classification de la forme du corps basée sur des connaissances d'experts et des mesures manuelles pour que les parties du corps segmentées soient classées de manière raisonnable.
- Dans le cadre de la recherche sur la modélisation 3D du corps humain, cette thèse propose une méthode de modélisation paramétrique d'un corps humain 3D personnalisé en intégrant les mesures manuelles, la numérisation 3D et les résultats de la classification des formes du corps pour étiqueter, corriger et reconstruire le modèle de corps humain 3D numérisé. Le modèle contient des informations sémantiques sur le corps humain qui peuvent aider les jeunes designers à concevoir des vêtements en 3D sans connaissance suffisante.
- Dans le cadre de la recherche sur la recommandation de patrons de vêtements, cette thèse propose un processus de conception paramétrique de patrons de vêtements personnalisés orientés vers l'ajustement qui améliore encore la vraisemblance des recommandations de patrons en intégrant les connaissances des experts dans le processus de conception des patrons.

L'introduction générale présente le contexte de cette recherche, y compris un large aperçu de la structure de base et des problèmes existants du système de recommandation de patrons de vêtements. En outre, les buts et objectifs de cette thèse ainsi que le plan sont présentés dans ce chapitre.

Le chapitre 1 donne un aperçu de la littérature pertinente et fournit l'état de l'art de la thèse, qui pose une base théorique pour les recherches suivantes. Cela inclut l'acquisition de données corporelles, la classification des formes corporelles, la modélisation 3D du corps et les techniques de création de patrons de vêtements, les concepts de conception de vêtements personnalisés, ainsi que les techniques utilisées

dans divers systèmes de recommandation existants, en particulier pour les recommandations de vêtements. Enfin, les principes de base et le schéma général d'un système de recommandation de patrons de vêtements orientés vers l'ajustement est présenté.

Le chapitre 2 décrit les outils d'acquisition de connaissances et les outils de calcul utilisés pour réaliser le système. Cela comprend les méthodes utilisées pour l'acquisition des données corporelles, les méthodes statistiques utilisées pour l'analyse et la modélisation des données corporelles, ainsi que les différents outils techniques utilisés pour la modélisation 3D du corps et le processus de conception paramétrique des patrons de vêtements.

Le chapitre 3 décrit la méthode de classification de la forme des parties du corps segmenté et un modèle de relation entre les mesures des caractéristiques et la forme des parties du corps. La comparaison des résultats prouve que la méthode proposée est plus précise et plus facile à interpréter que les méthodes classiques de classification du corps basées sur les mesures corporelles. Elle prend en compte les différences du corps humain de manière plus complète.

Le chapitre 4 présente la méthode d'étiquetage des points caractéristiques humains et la correction du modèle de corps humain. Enfin, une méthode de modélisation paramétrique est décrite pour obtenir un modèle de corps humain personnalisé pour un utilisateur spécifique en utilisant le modèle corrigé segmenté. En comparant les résultats de classification des modèles humains 3D avant et après correction, nous avons vérifié que la mesure manuelle peut corriger efficacement les modèles humains 3D et jouer un rôle auxiliaire dans la mesure humaine 3D. Cette méthode apporte une solution significative au problème de l'incapacité des modèles de corps humains 3D à capturer des données sur les zones cachées.

Le chapitre 5 décrit un processus de conception paramétrique de patrons de vêtements personnalisés orientés vers l'ajustement et une méthode d'évaluation de l'ajustement des vêtements. Les résultats expérimentaux montrent que le modèle de vêtement final

généré tient compte de l'influence des dimensions et de la forme des parties du corps, ainsi que des exigences stylistiques de l'utilisateur.

La conclusion générale résume les principales contributions de la thèse, et donne les perspectives de recherches futures.

Les principaux contenus de recherche de cette thèse sont :

- Cette thèse étudie comment résoudre le problème des classifications inappropriées des formes corporelles. La méthode de classification globale existante ne tient pas compte des caractéristiques des parties du corps humain. En revanche, la méthode de classification des parties du corps ne prend en compte que la caractéristique d'une partie du corps. Elle ne tient pas compte de l'impact des autres parties du corps sur la forme du corps. En outre, peu de recherches ont été menées sur les parties cachées de la personne, telles que la forme de la racine du bras. De plus, la forme des emmanchures (correspondant à la forme de la racine du bras) est étroitement liée à la conception structurelle du vêtement, ce qui affecte dans une certaine mesure l'ajustement et le confort du vêtement. Elle ne doit pas être ignorée et mérite d'être étudiée. Cette thèse propose de classer la forme du haut du corps en combinant des connaissances anthropométriques professionnelles, des méthodes de mesure manuelles et des méthodes de segmentation humaine. Elle prend en compte les différences du corps humain de manière plus complète.
- Cette thèse étudie comment construire un modèle 3D personnalisé du corps humain. Les modèles de corps humain 3D actuellement utilisés dans l'industrie de l'habillement sont pour la plupart rigides et manquent d'informations sémantiques sur les positions et les parties du corps. Il est donc difficile pour les concepteurs de créer des modèles précis, rapides et efficaces à partir de ces modèles. Cette thèse propose une nouvelle méthode de modélisation paramétrique personnalisée du corps humain en 3D basée sur l'étiquetage des positions clés et la segmentation optimisée des parties du corps. Le nouveau modèle contient des informations sémantiques humaines importantes sur les points de position clés étiquetés et les

- caractéristiques de chaque partie du corps. En outre, cette méthode apporte une solution significative au problème que les modèles de corps humain en 3D ne peuvent pas capturer les données sur les zones cachées.
- Cette thèse étudie comment créer rapidement des patrons de vêtements personnalisés. La création de patrons de vêtements est l'une des parties les plus importantes de l'industrie de l'habillement. Cependant, la création traditionnelle de patrons est un travail basé sur l'expérience, qui prend beaucoup de temps et qui ne tient pas compte des différences de formes corporelles. Cette thèse propose une méthode de conception paramétrique des patrons de vêtements basée sur les dimensions du corps acquises par un scanner corporel et les caractéristiques du corps (points de caractéristiques du corps et classification des formes des trois parties du corps segmentées) identifiées par les designers selon leurs connaissances professionnelles. Le modèle de vêtement final généré tient compte de l'influence des dimensions du corps et de la forme des parties du corps, ainsi que des exigences de style de l'utilisateur. En outre, la méthode que nous proposons permet aux concepteurs de gagner beaucoup de temps, et le coût de développement d'une chemise est nettement réduit. Même les utilisateurs n'ayant aucune connaissance en matière de modélisme peuvent développer des patrons de chemise professionnels en utilisant le système que nous proposons.

Cette thèse concentrée sur trois sujets de recherche clés pour la recommandation personnalisée de patrons de chemises a atteint des objectifs satisfaisants. Pour les recherches futures, d'autres éléments complémentaires peuvent être abordés consacrés aux aspects suivants :

- Pour parvenir à une meilleure conception personnalisée des vêtements, il faut tenir compte de l'ensemble "personne - vêtement - environnement". Cependant, nous ne considérons que la couche humaine dans ma thèse. En fait, il existe de nombreuses autres couches telles que les indicateurs physiques (couleur de la peau et traits du visage), les facteurs socioculturels (humeur et profession), les facteurs

- environnementaux naturels (saisons, température, humidité) et l'environnement social (par exemple, politique et économique).
- Dans cette thèse, les participants sont limités aux jeunes hommes chinois et nous n'avons examiné que la partie supérieure du corps dans l'étude actuelle. D'autres études pourraient utiliser les résultats de cette étude pour le corps entier et devraient cibler aussi les enfants, les femmes et les hommes d'âges différents. Pour les modèles humains 3D construits avec des connaissances sémantiques, la localisation précise et automatique des points de caractéristiques humaines et l'identification et la classification précises des nouveaux modèles restent des défis académiques qui doivent être résolus de toute urgence. Cela est particulièrement vrai pour les modèles comportant des caractéristiques obscures de l'indice de forme des parties du corps, ce qui nécessite des recherches approfondies.
- En raison de la quantité très limitée de données dans cette étude, seuls des modèles basés sur les données peuvent être construits. La base de connaissances ne concerne que le type spécifique de produits vestimentaires pour des groupes cibles spécifiques. Pour traiter davantage de données dans un environnement ouvert, nous devons améliorer les modèles pertinents pour les rendre plus flexibles et résoudre efficacement les conflits de données.
- Dans cette étude, les solutions de conception recommandées ont été affichées à l'aide des produits virtuels correspondants, ce qui a permis de réduire considérablement le temps et les coûts de conception. Cependant, il existe toujours un écart entre les vêtements réels et virtuels. Par conséquent, nous devons contrôler la relation entre les affichages d'essayage réels et virtuels pour obtenir des résultats d'évaluation plus précis.

Personalized pattern recommendation system of men’s shirts based on precise body measurement

Abstract

Commercial garment recommendation systems have been widely used in the apparel industry. However, existing research on digital garment design has focused on the technical development of the virtual design process, with little knowledge of traditional designers. The fit of a garment plays a significant role in whether a customer purchases that garment. In order to develop a well-fitting garment, designers and pattern makers should adjust the garment pattern several times until the customer is satisfied. Currently, there are three main disadvantages of traditional pattern-making: 1) it is very time-consuming and inefficient, 2) it relies too much on experienced designers, 3) the relationship between the human body shape and the garment is not fully explored. In practice, the designer plays a key role in a successful design process. There is a need to integrate the designer's knowledge and experience into current garment CAD systems to provide a feasible human-centered, low-cost design solution quickly for each personalized requirement. Also, data-based services such as recommendation systems, body shape classification, 3D body modelling, and garment fit assessment should be integrated into the apparel CAD system to improve the efficiency of the design process.

Based on the above issues, in this thesis, a fit-oriented garment pattern intelligent recommendation system is proposed for supporting the design of personalized garment products. The system works in combination with a newly developed design process, i.e. body shape identification - design solution recommendation - 3D virtual presentation and evaluation - design parameter adjustment. This process can be repeated until the user is satisfied. The proposed recommendation system has been validated by some successful practical design cases.

Key words: human- centered; 3D body modelling; designer’s knowledge; personalized pattern-making; parametric design; fit garment; intelligent recommendation system

Système de recommandation de patrons personnalisés de chemises pour hommes basé sur des mesures corporelles précises

Résumé

Les systèmes commerciaux de recommandation de vêtements ont été largement utilisés dans l'industrie de l'habillement. Cependant, les recherches existantes sur la conception de vêtements numériques se sont concentrées sur les évolutions techniques du processus de conception virtuelle, avec peu de retours de métier provenant des designers. La coupe d'un vêtement joue un rôle important dans l'achat de celui-ci par le client. Afin de développer un vêtement correctement ajusté, les stylistes et les modélistes doivent ajuster le patron du vêtement plusieurs fois jusqu'à ce que le client soit satisfait. Actuellement, le modélisme traditionnel présente trois inconvénients majeurs : 1) il est très long et inefficace, 2) il repose trop sur des concepteurs expérimentés, 3) la relation entre la forme du corps humain et le vêtement n'est pas pleinement explorée. Dans la pratique, le styliste joue un rôle clé dans la réussite du processus de conception. Il est nécessaire d'intégrer les connaissances et l'expérience du styliste dans les systèmes actuels de CAD de vêtements afin de fournir rapidement une solution de conception réalisable, centrée sur l'homme et à faible coût, pour chaque besoin personnalisé. En outre, les services basés sur les données, tels que les systèmes de recommandation, la classification des formes corporelles, la modélisation du corps en 3D et l'évaluation de l'ajustement des vêtements, devraient être intégrés dans le système de CAD de l'habillement afin d'améliorer l'efficacité du processus de conception.

Sur la base de ces besoins, cette thèse propose un système de recommandation intelligent composé de modèles de vêtements ajustables pour conduire à la conception de vêtements personnalisés. Le système fonctionne en combinaison avec un nouveau processus de conception nouvellement développé, à savoir l'identification de la forme du corps humain - la recommandation d'une solution de conception - la représentation virtuelle 3D et l'évaluation - l'ajustement des paramètres de conception. Ce processus peut être répété jusqu'à ce que l'utilisateur soit satisfait. Le système de recommandation proposé a été validé par quelques cas pratiques de conception réussis.

Mots clés: centré sur l'humain ; modélisation du corps en 3D; connaissances du designer; modélisme personnalisée; conception paramétrique; vêtement adapté; système de recommandation intelligent.